Durham E-Theses

Effect of vibration on condensation heat transfer coefficient

Khayat, Mazin N.

How to cite:

Khayat, Mazin N. (1973) *Effect of vibration on condensation heat transfer coefficient*, Durham theses, Durham University. Available at Durham E-Theses Online: http://etheses.dur.ac.uk/10290/

Use policy

The full-text may be used and/or reproduced, and given to third parties in any format or medium, without prior permission or charge, for personal research or study, educational, or not-for-profit purposes provided that:

- a full bibliographic reference is made to the original source
- a link is made to the metadata record in Durham E-Theses
- the full-text is not changed in any way

The full-text must not be sold in any format or medium without the formal permission of the copyright holders.

Please consult the full Durham E-Theses policy for further details.

EFFECT OF VIBRATION ON CONDENSATION

HEAT TRANSFER COEFFICIENT

by

Mazin N. Khayat. M.Sc. Dunelm.

Thesis submitted for the Degree of Master of Science

in the University of Durham.

Engineering Science Department.

April, 1973

ABSTRACT

The project deals with an investigation into the effect of vibration on condensation heat transfer. Saturated steam was condensed on a horizontal stainless steel tube which was transversely vibrated in the plane of the gravitational field.

The work involved the design, instrumentation and development of a test condenser which employed a reciprocating mode of vibration and was capable of operating at different amplitudes and frequencies.

An electric method employing a constant current to measure the condenser tube temperature was explained.

The experimental results showed improvements in the heat transfer coefficient with vibration, over its value with no vibration. Empirical correlation of the experimental data under vibrational conditions was established. Results for the static condenser tests were correlated with Nusselts classical theory of condensation.

Visual observations of the condensate orientation and drainage under vibrational conditions was reported.

Acknowledgements

I should like to express my thanks to Professors R.D. Hoyle and

H. Marsh for supervising my studies.

Thanks are also due to:-

Mr. D. Grant for his constructive contribution to the design of

the power supply circuit.

Mr. F. Venmore and the staff of the Workshop Department , for

building the experimental rig.

Mr. C. Campbell and the technicians of the Engineering Science

Department for their constant help during experimentation of the project.

I am indebted to my Parents for providing me with financial support .

CONTENTS

NOMENCLATURE

Fundamental Dimensions

H	Heat	
L	Length	
M	Mass	
t	Time	
T	Temperature	

A	Amplitude	L
$\bar{A}$	Cross-sectional area	L^2
B	Coefficient of expansion	$1/T$
$\bar{B}$	Dimensionless constant	-
C	Dimensionless constant	-
C_p	Specific heat at constant pressure	-
D	Diameter	L
F	Operator (signifying function of)	-
Gr	Grashof Number $= D\bar{o}^3.g.B.\Delta t/\gamma^2$	-
g	Acceleration due to gravity	L/t^2
h	Heat transfer coefficient	$H/L^2.T.t$
$\bar{h}_{fg}$	Specific latent heat	H/M
K	Liquid thermal conductivity	$H/L^2.T.t$
L	Length	L
$\dot{M}$	Mass flow rate	M/t

N	Dimensional Parameter $= \dfrac{4}{\pi}\left(\dfrac{A}{D_{\bar{o}}}\right)\dfrac{Rev.\,\mu_c\,\bar{h}_{fg}}{K\cdot D_{\bar{o}}^{2}\,(\theta_{sat}-\theta_{\bar{o}})}\times 10^{-5}$	
Nu	Nusselt Number $=$ h.D/K	-
$\bar{p}$	pressure	M/Lt^2
Pr	Prandtl Number for condensate	-
$\dot{Q}$	Heat transfer rate (Heat flux)	H/t
Re	Reynolds Number $\rho.v.D/\mu$	-
Rev	Vibrational Reynolds Number $\dfrac{\rho.A.W.\bar{D_o}}{\mu_c}$	-
r	Radius	L
S	Surface area	L^2
T	Cooling water temperature	t
v	Velocity	L/t
X	Characteristic length	L
Y	Local condensate film thickness	L
y	Co-ordinate normal to surface	L
θ	Condensate temperature	t
$\dot{\theta}$	Tube temperature	
μ	Liquid absolute viscosity	M/Lt
ν	Liquid Kinematic viscosity	L^2/t
ρ	Liquid density	M/L^3
Υ	Shear Stress	M/Lt^2
$\varnothing$	Angular co-ordinate	
W	Frequency	1/t
λ	Non-dimensional factor	-

Subscripts

c	Condensate	

exp	Experimental
i	Inside
in	Inlet
$\bar{L}$	Liquid
m	mean
O	Without vibration
$\bar{O}$	Outer
r.m.s.	Root mean square value
Sat	Saturation state
Sur	Surface
v	With vibration
$\dot{w}$	Water
$\triangle$	Difference

1. INTRODUCTION

1.1 General

In recent years, there has been growing interest in the field of coupled vibration and momentum and energy transport phenomena. An essential part of many industrial processes is the condensation of steam which usually occurs in surface condensers. Condenser research and development has been largely confined to stationary condenser elements, operating in a vapour atmosphere, where drainage of the condensate is restricted to the effect of gravitational forces. The need for increased efficiency in the operation of heat exchangers requires new techniques to obtain improvements in the transport phenomena.

In space applications, where gravitational forces are negligible, the condensate accumulates on the condenser element, and this results in the termination of the process. The removal of the condensate by new means is therefore necessary. Various methods are open to the designer;

i. scraping the condensate by mechanical means

ii. vibrating the condenser element to drain the condensate by momentum effects.

iii. rotating the condenser surface to impart centrifugal drainage effects.

iv. directing large vapour velocities to the condensate element to blow off the condensate.

These methods could contribute to the development of small size and light weight heat exchangers which are needed for industrial applications.

One of the interesting problems associated with rocket propulsion is the marked increase in the local heat transfer to the motor walls due to the effect of intense combustion oscillations that can occur in these motors. The wall temperature often rises to a point resulting in 'burn-out' and destruction of the motor. For these environments, the chief difficulty is to establish the relationship between vibration and heat transfer so that the problem may be overcome.

Many workers have attempted to exploit the influence of vibration upon heat transfer; their investigations may be split into three groups, the first two groups being of general interest and the last group being closely relevant to the work carried out by the author.

1.1 - 1

Heat Transfer from a Vibrating Heat Source to a Fluid

This method consists of subjecting a heated surface to a transverse oscillatory motion thereby creating an oscillatory relative velocity vector between the heated surface and the surrounding fluid

medium, thus imposing a forced convection effect. Scanlan[1] investigated the effect of transverse surface vibration on the heat transfer from a flat plate to water. The experiment revealed large increases in the overall coefficient of heat transfer (hv) at the larger amplitudes of vibration employed (about 2×10^{-3} m), hv reaching its peak value at a frequency of about 100 HZ; with further increase in frequency, the value of hv diminished, a fact which Scanlan claimed was due to the development of cavitation. Martinelli et al [2] investigated rates of heat transfer to water from an electrically heated 1.9×10^{-2} m $^{O \cdot D}$ horizontal tube immersed in a tank of water and subjected to transverse vibration with a frequency (f) range of 0 to 40 HZ and amplitude of vibration (a) from 0 to 2.5×10^{-3} m. It was found that the overall coefficient of heat transfer was unaffected at low values of vibrational Reynolds number (Rev); this result was attributed to the domination of free convection. However as Rev was increased above a critical value of 1,000, the rate of heat transfer was observed to increase rapidly by as much as 400 per cent of its corresponding value without vibration. This was due to the increasing effect of forced convection. Penney et al [3], studied the effects of low frequency large amplitude horizontal oscillations on heat transfer from a heated horizontal wire to both water and ethylene glycol. Tests in water with a basically similar apparatus, but employing vertical oscillations, were conducted by Deaver [4]. Both investigations found a critical Reynolds number (Rev) above which free convection had no

effect on heat transfer. In the range of free convection domination (low Rev), there was good agreement between the results for horizontal and vertical oscillations, but, at high Reynolds numbers (Rev) where forced convection dominates, the effect of vibration on heat transfer was more marked with vertically oscillated wire. Systematic analysis of the physical situation of the two cases may show that for horizontal oscillations, the cylinder moves through a relatively constant temperature undisturbed fluid, in a direction perpendicular to the direction of the convection currents, whereas for vertical oscillations, the cylinder moves in the same direction as the convection currents. The direction of the vibration vector relative to the direction of the gravitational forces, determines the character of the boundary layer flow and this is a primary controlling variable in these problems.

In the forced convection region, Deaven obtained the following relations:-

$$\frac{Nu}{Pr^{0.3}} = 0.35 + 0.48 \ (Rev)^{0.52} \qquad (1.1\text{-}1.1)$$

Lemlich (5) employed similar apparatus to that of Penney (3) and Deaver (4) but his investigations dealt with low-frequency 17 -37 HZ low-amplitude (up to 0.22×10^{-2} m) vertical vibrations. Lemlich obtained the following equation for his experiment data:-

$$\frac{hv}{ho} - 1 = constant \ X \ \frac{(Rev(A/Do)^{0.4} \ Pr^{0.6})}{(Gr.Pr)^{0.26}}$$

$$(1.1 - 1.2)$$

This agrees with Penney (3) and Deaver (4) as follows; the numerator represents a forced convection term of the vibrational disturbances, while the denominator represents a product which is a characteristic of free convection. Consequently, when the relative influence of the vibrational disturbances is small free convection predominates, and when the relative influence of vibration is pronounced forced convection predominates.

The influence of vibration upon the heat transfer rates from horizontal heated wires to air has also received attention. Lemlich (6) investigates this effect by subjecting electrically heated nichrome wires to vibration with a range of sinusoidal amplitudes from 0.7×10^{-3} to 2.9×10^{-3} m at frequencies from 39 to 122 HZ and over a range of temperature differenced between the wires and ambient air of $4^{\circ}C$ - $200^{\circ}C$. The results demonstrated that an increase in heat transfer coefficient of four times that without vibration was possible. The following relation was established from experimental data.

$$\frac{hv}{ho} = 0.75 + 0.0031 \frac{(Rev)^{2.05} (B.\Delta t)^{0.33}}{(Gr.Pr.)^{0.26}} \qquad (1.1 - 1.3)$$

This is applicable to both horizontal and vertical transverse vibrations. An attempt was made to observe the boundary-layer flow using smoke from a cigarette placed under the heated wires, but these observations cannot be regarded as accurate explanations of the boundary-layer flow. Fand-et-al(7) performed similar experimental work to Lemlich (6) but they used a 1.9×10^{-2} m O.D. cylinder. Their results showed that the effect of vibration upon the overall heat transfer coefficient (hv)

at an intensity below 9×10^{-2} m/sec. was negligible. Above this intensity

an increase in (hv) becomes apparent. The results were correlated by

the following equation:-

$$Nu_V = \text{Constant} \times (Gr.Pr)^{0.2} Rev. \qquad (1.1 - 1.4)$$

This is applicable for Rev $\geqslant$ 2200, Gr.Pr. $\geqslant 3 \times 10^4$ and (surface

temperature – ambient temperature) $> 22^{\circ}$K below this temperature

difference (hv) is found to be dependent on Δt. This equation is quite

different from that given by Lemlich (1.1 - 1.3) where (hv) is proportional

to (Rev) $^{2.05}$. This difference may be due to the fact that in Lemlich's

work the ratio A/Do is of the order of 100 times greater than that employed

by Fand. This ratio is one of the controlling variables in all fluid

mechanical phenomena involving vibrations.

1.1 - 2
Heat Transfer and Fluid Pulsation

In this method of vibration, the heated surface is held stationary

and acoustic vibrations are induced in the fluid medium confined by the

surface; the characteristic behaviour between vibration and heat transfer

is found to be very similar to that associated with mechanical surface

vibrations. This was demonstrated by Fand (8) who attempted to compare

the influence of mechanical and acoustical vibration on free convection from

an electrically heated horizontal cylinder. A photographic flow visulization

study was undertaken to clarify the characteristic orientation of the boundary

layer flow around the cylinder, smoke being used as the indicating medium.

The results indicated that the physical mechanism of interaction between

free convection and horizontal vibration is the same whether vibrations

are mechanically or acoustically induced. A fourfold increase of heat

transfer coefficient was observed at an intensity of vibration of 33.6 x 10^{-2} m/sec. and the critical intensity of vibration above which the heat transfer increased significantly was approximately 0.11 m/sec. Morrell (9) derived an approximate method for calculating heat transfer rates from a heated pipe to a resonated air stream flowing inside the pipe. This theory was based on the assumption that the customary empirical relation between Stanton number, Reynolds number and Prandtl number for steady fluid flow can be applied to oscillating flows as well. The analysis predicts a sh arp increase in heat transfer with increase in maximum pressure behind the shock wave. Jackson et al (10) imposed acoustic vibrations at different frequencies and pressure amplitudes on air flowing in a brass tube enclosed in a steam chamber. The experiments indicated that sound pressure levels below 118 decibels (15.9 N/m^2 (r.m.s.)) had little effect on heat transfer coefficient (hv), but above this level, significant increases in hv were apparent. Lemlich (11) adopted a similar procedure to (10) but he used pulsating water flow as a cooling medium instead of air. The pulsations were generated upstream of the test section by an electro-hydraulic pulsator operating at 1.5HZ. The pulsations were found to increase hv by as much as 80 per cent at a Reynolds number of 2,000, depending on upstream location of the pulsator. However, a decrease in hv was reported when the pulsator was located downstream from the exchanger. Feiler et al (12) carried out a thorough investigation into heat transfer from a heated flat plate to an air stream; large amplitude flow oscillations were imparted to this stream by a siren. High speed

schlieren photographs were taken of the thermal boundary layer adjacent

to the plate. The authors concluded from their photographs that the

boundary-layer thickness decreased in proportion to the increase in

heat transfer coefficient. Also that a flow reversal was occuring near

the wall at all frequencies during part of the cycle.

In general, an explanation for the interaction between transverse

vibration and free convection may be based on a study by Fand and Kaye

(13) who observed that vortices begin to develop above a horizontal

heated cylinder at precisely the same sound pressure level at which

the heat transfer rate begins to be significantly affected. The physical

mechanism whereby sound or vibration increase the heat transfer can

then be primarily attributed to the formation of the vortices on the

surface of the heated cylinder, thus providing a vigorous kind of motion

of the thermal boundary-layer round the cylinder and this is also dependent

on the direction of the vibration vector relative to the force of gravity

as mentioned earlier.

1. 1 -3

Heat Transfer by Condensation on Mechanically Vibrated Tubes

Although a considerable body of literature on interactions

between vibration and convective heat transfer may be found, there is

little published data on the influence of vibration on the process of

condensation. Raben et al (14) appear to be the first workers in this

field. Their aims were to improve heat transfer rates in saline-to-

fresh water conversion systems, to reduce scale formation on the

outside of the condenser tubes and to attempt to promote dropwise

condensation by vibration. The authors employed a transversely-

vibrated vertical aluminium tube 1.04m long and of 2.5×10^{-2}m O.D

$\times 2 \times 10^{-3}$m wall thickness. The tube was supported at its ends inside

a pyrex steam jacket and an electro-magnetic vibrator was linked

to the centre of the tube through a driving rod to impart transverse vibrations.

Tests were carried at a constant cooling water flowrate of 465 Kg/hr

and a constant inlet steam pressure of 1 bar. The maximum amplitude

of oscillation (H) ranged between 0.75×10^{-3} — 12.5×10^{-3}m,

at frequencies (F) ranging from 22.5 to 98cHz , thus giving a maximum

Rev of about 200,000. The resonant frequency of the tube was 38HZ.

The experimental observations showed that filmwise condensation was

predominant at all intensities of vibration, and improvements in the

steam heat transfer coefficient (hv) of up to 58 per cent were obtained.

(hv) increased with higher frequencies and higher amplitudes of

vibration.

All data for (hv) were given in the form:-

$$hv \propto ho.F^{0.246} \quad H^{0.205} \qquad (1.1 - 3.1)$$

This relation is valid only for $H.F^{1.2} > 10.6$. It is

important to realize that Raben's results did not demonstrate a critical

value of vibrational intensity above which heat transfer rates increased.

Using basically similar apparatus Raben also investigated the effect

of vibration on the water-side heat transfer coefficient. The test section

was heated by passing an electric current of up to 500 A through the

tube. The cooling water was passed in the tube at Reynolds numbers

between 1, 117 to 24,000, with and without oscillations. The vibrations

applied to the tube were in the frequency range of 17 - 144 HZ and

had amplitudes varying from 2×10^{-4} m to 9.7×10^{-3} m. No significant

increase in heat transfer coefficient was observed with vibration,

maximum increase being about 4 per cent. This small increase was

found to be independent of (Re). Dent (15) attempted a semi-empirical

approach using Nusselt's theory of condensation on a vertical plane,

to seek a correlation to Raben's (14) experimental findings. His

work was based on the theory of Dankwerts (16) and Mickley (17)

for the turbulent heat transfer between a fluid and a solid surface.

This theory shows that the vibrational heat transfer coefficient, (h_v),

is proportional to $\bar{S}^{0.5}$, where $\bar{S}$ is a mixing coefficient representing

the average rate of renewal of fluid lumps at the solid surface. Dent

assumed, that $\bar{S}$ is proportional to $V_v / \bar{\lambda}$ (where V_v is the resultant

velocity of the liquid film due to gravitation (Nusselt (18) and to tube

Vibration), and that $\bar{\lambda}$ is a mixing length of the order of the condensate

film thickness. To simplify the assumption further, he regarded $\bar{\lambda}$

to be constant after some value of vibrational intensity at which the

heat transfer coefficient (h critical) is just beginning to increase. Thus

a simple expression for (hv) was obtained:-

$$h_v = h \text{ critical} \left[\frac{(V_v)}{(V_{critical})} \right]^{0.5}$$

$$(1.1 - 3.3)$$

calculations of (Vv) and (V critical) were based on the same assumptions

that Nusselt used, namely, a Parabolic velocity distribution and a

linear temperature gradient through the condensate film. When

equation (1.1 - 3.3) is compared with Rabens experimental work,

-10-

good agreement is obtained at low amplitudes of vibration, but the results deviate sharply at higher amplitudes, apparently due to the domination of forced convection currents in the condensate film as found by Raben. Houghey (19) conducted work on condensation of saturated ethanol vapour on a longitudinally vibrated 2.3×10^{-2} O.D. x 0.20m long horizontal tube. Physical variables employed for the experiment were a range of amplitude (A) of vibration from 0 to.0015 m, a range of vibrational frequency (F) from 0 to 140 Hz. and a cooling water flow at Re $>$ 4000. A detectable increase in heat transfer was observed at a critical frequency of about 25cps for the entire range of vibrational amplitudes used. The experimental graphs indicated continuous increase in heat transfer coefficient (hv) with increasing frequency and amplitude of vibration. At the maximum intensity of vibration, a 20 per cent increase in (hv) occurred and this was also the maximum increase observed under the entire range of experimental conditions. The increase in (hv) was attributed to the formation of standing waves developed in the condensate film, thus promoting better convection and eddy transfer in the film. No analytical or empirical consideration was given, but it was assumed that the increase in heat transfer was a function of vibrational Reynolds number only. This gave a linear correlation of the data in the form:

$$\frac{hv}{ho} - 1 = 0.0018 \ A.F. \qquad (1.1 - 3.4)$$

where the condenser diameter and the condensate viscosity are constant. The equation was only applicable for A.F. $>$ 20.

In considering investigations of the effect of transverse horizontal

tube vibrations on condensation heat transfer, the only available

literature is provided by Dent (20). For this work a short copper tube

34.3×10^{-2}m long, 2.1×10^{-2}m O.D. $\times 0.11 \times 10^{-2}$ m wall thickness

was used as the test piece. The tube was mounted on a fork linked

to an electromagnetic vibrator and the test piece with its mountings

and cooling water connections were enclosed in a steel vessel to

which steam was supplied at a pressure slightly greater than 1 bar. The

experimental work covered a frequency range of tube vibration from 20

to 80 HZ and a range of amplitudes from 0 to 0.42×10^{-2}m. Results

with vibration showed a maximum increase of 15 per cent in the

condensation heat transfer coefficient (hv) over its value with no

vibration. In studying the mechanical performance of the experimental

apparatus as indicated by the experimental data, it can be seen that

higher amplitudes of vibration were not obtainable at higher tube

frequencies (since this was limited by the performance of the electro-

magnetic vibrator, (see section 2.3 - 1)). As a result, the maximum

possible amplitude of vibration was obtained at lower frequencies. This

method restricted the availability of higher vibrational intensities. The

maximum (Rev) attained in the experiment was about 34,000 compared

with (Rev) in the order of 300,000 covered by the author's experimental

investigation. Dent's experimental points showed considerable scatter

on the graph; a 15 per cent increase in (hv) was given at vibrational

intensities of 0.039 and 0.079 m/sec under the same experimental

-12-

conditions. Such characteristics may be due to large experimental errors. Experimental observations (reported in Chapter 5) show that vibration makes a very small contribution to (hv) up to a vibrational intensity of 0.06 m/sec. Dent also attempted to establish theoretical analysis for correlating his experimental findings, based on Nusselt's theory of condensation on a stationary tube. A perturbation method was proposed. Since condensation was not significantly increased with vibration, an assumption was made that the downward film velocity was due to gravitational force and to a perturbation velocity proportional to the vibrational intensity.

Dent introduced a perturbation parameter (E) and then made the assumption that (E) is equal to the ratio of vibrational amplitude (Amax) over tube diameter (Dö). The supplementary velocity was found by multiplication of (E) and the average velocity of tube vibration in the plane of gravitational field. The analysis proceeded according to Nusselt's theory assuming a linear temperature gradient through the condensate film and a laminar film flow on the surface. A dimensionless parameter for correlating experimental results was given in the form:

$$\frac{ND_o^2}{3} = \frac{4}{3\pi} \frac{(A\ max) \cdot Rev. \, h_{fg}}{(D_o) \cdot K \cdot (\Theta_{sat} - \Theta_o)}$$

(1.1 - 3.5)

In comparison with experimental results, the analysis showed a relatively rapid increase in heat transfer with vibrations and thus its validity for correlating the results is very limited. The condensate velocity is retarded during the lower displacement of the tube and this effect was not taken into account in the analysis. The increase in heat transfer was analytically

based on the positive effect of the cycle to increase drainage of the

condensate and consequently to reduce the film thickness. This assumption,

together with the initial assumptions, render the analysis inaccurate

for correlating the results. No empirical approach was attempted to

correlate the experimental results.

1.2

The Boundary-Layer

When a fluid flows along a stationary solid surface, the fluid

particles adjacent to the surface adhere to it and thus are at rest. At a

certain distance from the surface, the full stream velocity is reached. For

fluids of low viscosity such as air or water, the rise to the stream velocity

from zero velocity at the surface occurs within a relatively narrow layer

of fluid known as the "Boundary-Layer". The viscous forces within the

fluid tend to retard the flow relative to the boundary, thus establishing

a velocity gradient within the boundary-layer. Reynolds (21) showed

that there are two basically different forms of flow, laminar and turbulent

flow. In laminar flow, the fluid runs in stream-lines which flow side by

side in an orderly manner, while in turbulent flow, the stream-lines are

interwoven with each other in an irregular manner. As a consequence,

the individual fluid particles develop fluctuating motions. Reynolds

visualized turbulence as a series of eddies or vortices originating at or

near a solid surface, causing disturbance in the fluid stream. The movement

of the fluid by an eddy current from a region in which the main stream

velocity is low to a region of higher velocity involves a transfer of momentum between the two regions. Taylor (22) assumed that the transition from laminar to turbulent flow occurs as a result of momentary separation in regions of adverse pressure gradient in the fluid stream.

1.3

Heat Transmission in Condensate Film

Thermal transfer processes generally occur as a result of difference or gradient of temperature which depends upon the physical mechanisum of the process. Basically there are two processes whereby thermal energy is transferred. These are conduction and convection. In conduction, the heat is exchanged between adjacent bodies or parts of a body which are at different temperatures and the energy is diffused through the material by a thermal motion of the microscopic particles of which the material is composed. If conduction occurs in a moving fluid, the diffusion of the thermal energy will be affected by the relative motion of the fluid layers. This process is termed convection. Condensation may occur in two distinctly different forms. Filmwise and dropwise (Chapter 4). Only film condensation is dealt with in this work. In considering condensation on a stationary horizontal tube, the condensate film forms on the surface and flows down in a laminar motion (Nusselt (18)) under the influence of gravity. Since the liquid film adheres to the cooling surface, its temperature at this location is the same

as that of the surface, while the temperature of the liquid vapour

interface is slightly lower than the saturation temperature of the

vapour due to subcooling effect. The liquid film provides the major

resistance to the heat flow, and, since the flow is laminar, the

thermal transfer process is mainly of conduction through the film.

The condensate film thickness increases at successive downward

locations on the tube surface due to vapour condensing on the

interface at each location. The magnitude of the resistance to the

heat flow therefore varies down the surface in proportion to the

film thickness. For any condensation process on a stationary

tube, it is apparent that the gravitational force provides the sole factor

in draining the condensate and controlling the film thickness. The

main intention in this work is to impose vibration on the tube in an

attempt to increase drainage and therefore to decrease the film

thickness. This may amount to reducing the temperature gradient in

the film and hence improve the transfer process. The effect of

vibration on condensation heat transfer and its relation to amplitude and

frequency of vibration is experimentally investigated in this thesis.

1.4

Correlation of the Experimental Results

1.4-1 Stationary Tube

In attempting to explain and predict behaviour in physical

phenomena, there are two possible complementary methods;

experimentation and analysis. The former may generally be considered

as the initial method in any new field of study. Observations of the physical process assist in the development of quantitive theory in terms of general mathematical relationships governing the relevant phenomena.

For film condensation on a stationary tube, Nusselt (18) in 1916 established analytical results describing the heat transfer characteristics associated with the process (Chapter 4). Nusselts classical analysis has become a standard for correlating experimental results for stationary condensers. Limitation of Nusselts analysis for application to different condensation processes (e.g. for liquid metals) have been shown by different workers (Bromley (32) Sparrow (39)). However the validity of Nusselts analysis for such processes has been restored by introducing some modification to the theory. For film condensation of steam on a stationary horizontal tube, Nusselt's equation (4.2-19) is recommended by McAdams (22) and this equation was used to assess the experimental work (Chapter 4) of condensation on a stationary tube before imposing vibration.

1.4 - 2

Vibrating Tube

In dealing with analysis of heat transfer and condensation on a horizontally vibrating tube, the condensate orientation around the cylinder is in a non-uniform state owing to the mechanism involved between tube vibration, gravity and fluid motion. For a given frequency of vibration, the rate of disturbance of the condensate film varies with

respect to the instantaneous acceleration of the cylinder and it also varies along the cross section of the cylinder. In addition, the magnitude of the induced disturbances, depends on the intensity of vibration. Each cycle of motion acts as a disturbance and increasing the rate of such disturbances tends to increase the overall effect on the condensate instantaneous distribution around the cylinder. Furthermore, if the tube flexes during each cycle of vibration, the condensate near the centre of the tube is subjected to larger acceleration than the condensate draining near the ends of the tube. As an effect, the condensate orientation along the tube becomes non-uniform. Under all these circumstances the process becomes three dimensional and time dependant and complete analysis of the problem will be very complex. Consequently empirical methods would be very useful in establishing possible relations for correlating the important experimental variables. Such a procedure is explained in Chapter 5. The variables considered were tube frequency and amplitude of vibration and those associated with Nusselts theory of condensation on a horizontal tube.

2. INSTRUMENTATION AND MEASUREMENTS

General

In order to design experimental apparatus capable of fulfilling all requirements satisfactorily, all working conditions should be considered together with all possible difficulties that could cause failure. Some experimental difficulties may not be predictable beforehand and consequently the introduction of some modification to the final apparatus may be necessary.

In this investigation into the effect of vibration on condensation heat transfer, it was decided to position the condenser tube horizontally and to arrange a satisfactory means of vibrating the tube with different amplitudes and frequencies in the plane of the gravitational field. An adequate method of sealing the steam in the pressure vessel during tube vibration had to be found. Furthermore it was envisaged that the experimental programme could involve accurate measurement of mean tube temperature, cooling water temperatures, flow rate, steam pressure and temperature. Fig. 2.A shows a schematic diagram of the steam and cooling water systems. Figs. 2.B and 2.C are photographs of the actual apparatus.

2.1 Test Section

This comprised the Pressure vessel and the test condenser (Fig. 2.1). The vessel incorporated four windows for viewing the condensation process, and two condensate drainage pockets. Five tubes were welded to a common drainage tube that leads to the auxiliary
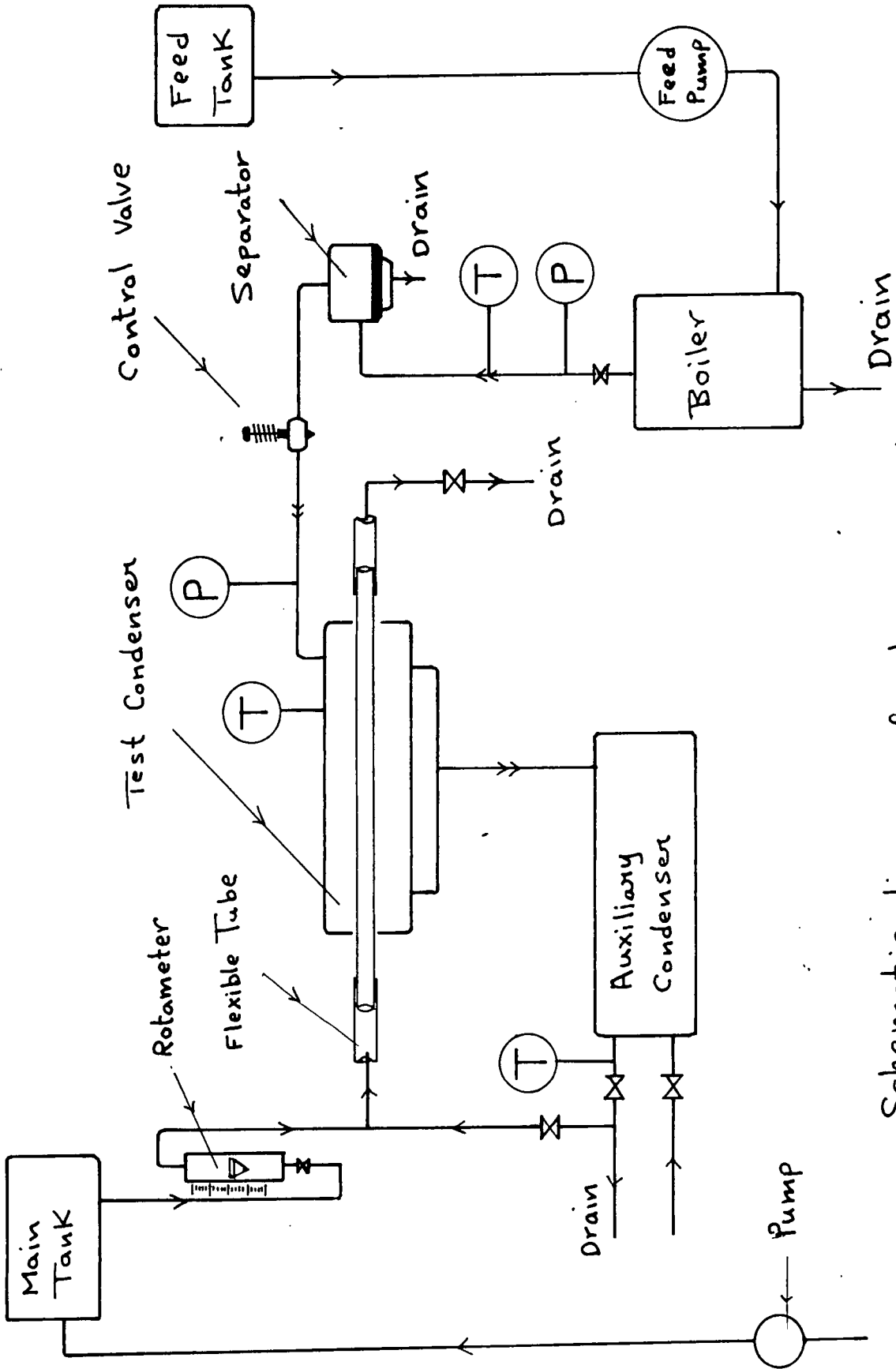
Schematic diagram of steam and cooling Water Systems

Fig 2.A
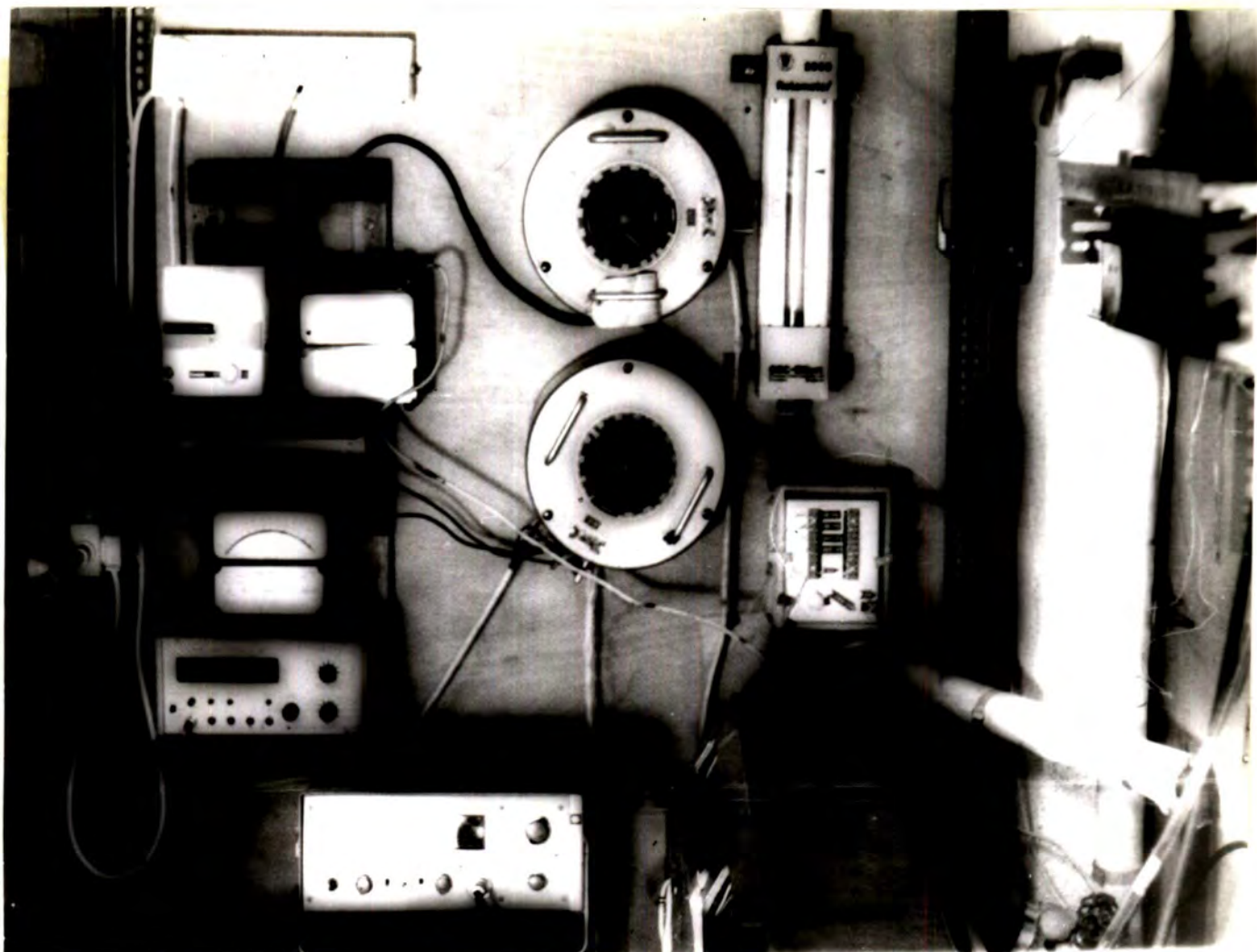
Fig 2.B   The instrument panel

Fig   2.C   The experimental apparatus

EN58B STAINLESS STEEL PLATE POSITIONED AT CENTRE OF EACH WINDOW

120°

120°

8·1×10⁻² m

12 ½" x 3" BSW BOLTS

2·16 x 10⁻² m

GOLDEN WALKERITE JOINTING 400 C°

6 x 10⁻² m

13 x 10⁻² m

1·2 m

FOUR GLASS WINDOWS

1·27 x 10⁻² m

1·27 x 10⁻² m

1·27 x 10⁻⁴ m

3·8 x 10⁻¹ m

3 x 10⁻² m

SECTION 'A'-'A'

8·54 x 10⁻⁴ m

3 x 10⁻⁴ m

1·47 x 10⁻² m

8·53 x 10⁻² m

5·18 x 10⁻² m
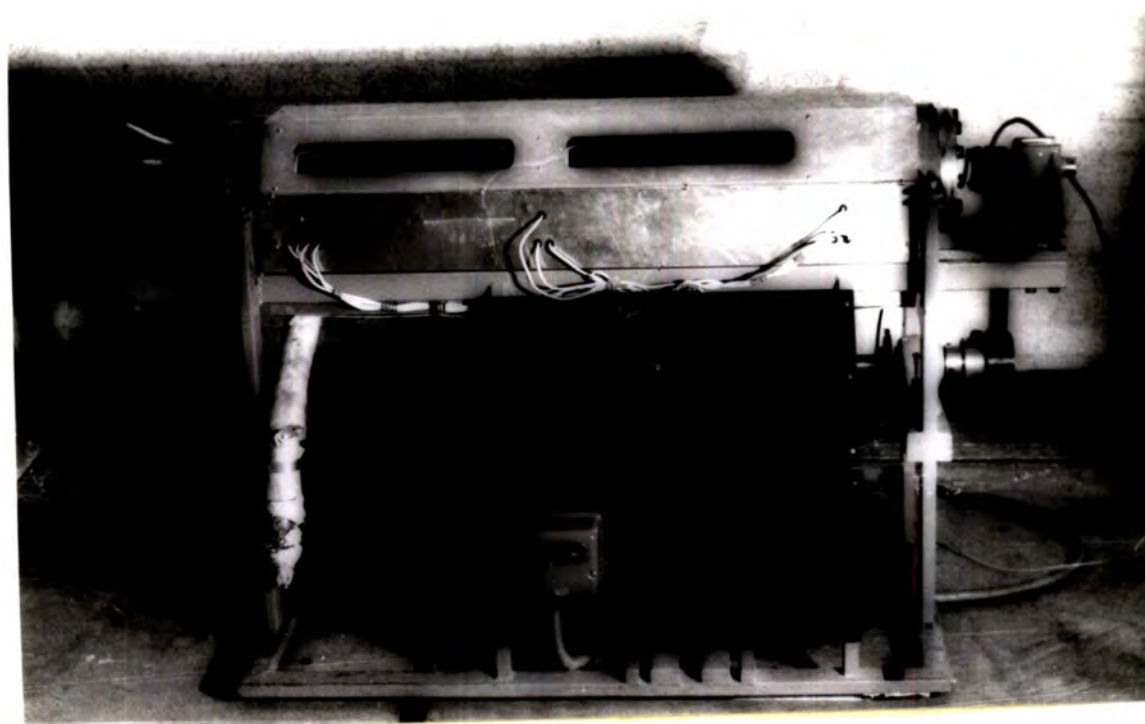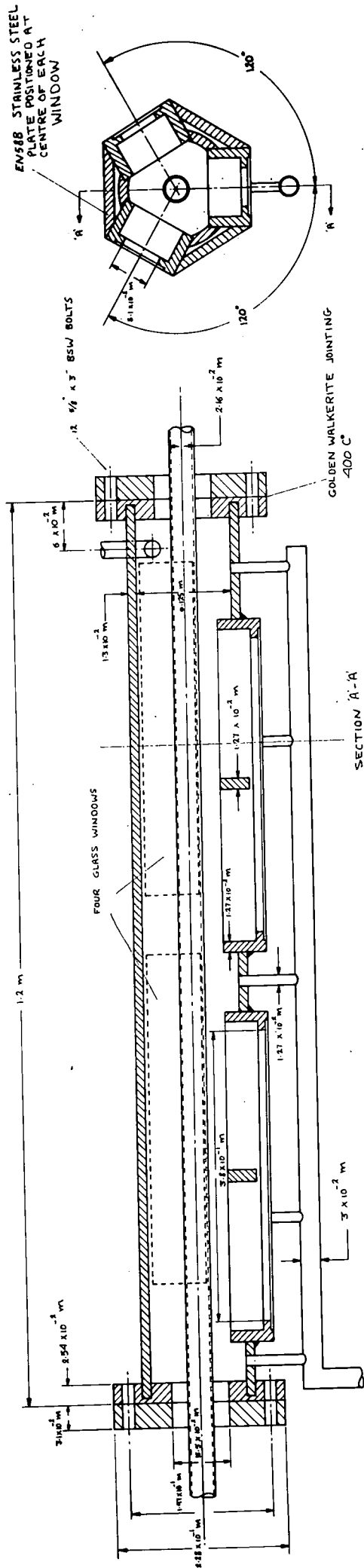
Fig 2.1

condenser. The vessel was externally heated to the steam saturation temperature by means of Electro-Thermal fibre-glass coated heating elements taped around the entire surface of the shell which was packed with 'stillite' mineral wool insulation. The entire vessel and insulation were enclosed in aluminium cover.

The test condenser consisted of 1.019 m long EN58B stainless steel tube. This tube passed through the pressure vessel end covers, each cover being secured to the vessel by means of twelve bolts.

0.034 m. O.D,

2.2 Steam Seal Design

The mode of vibration of the condenser tube necessitated a reliable seal to prevent the steam escaping to atmosphere under vibrational conditions.

Since relatively high amplitudes of vibration were to be employed, it was decided that steel bellows or any form of rubber seal would be inadequate. It was therefore decided to design a seal which had freedom to move with the tube without introducing any flexure. Fig.22 shows a diagrammatic sketch of the seal. This comprised a 'Teflon' disc mounted on the condenser tube inside the pressure vessel. A spring loaded stainless steel disc was screwed to the 'Teflon' disc to prevent deformation. The spring pressure, together with the steam pressure on the disc provided sufficient thrust to prevent the steam from escaping round the 'Teflon' seal. Two high temperature viton 'o' rings, chemically stable at temperatures up to 200°C were embedded in grooves machined inside the 'Teflon' and steel plate bores in order to prevent the

Pressure Vessel Cover

Outer Teflon Seal

Spring

Seal Compressor

Inner main Teflon Seal

Steel plate

Welded Steel Flange

Test Piece

Spring
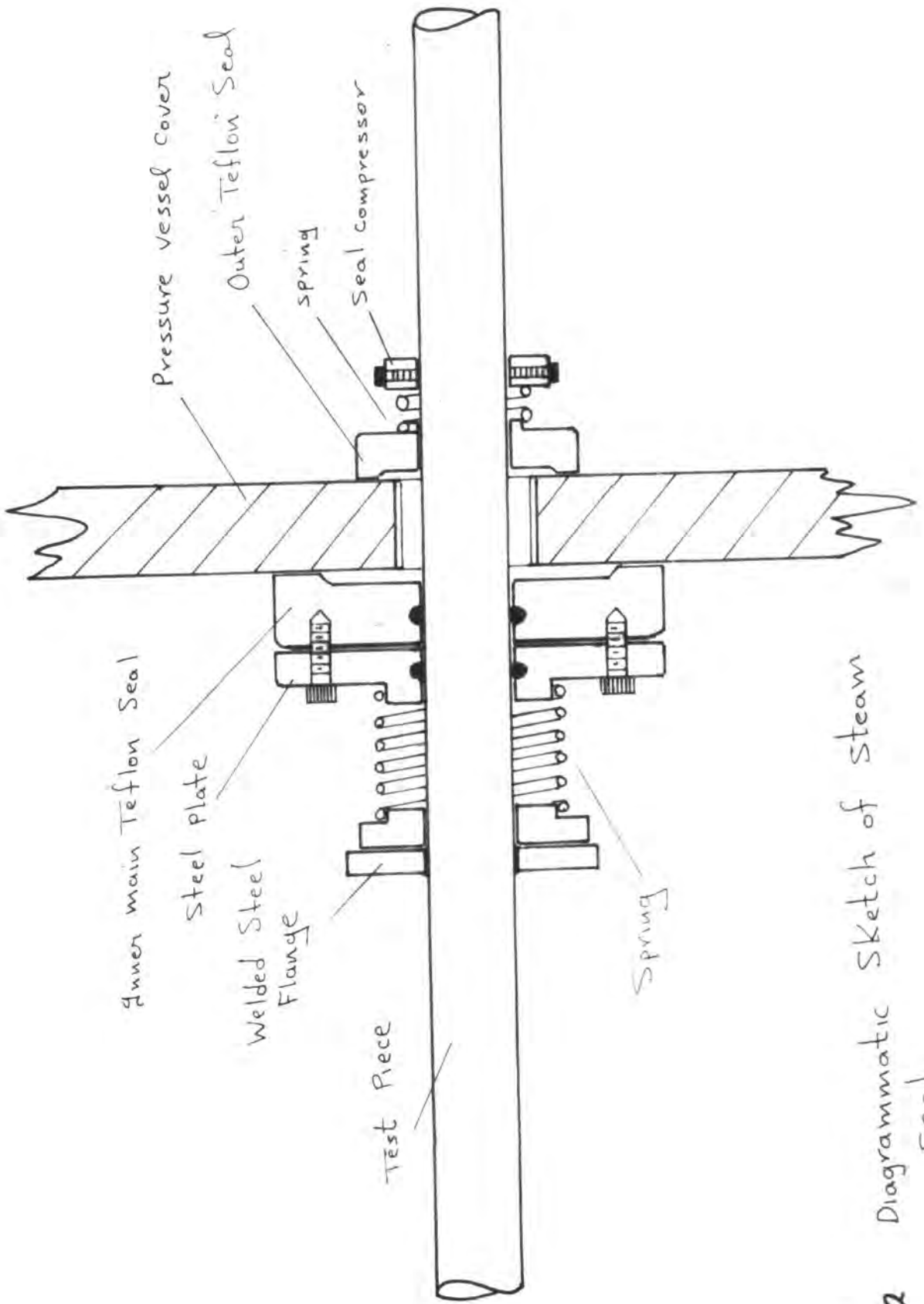
Fig 2.2 Diagrammatic Sketch of Steam Seal.

-24-

steam from escaping to atmosphere round the condenser tube. 'Teflon' was chosen because it combines a low coefficient of friction with a relatively high melting point (about $220^{\circ}C$).

2.3 Vibration Generating System

2.3-1 General

Originally the intention was to adapt two Electro-Magnetic Vibrators, one linked to each end of the tube, to generate the required transverse vibration. The vibrators would be fed from an oscillator through a twin channel amplifier. After a comprehensive investigation on the performance of this system, it was realized that many disadvantages were associated with it. At high frequencies, the useful power of the vibrator is dissipated in accelerating the moving parts of the vibrator. As a result high amplitudes of vibration can only be obtained from very large vibratiors controlled through extremely powerful amplifiers. The cost of these is relatively high, and such vibrators occupy a large floor area. This problem was solved by designing a vibration system incorporating two eccentric cams powered by an electric motor.

2.3-2 Design Configuration

The motor was mounted on the base of the pressure vessel supporting frame and drove a solid steel shaft. The shaft ran in two Hoffmann 0335 self aligning double roller Journal bearings which were mounted on two rigid supports welded to the supporting frame. These bearings were capable of taking moderate axial loads and shaft deflections.

A variable pitch eccentric cam was mounted on each end of the drive shaft. A 0.026 m long, steel tube, connected each cam to the condenser tube. A reciprocating mode of tube vibration was thus employed. The tube was constrained to move only in a vertical direction by means of two 'Teflon' lined channels mounted on the vessel supporting frame. The 'Teflon' served to insulate the tube electrically from the connecting arms.

2.3-3 The Electric Motor

One of the main requirements for the experimental work was that steady frequencies of vibration were to be employed, and, since the components of the moving system were relatively heavy, a powerful motor was needed. A Kopp AC variator was acquired for this purpose. This motor has a maximum of 3.8 K.W. power output, a speed range of 480 - 4320 r.p.m. and has a hydraulic clutch drive which incorporates an accurate mechanisum for control of motor shaft speed. The variator was coupled to the condenser drive shaft by means of a twin V belt and pulley system.

2.3-4 The Eccentric Cams

One of the experimental requirements was that the investigation could be carried at different amplitudes of condenser vibration. Therefore two identical variable amplitude mild steel cams were constructed to fulfil these requirements; each cam consisted of three parts;

        i - Slider
       ii - Holder
      iii - Screw adjuster

Adjusting Screw

Scale

Slider

Full - Scale

Section 'A'-'A'

Fig 2.3

-27-
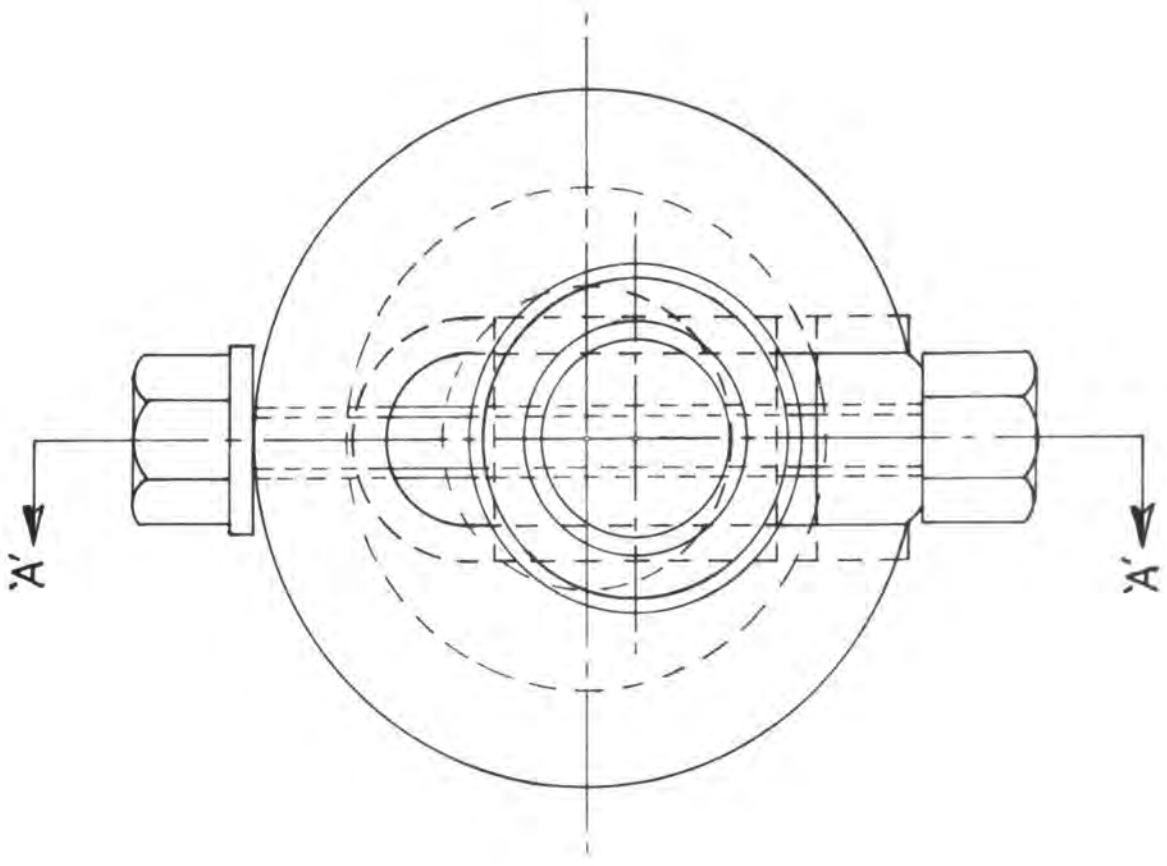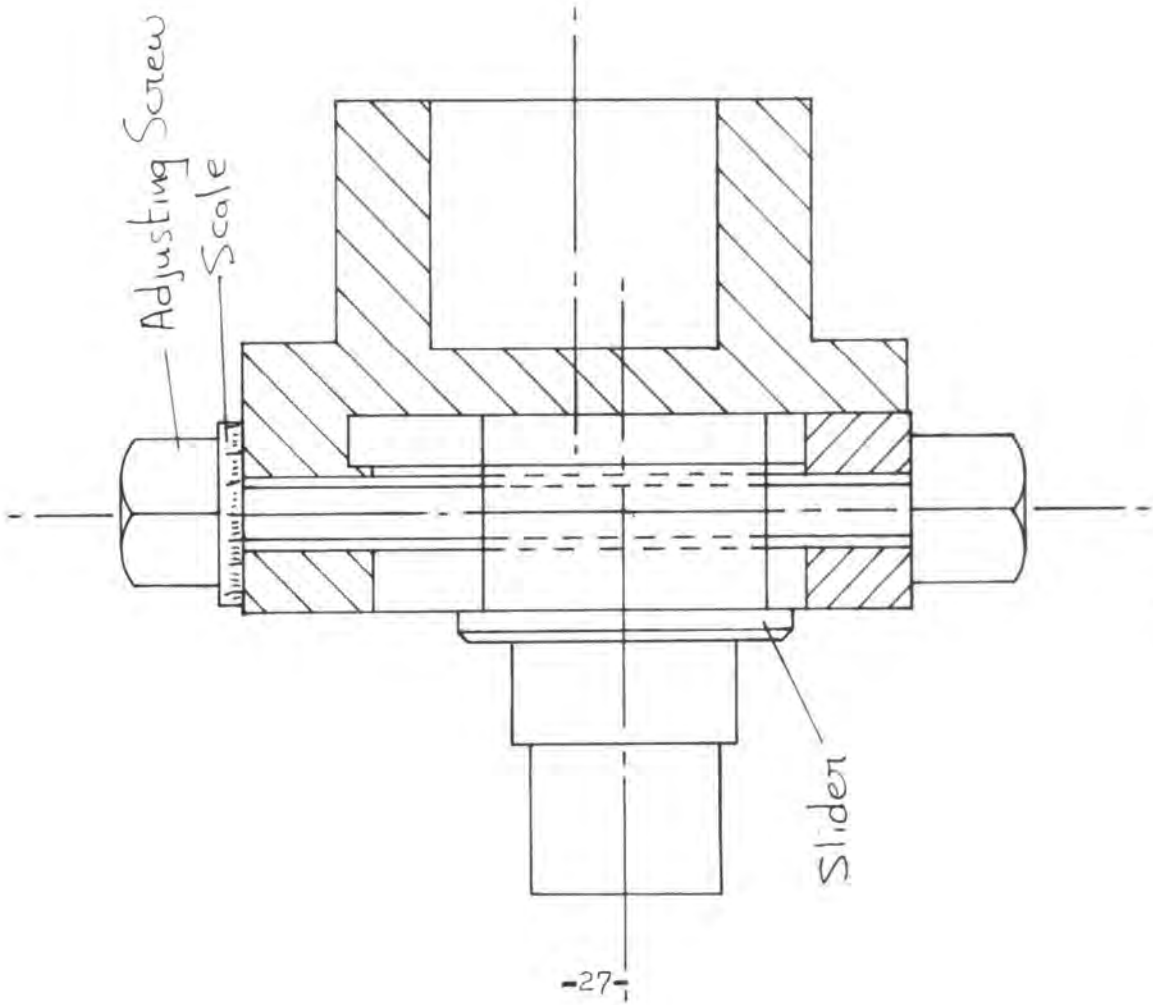
Fig. 2.3-4 shows a section through the cam. The slider was suitably shaped to run smoothly in a T section groove machined across a diameter of the holder. The screw adjuster, which passed through the holder along the groove was made to operate on the slider through a threaded hole machined in the T section of the slider. A locking screw was employed in the cam holder to screw the slider in position during cam operation. The projecting shaft of the slider imparted motion to the connecting arm via a Hoffman 0325 double roller self aligning ball journal bearing. The cam holders were counterbored to fit the overhanging ends of the drive-shaft, and locked by three screws.

2.4 Steam Generating System

All the experiments were carried out at a constant steam gauge pressure of six bars. The steam was supplied by a Clayton oil-fired steam generator model RO G-110. The system incorporated a steam accumulator which served as a steam separator as well as a liquid storage for the system. The steam from the boiler was supplied at a constant gauge pressure of ten bars and then passed through a diaphragm operated contol valve set at a gauge pressure of six bars. At this working pressure the measured temperature in the condenser corresponded to that of dry saturated steam. The remaining uncondensed steam together with the condensate was drained off to an auxillary condenser where it was totally condensed and passed to the main drain.

2.5 Cooling Water System

The condenser cooling water was obtained from a main reservoir

situated about thirteen meters above the experimental rig and it was passed through a flowmeter at the inlet to the condenser (Fig 2.A).

A flexible polythene tube was used to make the inlet and outlet connections to the condenser tube thus giving it freedom of movement.

During one stage of the experimental work, a range of inlet cooling water temperatures was required and this was achieved by connecting a line between the auxiliary condenser cooling water outlet and the test condenser cooling water passing to the flow meter. The desired cooling water temperature was obtained by adjusting the amount of cooling water introduced from the auxiliary condenser. The total flowrate of cooling water passing through the test section was controlled by valves placed on each of its sides. These valves were adjusted to maintain a high water pressure to obviate cavitation (see chapter 3).

2.6 MEASURING INSTRUMENTS

2.6-1 Condenser Tube Temperature

2.6-1A Introduction

In heat transfer investigations, one of the most critical measurements is that of the temperature of the wall separating the heated and cooled fluids, surface temperature being of particular interest.

In the process of condensation of steam on horizontal tubes, the condensate film thickness varies around the tube (Nusselt (18)). This means that the local temperature of the film, and, hence of the tube, will vary at any point around the tube. Nusselt assumed a constant tube outside wall surface temperature for his theoretical

consideration. Bromley . et.al. (23) have reported experimental

and theoretical investigations of the temperature distribution around a

condenser tube. For their experimental part, a stainless steel condenser

tube was used as the test section. The tube was enclosed in a 7.6×10^{-2}

m diameter glass jacket and revolved mechanically at the rate of one

revolution per fifteen minutes. Four thermocouples were installed at

regular intervals around the tube circumference. N-butyl alcohol vapour was

condensed on the outer surface of the tube, and water was used as the

cooling medium. The experimental data revealed a pronounced

variation of the tube local wall temperature with respect to the angular

position of the tube. The difference in temperature between the top and

bottom surfaces of the tube was of the order of $11^{\circ}C$ at water inlet and

outlet temperatures of $19.7^{\circ}C$ and $24.4^{\circ}C$ respectively. However the

authors theoretical data showed that errors introduced by using Nusselt's

equation (based on constant wall temperature) for calculating the heat

flow across the condenser tube, were negligible.

It was thus concluded that a number of thermocouples would

have to be mounted on the condenser wall in order to obtain a reasonable

accuracy of average wall surface temperature in the order of $\mp 1^{\circ}C$. The

disadvantage of this method was that the sensors would interfere with

the condensation process, and further more the vibration of the test

section might cause the sensors to break away from the surface. In

addition, the insertion of thermocouples in holes or grooves under these

circumstances would considerably weaken the test piece and disturb the

surface conditions.

It was decided that the use of thermocouples for this
measurement would present considerable difficulties, and therefore
attention was turned to an electrical method whereby the condensate tube
itself is used as a resistance thermometer. The tube surface temperature
is derived from the mean tube temperature and the corresponding heat
flux to the cooling water.

2.6-1B Constant Current Supply

The basic principle underlying the measurement of the mean
condenser temperature was to pass a constant electrical current from a
stable supply through the condenser tube and measure the voltage drop
along the test section.

Watson.et.al. (24) used an A.C bridge circuit incorporating
an inductive voltage divider for measuring the variation in tube
resistance with respect to temperature. A similar procedure was used
by Dent (20) who employed a Kelvin double bridge D.C. circuit. The
disadvantage of this method is that the accuracy is dependent on the
stability of standard resistors in the circuit and on the accuracy of the
bridge balance. The circuits are also subject to stray thermal emf's
although these can be eliminated by reversing the polarity of the tube
connections and repeating the reading. It should be noted that these
measurements do not display instantaneous temperature variations and
this could be a disadvantage if a record of the signal is required.

The constant current supply employed for the work is based on
the 'Howland' current generator with a triple output stage capable of
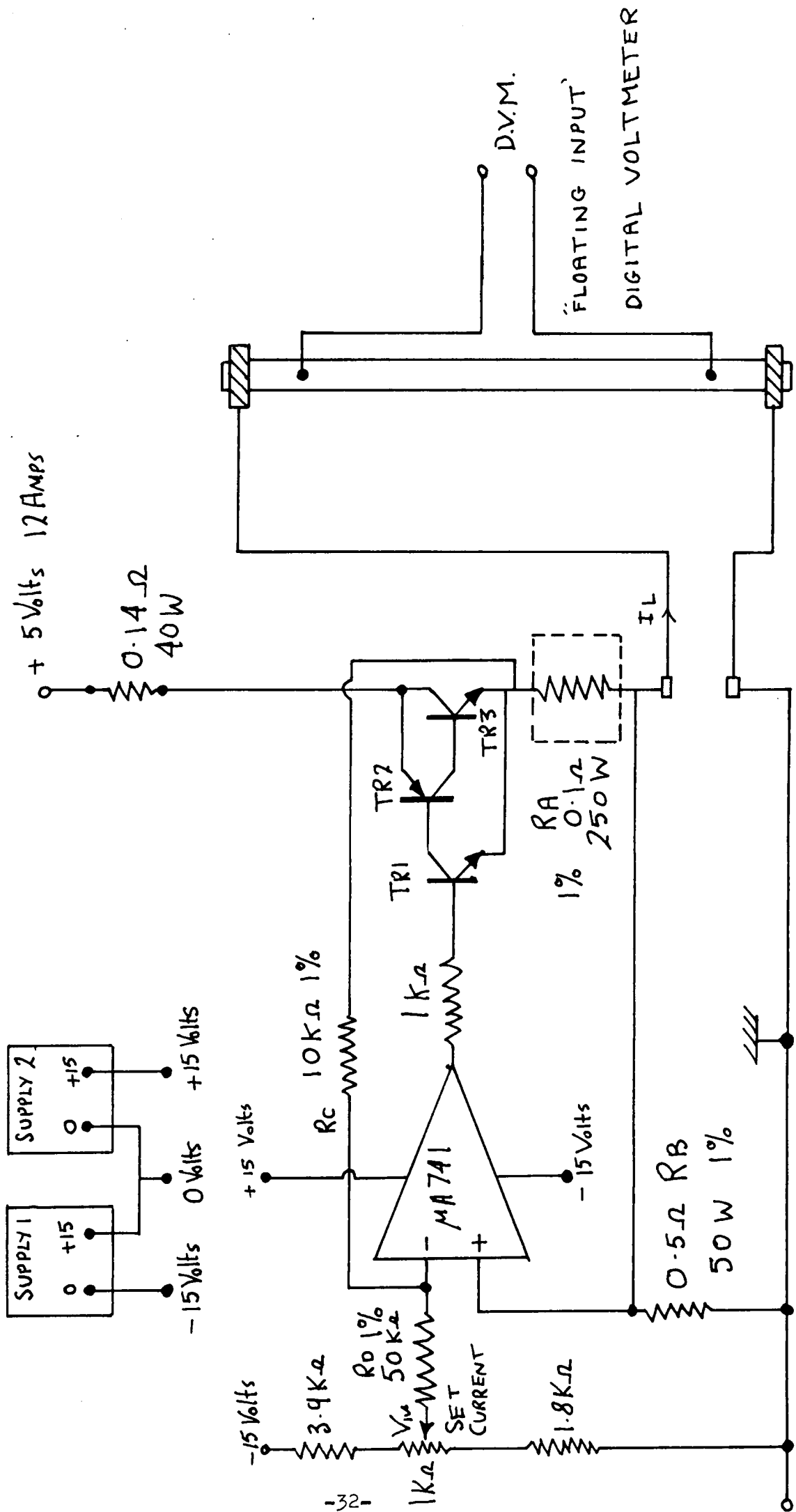
Fig 2.6-181

10 AMP CONSTANT CURRENT SUPPLY.

-32-

controlling currents up to 15 amps to within $\mp$ 0.1 Amp (see Fig. 2.6 -

1B for the circuit diagram). The current through the load resistor (the

condenser tube) is given by:-

$$IL = \frac{Vin}{RB}$$

and $$\frac{RC}{RD} = \frac{RA}{RB}$$ (Matched resistors)

where   IL: Load current

RD: CGS HSA 50 power resistor

RA: 5 CGS HSA 50 power resistors

Vin: reference voltage.

The resistors RA and RB are of the low temperature wire-wound type,

mounted on large heat sinks. All the circuit parts were mounted on a

'Tufnol' plate which was enclosed inside a steel box (Fig.2.6-1B2).

A fan was used to carry heat away from the sinks to eliminate damage to

the heated parts of the circuit.

2.6 - 1C Electrical Couplings to Tube

The constant current was applied to the tube via large brass

clamps at each end and the voltage was measured between two points

1.019 m apart (the test section) where the wires to the voltmeter were

welded to the tube body. A standard ammeter was connected in series

with the load to check that the current was constant. Stainless steel

wiring was used to avoid thermo-electric emf's at the junctions.

2.6 - 1D Sensitivity of Tube Temperature Measurement

The material and dimensions of the tube are important factors

in choosing the tube to perform as a resistance thermometer. The tube resistance between electrodes.

$$R = \frac{\rho L}{A} \quad \text{ohms} \quad (2.2)$$

where ρ: Specific resistance of tube material $\Omega.m$

     L: Length between electrodes   m

     A: Cross-sectional area of tube m^2

If a current I amp is applied through the tube, then the voltage drop,

$$V = IR$$

or $V = \frac{I \rho L}{A} \quad \text{volts} \quad (2.3)$

If α $c^{o\,-1}$ is the temperature coefficient of resistance of the material, the sensitivity of voltage variation with respect to temperature change

$$S = \frac{I \rho L \alpha}{A} \quad V/C^o \quad (2.4)$$

From this relation and the electrical properties of metals, taken from Kaye and Laby (25) it was found that stainless steel has a higher sensitivity compared with other metals. It also has superior structural properties, and it was therefore decided that stainless steel was a practical choice for the tube material.

From equation 2.4 the sensitivity of the test section of the tube was calculated, using the following values based on the mean composition of the stainless steel tube elements and its physical dimensions:

     α : $0.001 \; {}^oC^{-1}$

     ρ : $78 \times 10^{-8} \; \Omega.m$

     L : 1.019 m

     A : $2.39 \times 10^{-4} \; m^2$

From equation 2.2

$$R = 3.33 \times 10^{-3} \text{ ohm}$$

If a constant current of 10 amps is applied to the tube, the voltage drop

$$V = IR$$

$$= 33.3 \text{ mv}$$

and from equation 2.4

$$S = 33.3 \ \mu v/^\circ C$$

Using a digital voltmeter with a sensitivity multiplier of (x4) this gives a value for S of 95.6 $\mu v/^\circ C$. The actual sensitivity obtained from the test apparatus is found from calibration to be about twice this value.

2.6 - 1E Self Heating Effect of Condenser Tube

For a constant current (I) of 10 amps flowing through the tube, the heating effect is $I^2 R$ where the tube resistance is approximately 3.33×10^{-3} ohms, hence the heating effect is 0.333 watt. From the experimental results, the heat transfer rate ($\dot{Q}$) due to condensation is of the order of 20 KW and thus the heating effect due to the electrical current represents .0013 per cent of ($\dot{Q}$). It is therefore reasonable to neglect this effect in these experiments.

2.7 Steam Temperature and Pressure

The temperature of steam was measured in the vicinity of the condenser tube by means of three pyrotenax cr/Al thermocouples having an accuracy of ∓ 0.5 per cent. These thermocouples were mounted
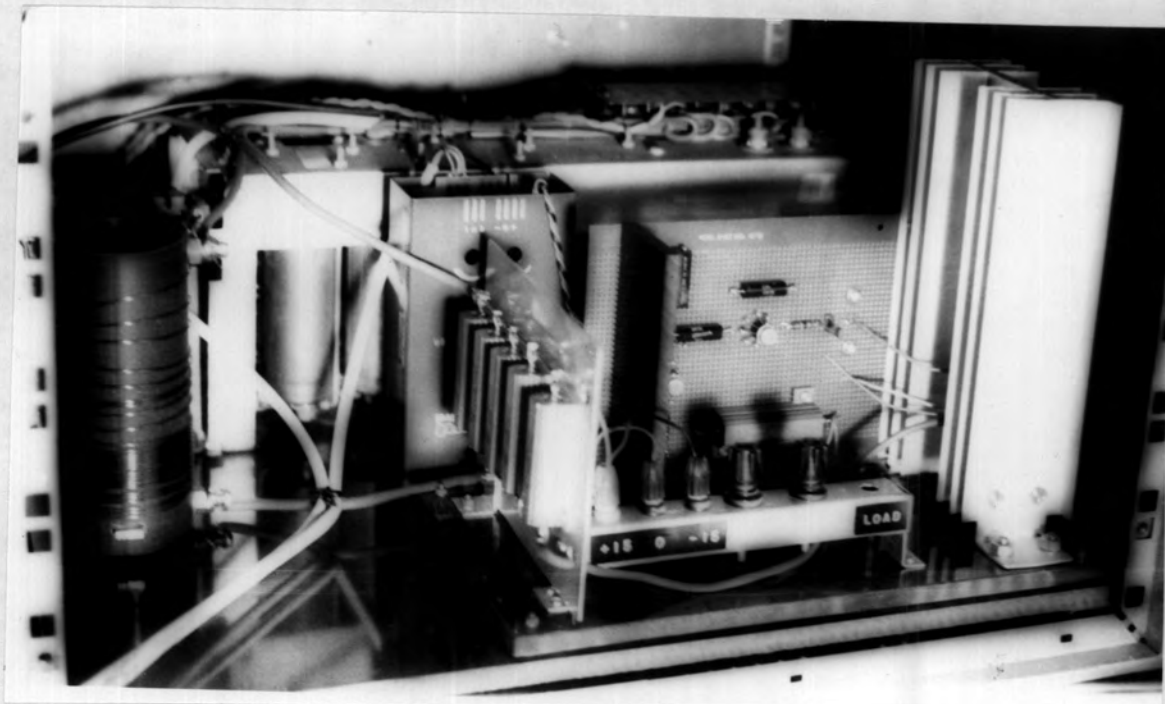
Fig 2.6-IB2   The constant current transistorized circuit
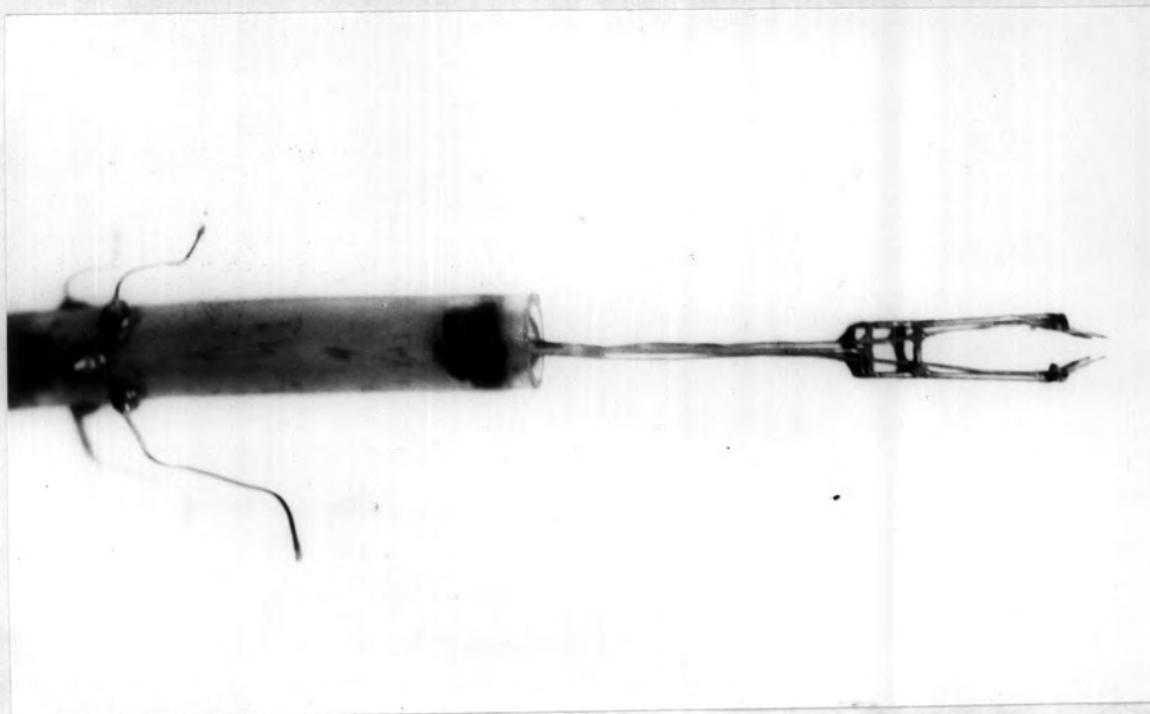
Fig 2.8   The cooling water thermocouples and holder

in different positions in the upper half of the pressure vessel, and their

output terminals were joined to a selector switch connected to an

electric thermometer (Comark type 1601) having an accuracy of

$\mp 2^{\circ}$C over a range of 0 - 300°C. A mercury-in-glass thermometor was

also mounted inside the vessel behind one of the glass windows to

check the temperature in this vicinity. The steam pressure in the

condenser vessel was measured by a Budenberg standard test gauge with

accuracy of ∓ 0.25 per cent.

2.8 Cooling Water Temperature Measurement

The cooling water inlet and outlet temperatures were each

measured with a pair of cu/con thermocouples enclosed in a stainless

steel sheath. Each thermocouple was prepared and spot welded

according to the method of Link (26). Finally it was covered with a thin

layer of 'Araldite' resin to prevent corrosion and breaking down of

insulation due to the ingress of water. The thermocouples were tested

for electrical insulation from the sheath and for temperature response

before installation. A pair of thermocouples were mounted on each

of two stainless steel forks (Fig. 2.8) constructed to support the

thermocouples rigidly inside the condenser tube. The length of each fork

was carefully chosen so that when the termocouples were inserted inside

the condenser, they were exactly positioned at the inlet and outlet

of the test section of the condenser (coinciding with the positions of the

condenser voltage tappings). The supports were fixed to the polythene tube

by means of brass screws soft welded to the ends of the fork. The

thermocouple leads were taken out of the water line through hollow brass screws secured to the tube wall. 'Araldite' resin was used to seal the holes in these screws. The thermocouple leads were connected to a Comark multi-channel selector unit type 1697. A single cold junction was used in the circuit, consisting of cu/con thermocouple positioned in a Zeref ice-point reference chamber. The system maintained a water/ice mixture at atmospheric pressure giving a convenient ice point reference to within $\mp 0.2^{\circ}C$ with great stability over a wide range of ambient temperatures. The voltage output from the thermocouples was accurately measured by a Solartron digital voltmeter type LM 1420.2. Voltmeter sensitivity (X4) was used during experiments to improve accuracy.

2.9 Tube Frequency

Accurate measurement of tube frequency was obtained by a digital frequency counter type Advance TC 11A. The signal source was obtained from an electro-magnetic transducer in co-operation with a slotted steel disc. Six slots were machined at equal intervals round the disc rim. The disc was mounted on the condenser drive shaft, and the transducer was placed radially with respect to the axis of the disc. (Fig.2-9A). As the shaft rotated, an electric pulse was generated each time after a slot passed the magnetic pick-up (Fig. 2.9B). Thus for one shaft rotation, six consistent signals were generated. These signals were fed to the counter which was adjusted to count over a period of ten seconds, thus displaying a shaft frequency of cycles per minute.

Fig 2.9A   magnetic pick-up
and slotted disc
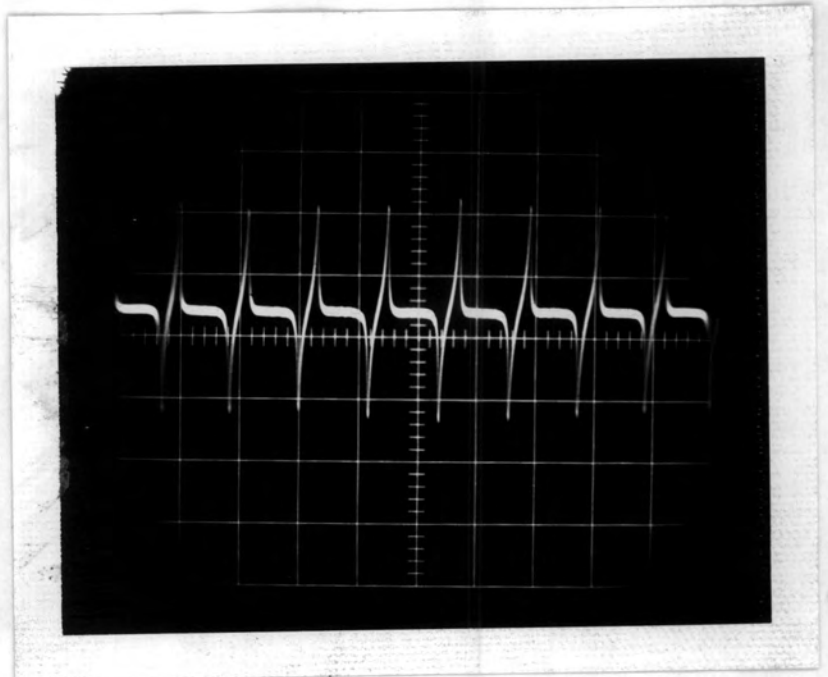
Fig 2.9B   signal disply
from pick-up and disc

Owing to the mechanical construction of the vibration system, the drive shaft frequencies give direct measure of condenser frequencies.

2.10 Instruments Calibrations

2.10-1 Thermocouples Calibration

The cooling water thermocouples were individually calibrated against a standard mercury-in-glass thermometer having an accuracy of $\mp 0.5^{\circ}C$. Water was brought to boiling point, and the individual thermocouple hot junctions and the thermometer were inserted near the centre of the water bath. The water was allowed to cool to room temperature during which period successive readings of thermocouple emf's and corresponding thermometer temperatures were recorded. The calibration curves obtained for the thermocouples were found to correspond with those given in standard tables for cu/con thermocouples to within $\mp 0.5^{\circ}C$. The accuracy of the thermometer used for measuring the steam temperature was checked by similar procedure.

2.10-2 Tube Temperature Calibration

The condenser wall temperature was calibrated by heating the tube inside the pressure vessel, and was then allowed to cool down over a long period of time (8 hours). The pressure vessel heating elements were utilized as the heat source. Initially they were re-wrapped round the vessel in successive stages. After each stage the vessel was heated over a period of 16 hours, and the temperatures inside the vessel at the middle and extremes were observed. By means of trial and error, a stage

Tube Temperature Calibration Graph

Fig 2.16-2

Voltage Drop mV

Mean Tube Temperature °C

-41-
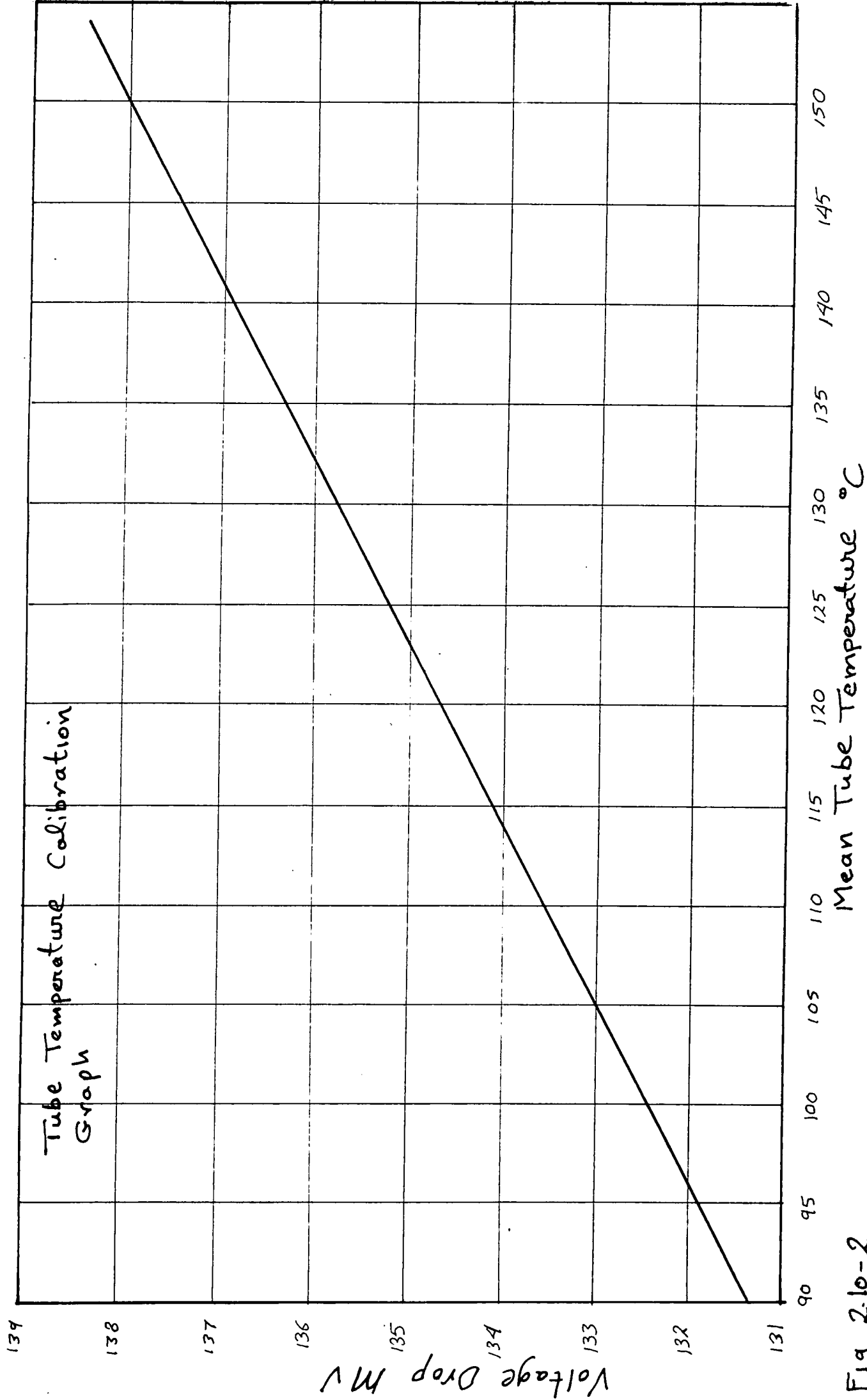
was reached where a constant temperature within $\overline{+}1^{\circ}$C was maintained inside the vessel.

Prior to calibration, the tube ends and the vessel windows were lagged in order to maintain a constant temperature along the test section. The tube was then heated to a temperature of 180°C and maintained at this temperature for a period of 10 hours to attain steady state conditions. The inside surface wall temperature of the condenser, was checked by a thermocouple traversed along the tube to ensure that the temperature on both sides of the wall and along the tube was constant when taking calibration readings. The tube was allowed to cool down to room temperature. During this period, the tube temperature and voltage drop along the test section were recorded. Because of the good thermal insulation, the calibration period lasted about 8 hours. A number of calibration points (about 10) were further obtained by this method, simply by altering the initial set temperature of the apparatus. The tube resistance was checked regularly during experiments to detect any drift but was found to be extremely consistant. The calibration curve is shown in fig. 2.10-2

2.10-3 Tube Amplitude

Under working conditions, the condenser tube flexed as expected. The magnitude of flexure increased with the frequency of vibration as the tube approached its natural frequency of vibration (about 2600 cpm). This necessitated measurement of dynamic amplitude which was calibrated with respect to the static amplitude and to tube frequency. A travelling microscope was positioned level with the condenser tube which was focussed

on the top of the tube when at its highest position : the tube was then brought

down to its lowest position by manually turning the drive shaft, and the

total vertical displacement was measured on the microscope vernier scale.

The dynamic tube displacements were similarly measured at a range of set

frequencies from 0 - 2,000 c.p.m.

For all experimental calculations, half the average peak-to-peak

amplitudes were considered. The mean dynamic amplitude over the length

of the test section, was found to be equal to the static amplitude, plus $2/\pi$

times the increase over the static amplitude, as follows:
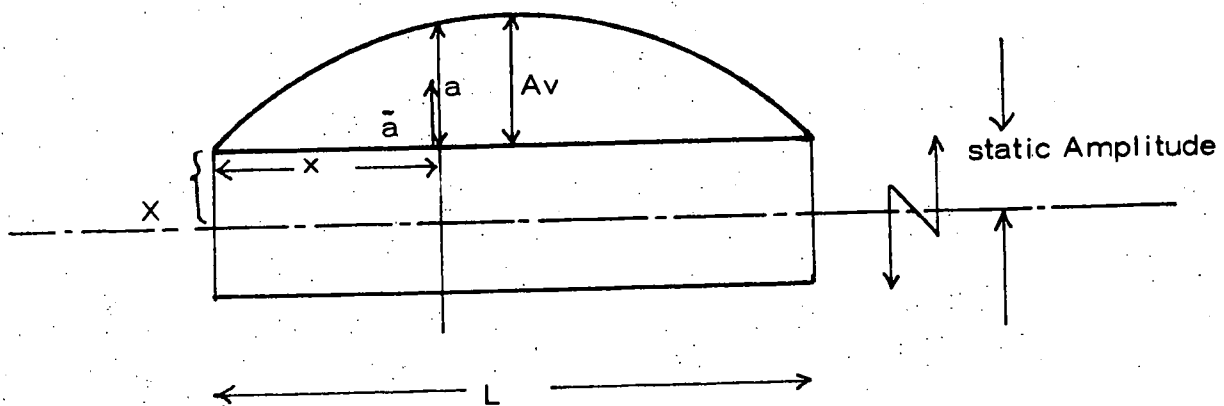
Fig. 2. 10-3

For the deflection of the tube, due to vibration (see Fig. 2. 10-3);

$$\bar{a} = a \sin wt \qquad (2.10 -1)$$

$$a = Av \sin \pi \frac{x}{L} \qquad (2.10 -2)$$

Av: maximum deflection
a : Maximum deflection at x

The mean deflection of the tube over the length L is

$$\bar{A} = \frac{Av}{L} \int_{0}^{L} \sin \pi \cdot \frac{x}{L} \, dx \qquad (2.10 -3)$$

$$= 2 \frac{Av}{\pi}$$

The mean dynamic amplitude $= \bar{A}$
$$= \text{static amplitude} + \frac{2}{\pi} \; Av.$$

-43-

2.11 Promotion of Film Condensation

Condensation of vapours on a metal surface can occur in two forms; dropwise and filmwise condensations. The mechanisum or the rate of heat transfer associated with film condensation is quite different from that associated with dropwise condensation. For practical reasons (see chapter 4) film condensation was employed during all experimental work. Before each run, the condenser surface was prepared according to the method of Drew (27) to give satisfactory film condensation over a prolonged period of time. The metal surface was initially cleaned and washed with water and then scoured with very fine emery paper. This was followed by thorough washing with Decon 75 degreasing agent. Then it was rinsed and rubbed with powdered magnesium and finally, thoroughly rinsed with water. This treatment was found to promote a very satisfactory film for at least 24 hours of condensation.

2.12 Experimental Test Procedure and Measurements

Prior to each experimental run, the pressure vessel was heated to a temperature of $2^{o}C$ above the steam saturation temperature, thus avoiding condensation of steam on the vessel inner wall. This insured that a steam dry saturation temperature was maintained inside the vessel. The cooling water was set to flow at a constant rate. The steam control valve was adjusted to give a pressure of 6 bars, at which pressure, the steam was introduced to the vessel, dry saturated. This could be observed from the steam pressure and temperature inside the vessel. Between each change of experimental conditions, a period of

fifteen minutes was allowed to pass before taking readings so that the whole apparatus could attain a steady state.

2.13 Source of Experimental Errors

The validity of the experimental measurements for establishing

the physical nature of the process under consideration, is largely

dependent on the accuracy of prediction of the experimental

uncertainties associated with various experimental measurements. These

uncertainties may be introduced due to the performance of the

measuring instrument or due to the random nature of the measured quantity.

The individual measurements are combined to give a particular result which

is of main interest. It is of importance to assess the uncertainty in

the final result due to uncertainties in the primary measurements which

are in this case:-

      i. – Cooling temperature
     ii. – Steam temperature and pressure
    iii. – Condenser wall temperature
     iv. – Condenser surface area
      v. – Condenser amplitude and frequency of vibration.

The cooling water inlet and outlet temperatures were measured to within

$\mp 0.5^{\circ}C$. The error was mainly caused by fluctuations of the water

local temperature due to the eddy mixing of the thermal fluid layers.

Consequently judgement of the temperature depended on average observed

values. The steam temperature measurement was within $\mp 3^{\circ}C$ and

since a standard calibration pressure gauge was used, errors in

indication of steam pressure were very small. The condenser wall

temperature was observed to be quite stable when experimental steady

states are maintained. The accuracy of wall temperature indication was mainly dependent on the performance of the constant current circuit, and was in the order of (0.5 - 1°C). The condenser frequency was very accurately indicated by the digital counter and the error did not exceed $\mp$ 5 counts for typical experimental frequencies. The errors involved in measuring tube amplitude were very small since a precision instrument was used for this purpose.

The overall error in the measurement of the condensation heat transfer coefficient, was in the order of (5 - 8)%. This is a typical value associated with such experiments.

3. CAVITATION

General

In studying the effects of vibration on condensation heat transfer, it is of major importance to investigate and eliminate the problems that may affect the heat transfer process. Some problems concerning the condensation process have been dealt with in the previous chapter. It is of equal importance to consider the problems associated with the cooling fluid since the performance of the fluid is directly related to the transfer process.

The risk of formation of air cavities in the cooling liquid when subjected to severe vibrational intensities is the prime concern. Liquids have a very small coefficient of compressibility and quite large changes of pressure are accompanied by small changes in the specific volume of the liquid. A liquid which has not been specially treated cannot withstand tensile stresses, and tends to form cavities which then expand to relieve the negative pressure. This phenomenon is believed to be associated with tiny pockets of undissolved gas (usually air saturated with vapour) in the liquid. The inward force at the boundary of small spherical bubbles due to surface tension, is too strong to be balanced by the vapour pressure, and gas subjected to this pressure will quickly pass into solution in the liquid. When the liquid is displaced, the tensile stresses within the cavitated portion drop, and the cavities collapse violently.

Cavitations were originally observed while testing ships propellers, when the practical significance of this effect was studied and it was found that the drag of submerged bodies moving through a liquid,

rises when cavitation appears. Consequently the efficiency of pumps turbines and propellers drop with the development of cavitation. Furthermore significant damage is imparted to such components if cavitation is prolonged.

Plesset (28) studied the cavitation phenomenon of liquid flow over a submerged body. He defined three liquid flow regimes; non cavitating flow, cavitating flow with relatively small number of cavitation bubbles and a cavitating flow with a large single cavity about the body. His main consideration was to derive the equation of motion for the second mode of flow. He assumed that the pressure coefficient in the flow field is the same as that for non-cavitating flow, and then applied this to analysis of experimental observations made in a high speed water tunnel. Sutton (29) carried further investigations to find the effect of transient strain waves caused by cavitation, by employing an Ultra-high-speed photographic technique and he reported that the stresses due to cavitation could be as high as 1.38×10^8 N/m^2.

3.1 Formation of Wakes and Cavities

When a body which is not particularly stream-lined moves through a fluid with high enough velocity, the flow separates from the body surface thus forming a wake region or a vapour-gas cavity in the interior of the displaced fluid. The formation of cavitation arises from the effect of pressure differential forming within the liquid mass. The motion of the body in the fluid gives rise to a reduced pressure ($\bar{P}r.$) in the fluid, when ($\bar{P}r$) is decreased to a value below the vapour pressure

($\bar{P}v$), vapour bubbles suddenly form and their existence is prolonged

until ($\bar{P}r$) rises to a value above ($\bar{P}v$) at some stage in the process,

when the vapour condenses causing the cavities to collapse.

The formation of water cavitation is more pronounced with the

greater amount of gases dissolved in the water. However, if the water

is airfree, it can withstand higher tensile stresses and a pressure

below the vapour pressure, without the formation of cavities. Changing

conditions of pressure velocity and temperature to values favourable

for enhancing vaporization rates, will cause cavitation growth.

3.2 Types of Cavitations

The cavitation phenomena may be classified into four main

groups

1. Travelling cavitation

2. Fixed cavitation

3. Vortex cavitation

4. Vibrating cavitation

With travelling cavitation, individual transient bubbles form and

expand in the liquid and move with it, then they shrink and collapse.

The movement of such cavities is the distinguishing factor from other

transient cavities. They may be observed at the low-pressure points along

a solid boundary or in a high turbulence region in a turbulent shear field.

Fixed cavitation is identified by a liquid flow which detaches

itself from a rigid immersed body or a flow passage forming a cavity

attached to the solid boundary. This may have the appearance of a highly

turbulent boiling surface.

Vortex cavities have the charecteristics of slow rates of collapse and occur in the cores of vortices which form in zones of high shear. They can be clearly observed on the tips of propellers and may take the form of travelling or fixed cavities, vortex cavities can also form in the wake caused by the boundary-layer separation from some objects (e.g. a sphere) immersed in the liquid flow. In this case, vortex cavities may be identified from travelling cavities, in that the cavitation occurs on the surface of the separation zone but not on or adjacent to the immersed body.

Vibrating cavitation is the main type concerning this work. It has a major feature, in that a given element of liquid is exposed to many cycles of cavitation (in the time order of few milliseconds) while in the alternative types of cavitations described above, the liquid element passes through the cavitation stage only once. For a vibrating cavitation forming in a fluid continuously flowing through a transversly vibrating tube, the forces that cause cavities to form and collapse, are due to high-frequency high-amplitude tube vibrations which cause severe pressure pulsation in the liquid. Cavities are formed when the magnitude of the varying liquid pressure drops to a value below or equal to the vapour pressure.

3.3 Effect of Cavitation on Heat Transfer

When cavities which contain appreciable amount of gas collapse, the gas temperature at the end of collapse is very high, since the time for

collapse is so small that there is not sufficient time for cooling by a surrounding liquid. The collapse of cavities near a metallic surface may raise its temperature to a significant level. Since the heat transfer coefficient between the solid and the liquid increases with increased temperature differences between the solid and the main body of the liquid, the presence of cavitation in a transfer system will cause considerable experimental and theoretical errors when predicting the values of heat transfer coefficients. The errors are further exaggerated by the fact that some cavitations tend to decrease the area of the transfer surface in contact with the liquid. The liquid gains heat much more rapidly than the vapour owing to its higher thermal conductivity, and this tends to decrease the heat transfer rate.

In general when heat transfer coefficients are to be measured, cavity formation should be avoided in order to improve experimental accuracy.

3.4 Calculation for the Risk of Cavitation in Condenser Cooling Water.

The main factors that affect the initiation and growth of cavities in a flowing liquid are, the flow pressure, the velocity of the liquid, the boundary geometry and the critical pressure at which cavities are formed. Other factors include the various properties of the liquid, such as viscosity, surface tension and vaporization characteristics. It is extremely difficult to include all these factors in developing cavitation parameters, but the usual practice is to consider the basic parameters, and then the effect of secondary variables may be indicated as a deviation from the predicted

basic parameters.

In considering water flowing through a transversley vibrating tube, the primary experimental concern is directed toward the variation in pressure across the water path. This has a value $(\bar{P}_L)$ at some point in the liquid stream and $(\bar{P}w)$ at the tube wall. Vapour will suddenly form when $(\bar{P}w)$ is reduced below the vapour pressure of the cavities.

Prandtl (45) gave the following relation as a measure of the risk of cavitation:

$$\lambda = \frac{(\bar{P}_L - \bar{P}\bar{w})}{\frac{1}{2} \cdot \rho \cdot v^2}$$

(3.4)

where λ is a non-dimensional cavitation factor and V is the liquid velocity in the direction of oscillations.

At a particular value of tube frequency (W) and using the maximum amplitude of vibration (0.015 m) employed during experimental tests, the risk for presence of cavitation in the cooling water flowing inside the test peice may be found as follows; it is assumed that air will come out of solution when $(\bar{P}\bar{w})$ is reduced to atmpspheric pressure (this is the least possible value at which cavitation could develop) i.e. when $(\bar{P}_L - \bar{P}\bar{w})$ is equal to the available head of water. Prandtl (45) illustrated a cavitation diagram for his experiment on a vibrating isolated blade profile, immersed in a water tank. It is considered that the characteristics of the cavitation process for a vibrating blade are similar to those for a vibrating tube. Therefore, the largest cavitation factor ($\lambda = 1.0$) for the blade given by Prandtl diagram was used in equation (3.4) to predict the least possibility for cavitation to form in

-52-

the water path.

From equation (3.4):-

$$V^2 = \frac{2(\bar{P}L - \bar{P}w)}{\lambda \cdot \rho}$$

$\bar{P}L - \bar{P}w \ : \ N/M^2$

$\rho \ : \ Kg/M^3$

Where $V = AW$

Head = 13 metres.

Therefore ,

$$W^2 = \frac{2 \times 1.3 \times 10^4 \times 9.81}{1000 \times (1.5)^2 \times 10^{-4}}$$

$W = 1030 \quad rad/sec$

$W = 9840 \quad cpm$

This demonstrates for the experimental environments that cavitations do not develop below a frequency of about 10,000 cpm. This is well above the maximum frequency used (2,000 cpm) in the experimental programme and the risk of such effect was therefore not possible.

4. CONDENSATION ON STATIONARY SURFACE

4.1 Filmwise and Dropwise Condensation

When saturated vapour comes in contact with a surface whose temperature is lower than the saturation vapour temperature, liquid condensate forms on the surface. The condensate thus formed will be subcooled to some extent from being in contact with the cooled surface, and the process of condensation will proceed as long as the surface temperature is lower than the saturation temperature. If the liquid condensate wets the surface, it spreads out and forms a stable film. This process is termed filmwise condensation. When the condensate film has established itself on the surface, the vapour condenses on the liquid at the interface and the heat is transferred to the surface through the liquid film. Film condensation can be promoted by using clean steam condensing on a clean surface or on a surface contaminated with a non-wetting agent. The vapour condenses in the form of very tiny drops that grow in size, adhere to each other and then roll down the surface under the influence of gravitational force. This process is termed dropwise condensation and its significant feature is that a large part of the condensing surface is not covered by a condensate film. As a result, the heat transfer coefficients associated with this process can be more than five fold greater than those of film condensation. This was demonstrated by McAdams (22) and Shea et al (30).

Dropwise condensation can only be maintained under carefully

controlled conditions. In practice, filmwise condensation is predominant and it could be more advantageous to expand the knowledge of film condensation in order to improve the efficiency of the process for use in different applications.

Filmwise condensation was solely employed for the work presented in this report.

4.2 Nusselts Theory of Filmwise Condensation on Horizontal Tubes.

Nusselt in 1916, developed an equation for calculating the heat transfer coefficient of pure saturated vapour condensing on a cold clean surface. This theory was based on the following assumptions:-

i. the vapour condenses in the form of continuous film flowing in a laminar form down the tube, due to the effect of gravity.

ii. the temperature difference between the vapour and cooling surface is constant.

iii. the effects on the condensate film thickness caused by the vapour velocity are neglected.

iv. the heat given up by the vapour is the latent heat and it is transferred through the film purely by conduction.

v. the temperature gradient through the film is linear.

In deriving the theory, Nusselt considered small element of condensate film on the surface of a tube of outside diameter $D\bar{o}$, situated at an angle $\emptyset$ to the horizontal plane and moving downward round the tube with a local speed (V) tangential to the tube surface and at a distance (y) from the surface (Fig. 4.2 - 1). The shear stress occuring in the liquid element at (X) can be expressed by:-
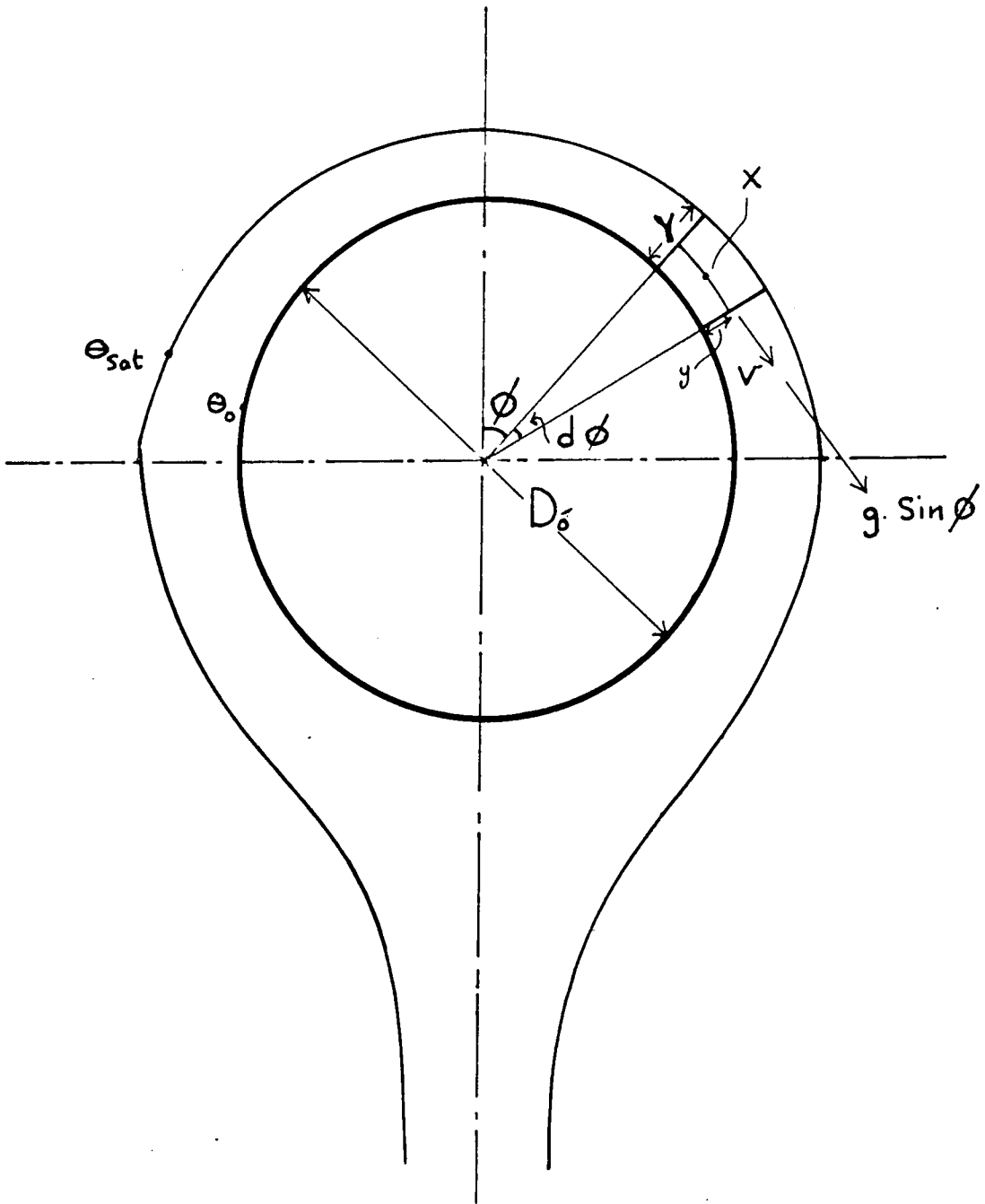
Fig 4.2-1

$$\Upsilon = \int_c^{\mu} \frac{dv}{dy}$$

$$(4.2 - 1)$$

The equation of mechanical equilibrium for an element of film between

(y) and (y + dy) of unit length gives:-

$$\left(\frac{D\bar{o}}{2} + y\right) d\emptyset.d\,\Upsilon = - \varrho.g\sin\emptyset.dy.\left(\frac{D\bar{o}}{2} + y\right) d\emptyset$$

$$\frac{d\Upsilon}{dy} = - \varrho.g\sin\emptyset$$

$$(4.2 - 2)$$

Equating equations 4.2 - 1 and 4.2 - 2 gives:-

$$\frac{d^2 v}{dy^2} = - \frac{\varrho.g.\sin\emptyset}{\int_c^{\mu}}$$

$$(4.2 - 3)$$

By integration:

$$V = \frac{-\varrho.g\,\sin\emptyset}{2.\int_c^{\mu}}\, y^2 + C_1 y + C_2$$

$$(4.2. - 4)$$

From Nusselts assumption, the vapour is virtually at rest, no sensible

friction occurs at the vapour-liquid interface, and the liquid adheres to the

tube wall.

Hence the boundary conditions are:-

$$\left[\frac{dV}{dy}\right]_{y = Y} = 0$$

$$V = 0 \quad \text{at} \quad y = 0$$

Applying these conditions to equation 4.2 - 4 gives:-

$$V = - \frac{\varrho.g\,\sin\emptyset}{\int_c^{\mu}}\, (y^2 - 2\,y.Y)$$

$$(4.2 - 5)$$

This expression shows that the velocity distribution across the film is

parabolic. The mean velocity of the liquid film is:-

$$V_m = \frac{1}{Y} \int_o^Y V \cdot dy$$

$$V_m = \frac{\rho \cdot g \cdot \sin \emptyset \cdot Y^3}{3 \cdot \mu_c} \qquad (4.2 - 6)$$

Consider one side of the tube ($\emptyset = o - \pi$); the mass flow of liquid in

the film;

$$(\frac{\dot{M}c}{2}) = Y \cdot \rho \cdot V_m \qquad (4.2 - 7)$$

$$\dot{M}c: \text{Total mass flow}$$

the heat flow due to condensation of mass $\dot{M}c$ can be expressed by;

$$\frac{\dot{Q}}{2} = \bar{h}_{fg} (\frac{\dot{M}c}{2}) \qquad (4.2 - 8)$$

Combining equations 4.2 - 6, 4.2 - 7 and 4.2 - 8 gives;

$$(\frac{\dot{Q}}{2}) = \frac{\rho^2 \cdot g \cdot \bar{h}_{fg} \cdot Y^3 \cdot \sin \emptyset}{3 \cdot \mu_c} \qquad (4.2 - 9)$$

$$d(\frac{\dot{Q}}{2}) = \frac{\rho^2 \cdot g \cdot \bar{h}_{fg} \cdot d(Y^3 \cdot \sin \emptyset)}{3 \cdot \mu_c} \qquad (4.2 - 10)$$

From Fourier's law of conduction, this amount of heat is equal to the

heat conducted through the film (curvature is neglected since it is small),

thus:-

$$\frac{(d\dot{Q})}{(2)} = \frac{K \cdot (\Theta_{sat} - \Theta_{\bar{o}})}{Y} \frac{D\dot{o}}{2} d\emptyset \qquad (4.2 - 11)$$

$$\text{let } \bar{B} = \frac{3 \cdot \mathcal{V} \cdot K \cdot D\bar{o} (\Theta_{sat} - \Theta_{\bar{o}})}{2 \cdot \rho \cdot g \cdot \bar{h}fg} \qquad (4.2 - 12)$$

Combining equations 4.2 - 12, 4.2 - 11 and 4.2 - 10 gives

$$\bar{B} \cdot d\emptyset = Y \cdot d(Y^3 \cdot \sin \emptyset) \qquad (4.2 - 13)$$

Solution to this equation gives:

$$Y = \left[\frac{4 \cdot \bar{B} \cdot \int_o^\emptyset \sin^{\frac{1}{3}} \emptyset \cdot d\emptyset}{3 \cdot \sin^{4/3} \emptyset} \right]^{\frac{1}{4}} \qquad (4.2 - 14)$$

The local heat transfer coefficient (h_{NU}) at $\emptyset$ becomes

$$h_{NU} = \frac{K}{Y} \qquad (4.2 - 15)$$

The mean heat transfer coefficient (h_{NU}) is obtained by integration over

$\emptyset = o - \pi$, thus;

$$h_{NU} = \frac{K}{\pi} \cdot \int_o^\pi \frac{d\emptyset}{Y} \qquad (4.2 - 16)$$

combining equations 4.2 - 16, 4.2.-14 and 4.2 - 12 gives;

$$h_{NU} = \overset{\llcorner}{A} \left[\frac{2 \cdot K^3 \cdot \rho \cdot g \cdot \bar{h}_{fg}}{3 \cdot \nu \cdot D\dot{o} (\Theta_{sat} - \Theta_{\bar{o}})} \right]^{0.25} \qquad (4.2 - 17)$$

where $\overset{\llcorner}{A} = \int_o^\pi \frac{\sin^{\frac{1}{3}} \emptyset \cdot d\emptyset}{\frac{4}{3} \cdot \int_o^\emptyset \sin^{\frac{1}{3}} \emptyset \cdot d\emptyset} \qquad (4.2 - 18)$

By graphical integration, Nusselt reported a value of 2.52 units for $\overset{\llcorner}{A}$.

The values for the integral at $\emptyset$ between O to π are tabulated in Jakob (31)

From equation (4.2 - 17),

$$h_{NU} = 0.72 \left[\frac{\rho \cdot g \cdot h_{fg} \cdot K^3}{\nu \cdot D\dot{o} \cdot (\Theta_{sat} - \Theta_{\bar{o}})} \right]^{0.25} \qquad (4.2 - 19)$$

The constant in Nusselts equation depends on the evaluation of the integral $\frac{4}{3} \cdot \int_o^\pi \sin^{\frac{1}{3}} \emptyset \cdot d\emptyset$. Nusselt reported a value of 3.428 at $\emptyset = \pi$.

Bromley. et. al (32) re-evaluated this integral using the gamma function

by Pierce (33) and they reported a value of 3.4495 $\mp$ 0.0002. Thus

Nusselt equation was corrected to:-

$$h_{NU} = 0.728 \left[\left(\frac{(\rho \cdot g \cdot \bar{h}_{fg} \cdot K^3}{(\nu \cdot D\bar{o} \, (\Theta_{sat} - \Theta_o)} \right) \right]^{0.25} \qquad (4.2 - 20)$$

4.3 Improved Analysis of the Condensation Process

Nusselt, in his theory of laminar film condensation, ignored

the effect of condensate subcooling below the vapour saturation temperature.

Bromley (32), working on the effect of the heat capacity of condensate,

modified Nusselt's theory of condensation on horizontal and vertical tubes.

His analysis of the condensation of vapours at high pressure and with large

temperature difference between the vapour and cooling surface, revealed that

the contribution of the sensible heat associated with subcooling, to the

heat flow, may have an appreciable magnitude in comparision with the

latent heat of vapourization. As a result, the subcooling effect could have

a significant effect on the predicted values of the heat transfer coefficient.

Nusselt derived an alternative expression to equation (4.2 - 19) in

order to account for the effect of subcooling, but his theory predicted a

decrease of heat transfer coefficient. Bromley's argument contradicted this

effect on the basis that Nusselt had made a fundamental error in writing

his enthalpy balance. Bromley's analysis was based on a linear

temperature profile across the condensate film, his correction for calculating

the heat transfer coefficient presented a multiplication factor to the right

hand side of equation (4.2 - 19). This is of the form:-

$$\left[1 + \frac{0.375 \, C_{pc} \, (\Theta_{sat} - \Theta_o)}{hfg} \right]^{0.25}$$

Rohsenow (37) varified and improved Bromley's theory by

attempting to find the correct non-linear temperature distribution in the film.

-60-

His analysis gave the following correction factor:-

$$\left[1 + \frac{0.68 c_{pc} (\Theta_{sat} - \Theta_{\bar{o}})}{\bar{h}_{fg}} \right]^{0.25}$$

For condensation of steam, the values of $\bar{h}_{fg}$ are relatively large therefore the term $\frac{c_{pc} (\Theta_{sat} - \Theta_{\bar{o}})}{\bar{h}_{fg}}$ is very small and the effect of subcooling on steam condensation is insignificant.

$$\frac{Nu_d}{0.733 \left[\frac{\varrho \cdot g \cdot \bar{h}_{fg} \cdot d^3}{k \cdot \nu \cdot (\Theta_{sat} - \Theta_{\bar{o}})} \right]^{1/4}}$$

Sparrow and Gregg's
Heat transfer results for
Laminar Condensation
on horizontal cylinders

Fig. 4.3 - 1
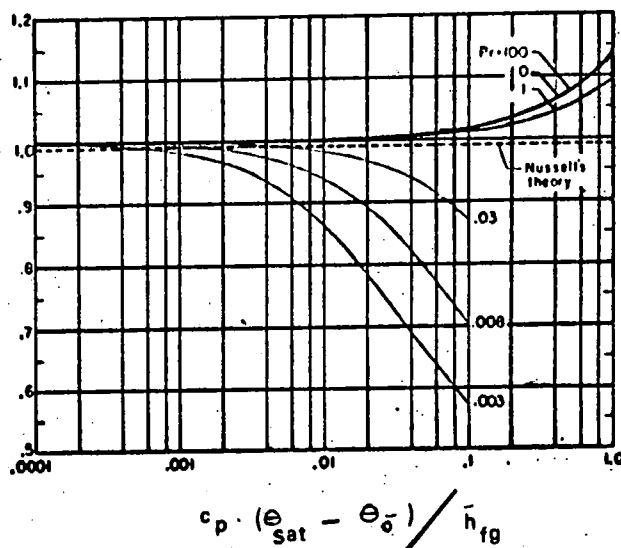
Sparrow and Gregg (38,39) applied the boundary-layer approach

to their analysis of film condensation on vertical plates and horizontal

cylinders. Inertia and convection terms in the condensate film were

considered and a zero shear stress at the interface was assumed. Solutions

were presented for condensate Pr range from 0.003 to 100. The results

are shown together with Nusselts results in fig. 4.3 - 1.

It can be seen that for values of $C_{pc} \frac{(\Theta_{sat} - \Theta_{\bar{o}})}{\bar{h}_{fg}} \leqslant 0.2$

and pr $\geqslant$ 1, there is a very close agreement between Nusselts theory and

Sparrow and Gregg's analysis (the maximum deviation is about 3 per cent).

In general, it can be shown from the preceeding discussion that for condensation of steam on horizontal tubes, the effects of inertia in the liquid film, the non-linearity of temperature distribution in the film and the subcooling effects are insignificant due to the high values of $\bar{h}_{fg}$ and Pr.

The experimental results reported in this work were carried out at $Pr = 1.16$ and $C_{p_c} \cdot (\Theta_{sat} - \Theta_o) / \bar{h}_{fg}$ in the order of 0.03. Thus the contribution of the analysis for the subcooling effect and the boundary layer analysis has a negligible effect on using Nusselts theory for predicting the values of the heat transfer coefficents presented in the thesis.

4.4 Evaluation of Experimental Data

The method employed for evaluating the heat transfer coefficient (ho) from test data is applicable to the case of both a static and an oscillating tube. A sample calculation for finding (ho) and (h_{NU}) is shown below to demonstrate the procedure involved in determining the two quantities. The following data are recorded from a typical experimental test for condensation on a stationary tube and from standard tables;

Steam pressure = 6 Bars
Steam saturation temperature Θ_{sat} = 158.8 °C
Mass flow rate of cooling water $M\bar{w}$ = 1204 Kg/hr
Inlet cooling water temperature T_{in} = 26.2 °C
Outlet   "   "   " To = 41.5 °C
Mean condenser tube wall temp. $\bar{\Theta}m$ = 131.5 °C
Steam shell temperature = 161.0 °C

Specific heat of cooling water $C_{p\bar{w}}$ = 4180 J/kg °C
Thermal conductivity of tube K = 26 J/s.m °C
Outside surface area of test piece $S\bar{o}$ = 0.108 m²
Outside diameter   "   "   " $D\bar{o}$ = 0.034 m
Inside   "   "   "   " D_i = 0.029 m

The heat flux $\dot{Q} = \dot{M}w \cdot C_{pw} \cdot (To - Tin)$

$$= 21389 \text{ J/S} \qquad (4.4 - 1)$$

the difference between the inside and outside tube temperatures can be found from Fourier's law of conduction:

$$\Theta_o - \Theta_i = \dot{Q} \cdot \frac{\log_e \frac{Do}{Di} \cdot Do}{K \cdot 2 \cdot So} \qquad (4.4 - 2)$$

$$\Theta_o - \Theta_i = 21.54^{\circ}C$$

Assuming a linear temperature drop across the wall.

$$\Theta m = \frac{\Theta_i + \Theta_o}{2} \qquad (4.4 - 3)$$

$$\Theta_o = 142.3^{\circ}C$$

also the heat flux $\dot{Q} = ho \cdot So \ (\Theta_{sat} - \Theta_o) \qquad (4.4 - 4)$

$$ho = 11903 \text{ J/m}^2 \text{ S } ^{\circ}C$$

4.5 Comparision of Experimental Results with Nusselts Theory

In order to compare the experimental results with the theoretical equation of Nusselt for laminar flow of condensate on a horizontal tube (equation 4.2 - 19) experimental data of static tube tests were obtained at a range of cooling water Re from 12000 - 19000 for a range of $(\Theta_{sat} - \Theta_o)$ of 13.7 - 17.6°C and a constant steam pressure of 6 bars. Corresponding values for the heat transfer coefficient were obtained from Nusselt's theory, using condensate physical properties (visocity, thermal conductivity and density) based on average film temperature. The results are tabulated in Appendix 1. It can be seen that the experimental values are + 5% to + 15% in excess of the corresponding values predicted by Nusselts equation. The average increase

is about 9%. Similar observations were reported by McAdams and Frost

(34) on their work of steam condensation on a 1.65×10^{-2} m O.D.

horizontal tube, at a range of Δt (saturation temperature - tube surface

temperature) of 12 to $24^{\circ}C$ and a range of experimental heat transfer

coefficient (hexp) of 19307 - 11925 $J/m^2 S^{\circ}C$. They reported increases

of $0 - 30\%$ in the values of (hexp) over those of (h_{NU}). Wallace.et.al

(35) working in the same field and using a 2.1×10^{-2} m O.D. tube

reported 50 - 70% increases of (hexp) over (h_{NU}) for a range of hexp from

21579 - 24418 $J/m^2 S^{\circ}C$ and Δt between 5 - $6^{0}C$. Othmer (36) condensed

steam on a large diameter tube $(7.35 \times 10^{-2}$ m O.D.$)$ at a range of Δt

from 1 - $11^{\circ}C$ and (hexp) of 9653 - 28393 $J/m^2 S^{\circ}C$. In comparision with

(h_{NU}), the deviation of (hexp) was reported to be - 30 to + 20 per cent.

From these results, it can be seen that the accuracy of

Nusselt's theory is dependent on Δt and on tube diameter.

The experimental results reported in Appendix 1 are in good

agreement with McAdam's results which were carried out under similar

physical conditions.

In general, the average ratio of (hexp) to the predicted (h_{NU})

may vary between +5 to +30 per cent.

5. DIMENSIONAL ANALYSIS

5.1 Application of the Method of Dimensions for Correlating Experimental Data.

A purely analytical solution to the physical processes involving condensation on a vibrating tube is extremely complex (as explained in Section 1.4 - 2). Alternatively the experimental results may be treated by the theory of dimensions to establish correlations for the experimental data. In this method the dimensions of the physical quantities involved in the process can be manipulated algebraically, and the results can be interpreted graphically to provide a great deal of information.

In general, dimensional analysis involves the combination of the individual variables into dimensionless groups which are fewer in number than the original variables. The method indicates the relative importance of the various parameters by consideration of their orders of magnitude.

The method of dimensions has the limitation that it is concerned with physical dimensions as the main properties and not with numerical measures; therefore it yields no numerical values to express the form of which one dimension varies with the other. However it proves a general functional relationship between the physical quantities and it provides a logical basis for an empirical representation of the experimental results.

5.2 Derivation of the Dimensionless Equation for Film Condensation on a Vibrating Horizontal Tube.

It is important to establish a proper understanding of the problem related to condensing systems undergoing mechanical oscillations in order to choose the important variables that may have a significant influence on the phenomena. When steam $_\wedge^{at}$ saturation temperature (Θ_{sat}) is passed over a smooth horizontal tube whose temperature is $\Delta\Theta$ below the saturation temperature, the condensate forms on the wall a film which acts as an insulating layer to the heat transfer. As a result, the rate of condensation is influenced by the condensate coefficient of thermal conductivity (K). The main geometric variable in the problem is the thickness of the film which depends on the rate of condensation and on the nature of drainage of the film. The rate of condensation depends on the latent heat of vaporization $(\bar{h}_{fg})$ of the fluid. The facility with which the condensate flows from the wall is determined by its viscosity (μ) density (ρ) and the gravitational force. Furthermore, since the thickness of the film varies round the tube's cross-section, the tube diameter $(\bar{Do})$ has an influence on the magnitude of the heat transfer coefficient.

If the tube is undergoing mechanical oscillations, the vibrational intensity will affect the condensate drainage and it will consequently influence the film thickness. Thus both the frequency $_\wedge^{(W)}$ and amplitude $_\wedge^{(A)}$ of vibration become important in assessing the magnitude of the heat transfer coefficient (hv).

-66-

In view of the preceding discussion, there exists a relationship of the form:-

$$hv = F (g, D\bar{o}; \hat{\mu}_c , \rho , h_{fg}, K,$$
$$\triangle \theta , W , A)$$

$$(5.2 - 1)$$

For given conditions, the unknown functions yeilding

(hv) may be written in exponents form, and by substituting for the

fundamental dimensions, using the (H M L T t) system suggested by

Ede (46) and Welty (47), equation (5.2 - 1) becomes:-

$$\frac{H}{L^2.t.T.} = F1 \left[\frac{L}{t^2}\right]^a \left[L\right]^b \left[\frac{M}{Lt}\right]^c \left[\frac{M}{L^3}\right]^d$$

$$\left[\frac{H}{M}\right]^e \left[\frac{H}{Lt}\right]^f \left[T\right]^j \left[\frac{1}{t}\right]^n \left[L\right]^p$$

$$(5.2 - 2)$$

The dimensionless coefficient F1 and all exponents are of given value

only at point conditions. If any condition (such as frequency) is changed,

then F1 and all the exponents may change. This indicates a

relation between (hv), the variable, and F1. If all variables that are

related to the system are included in equation (5.2 - 1), the relative

size of the various components necessary to render equation (5.2 - 1)

dimensionally homogeneous can be established.

Since the net dimensions on each side of equation (5.2 - 2)

must be the same, the sum of the exponents involved in any one

dimension must be the same on both sides of the equation. Thus solving

for the exponents yields:-

-67-

$$hv = F, \; (g)^a \; (Do)^b \; \left(\frac{\mu}{c}\right)^{e-d} \; (\rho)^d \; (\bar{h}_{fg})^e \; (K)^{1-e}$$

$$(\Delta\theta)^{-e} \; (W)^{d-2a} \; (A)^{2d-a-b-1}$$

<div align="right">(5.2 - 3)</div>

Separation of the variables gives:-

$$\frac{hv.A}{K} = F2 \left[\frac{g}{AW^2}\right]^a \left[\frac{Do}{A}\right]^b \left[\frac{\rho.w.A^2}{\mu_c}\right]^d \left[\frac{\mu_c \cdot \bar{h}_{fg}}{K \cdot \Delta\theta}\right]^e$$

<div align="right">(5.2 - 4)</div>

Equation (5.2 - 4) may be interpreted for correlating the

performance of the vibrating heat exchanger.

5.3 Interpretation of the Dimensionless Parameters

It is advantageous to relate the correlation process to

Nusselt's theoretical analysis for condensation on a stationary tube

(Chapter 4). This can be achieved by changing equation (5.2 - 4)

into a new set of dimensionless products. It is permissible to multiply

any of the non-dimensional groups by any dimensionless quantity,

provided that a new function and exponents are presented. Thus equation

(5.2 - 4) can be interpreted as:-

$$\frac{hv.Do}{K} = Nuv = F_3 \left[\frac{AW^2}{g}\right]^{a_1} \left[\frac{A^2w^2}{Do \cdot g}\right]^{b_1} \left[\frac{\rho.\sqrt{g.Do} \cdot Do}{\mu_c}\right]^{c_1}$$

$$\left[\frac{\mu_c \cdot \bar{h}_{fg}}{K.\Delta\theta}\right]^{d_1}$$

<div align="right">(5.3 - 1)</div>

Where $F_3, a_1, b_1, c_1,$ and d_1 are non-dimensional constants.

It is clear from this equation that the last two dimensionless parameters involve all the physical quantities associated with the analysis of condensation on a stationary tube (equation 4.2 - 19). Equation (5.3 - 1) can be written as:-

$$Nuv = \bar{B}_1 \left[\frac{\rho \sqrt{D_{\bar{o}} \, g} \cdot D_{\bar{o}}}{\mu_c} \right]^{c_1} \left[\frac{\mu_c \cdot \bar{h}_{fg}}{K \cdot \triangle \Theta} \right]^{d_1} +$$

$$\bar{B}_2 \left[\frac{A \, W}{g} \right]^{a_1} \left[\frac{A^2 W^2}{D_{\bar{o}} \cdot g} \right]^{b_1} \left[\frac{\rho \cdot \sqrt{g \cdot D_{\bar{o}}} \cdot D_{\bar{o}}}{\mu_c} \right]^{c_2} \left[\frac{\mu_c \cdot \bar{h}_{fg}}{K \cdot \triangle \Theta} \right]^{d_2}$$

$$(5.3 - 2)$$

If c_1 and d_1 are taken as equal to c_2 and d_2 respectively, then:-

$$\frac{Nuv}{\left[\frac{\rho \cdot \sqrt{g \cdot D_{\bar{o}}} \cdot D_{\bar{o}}}{\mu_c} \right]^{c_1} \left[\frac{\mu_c \bar{h}_{fg}}{K \cdot \triangle \Theta} \right]^{d_1}} = \bar{B}_1 + \frac{\bar{B}_2}{\left[\frac{A \cdot W^2}{g} \right]^{a_1} \left[\frac{A^2 \cdot W^2}{D_{\bar{o}} \quad g} \right]^{b_1}}$$

$$(5.3 - 3)$$

Where B_1 and B_2 are dimensionless constants, it will be seen that if c_1 and d_1 are substituted by the numerical values of (0.25) and (0.5) respectively, the denominator on the left hand side of equation (5.3 - 3) becomes proportional to the theoretical Nusselt number for condensation on a stationary horizontal tube. Its value is

dependent on the constant B_1, since, if either A or W tends to zero, the right hand side of equation (5.3 - 3) will be reduced to B_1.

On the basis of this discussion, the values of C_1 and d_1 can be taken from Nusselt's theory (as 0.25 and 0.5 respectively) and the values of the dimensionless constants B_1, B_2, a_1 and b_1 must be deduced from empirical correlations; thus equation (5.3 - 3) becomes:

$$\frac{Nuv}{\left[\frac{\ell \cdot \sqrt{D_{\delta} g} \cdot D\bar{o}}{\mu / c}\right]^{0.25} \left[\frac{\mu_c \cdot \bar{h}_{fg}}{K \cdot \Delta \Theta}\right]^{0.5}} = B_1 + B_2 \left[\frac{AW^2}{g}\right]^{a_1} \left[\frac{A^2 W^2}{D_{\delta} g}\right]^{b_1}$$

(5.3 - 4)

$$\text{or} \quad \pi Nu = B_1 + B_2 \left[\pi_a^{a_1} \cdot \pi_b^{b_1}\right]$$

(5.3 - 5)

where π_{Nu}, π_a, π_b are non-dimensional parameters which correspond to parameters in (5.2 - 4)

Thus the number of the non-dimensional parameters has been reduced to three, and further procedure to develop equation (5.2 -4) will be entirely dependent on experimental results for finding the non-dimensional constants.

5.4 Experimental Data and Dimensionless Parameters

The results of the dimensional analysis of heat transfer related to condensation on a vibrating condenser yielded 5.3 - 4. The nature of the functions B_1 and B_2 and the exponential relationship in the equation can be found from experimental data. Two series of experiments are required. In one series, the relation between the group π_{Nu}

Fig 5.4-1

Average Dynamic Amplitude $\pm A \times 10^{-4}$ m.
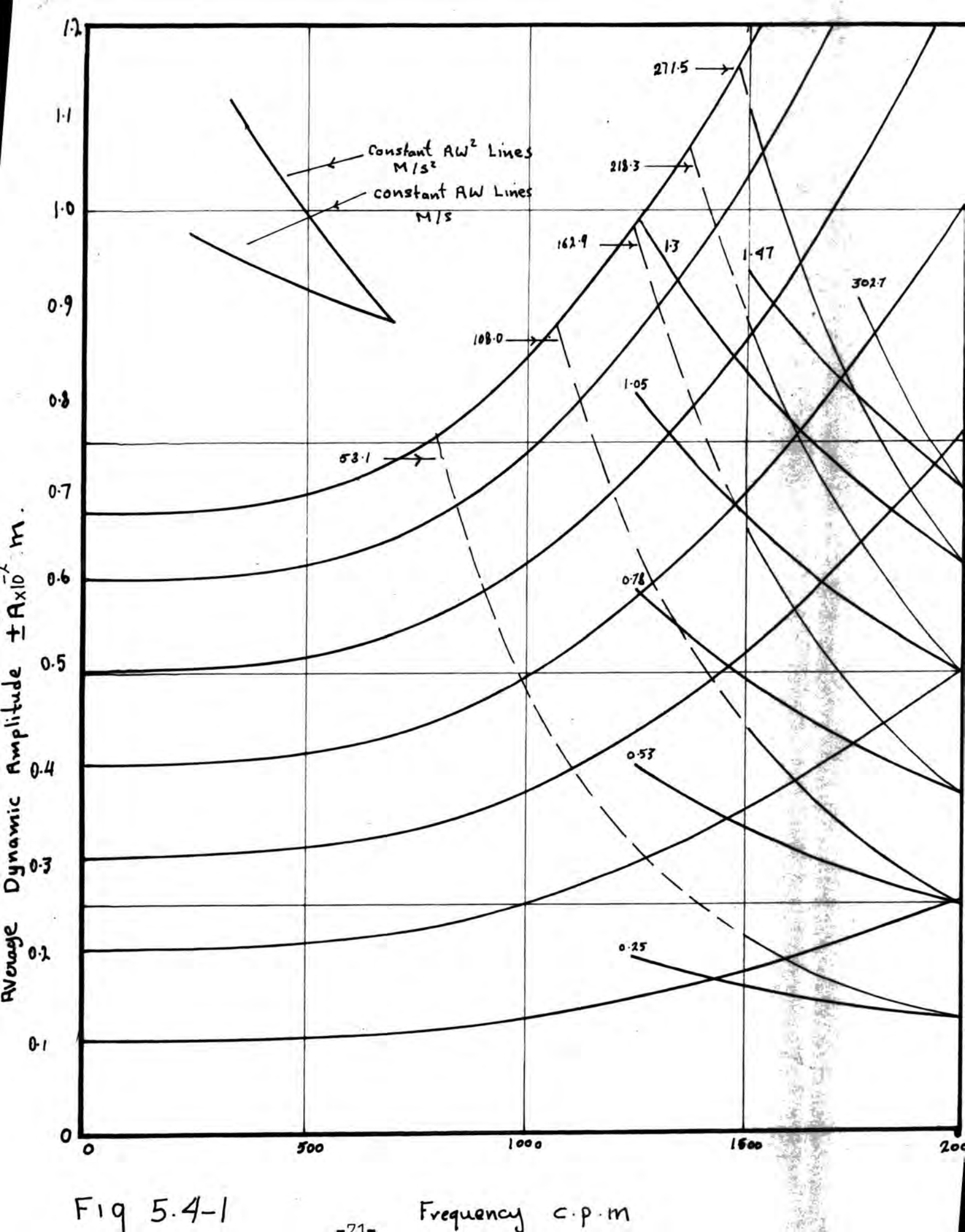
Frequency c.p.m

with the group π_a may be determined for selected values of the group π_b, and in the other series, the relation between the group π_{Nu} with the group π_b may be determined for selected values of the group π_a. The difficulty in this procedure is that the amplitude of vibration is entirely dependent on the frequency of oscillations (because of tube flexure). Therefore the selected values of AW and AW^2 are obtained by governing the frequency of vibration and finding the static amplitude that gives the required value of the dynamic amplitude at any particular frequency. This relation is obtained from calibration curves of amplitude with respect to frequency of oscillation (Fig. 5.4 - 1). One series of experimental results was obtained for each of seven constant values of AW^2 ranging from 0 - 302.7 m/s^2 at a range of frequencies from 1500 to 2000 cpm (Appendix 2). The second series covered a range of seven constant AW values of 0 to 1.47 m/s at a range of frequencies from 1250 to 2000 cpm (Appendix 3). It is emphasized that the ranges of experimental variables were chosen to cover the maximum obtainable performance of the condenser. Experiments at low frequencies were avoided since, at low amplitudes, no significant increase in the heat transfer coefficient was observed. The effective region of condenser dynamic performance (at higher values of Rev) on heat transfer coefficient is indicated by the constant AW and AW^2 curves of Fig. 5.4 - 1.

5.5 Correlation of the Experimental Data

The function B_1 was simply calculated from the experimental data at $W = 0$, giving B_1 equal to π_{Nu} (see equation (5.2 - 5))and the

numerical value of this function was found to be equal to (0.73). This corresponds to the value of Nusselt's constant (0.72) for his theoretical analysis of condensation on a horizontal tube.

The exponents a_1 and b_1 in equation (5.3 - 4) were found from graphical plots of the experimental data as follows. For evaluation of a_1, five groups of experimental points were plotted, each group representing a plot of $\log_{10} (\pi_{Nu} - 0.73)$ as a function of $\log_{10} (\pi_a)$ and at a different constant value of (π_b). The graphs showed some scatter of the experimental data. To improve the correlation, it was necessary to programme each group of experimental points to find the equation of least square fit through the results. The experimental and computed results are shown on Fig 5.5 - 1 and are represented by straight lines having approximately the same slope. This justifies a relation of equation (5.3 - 4). The value of the exponent a_1 represents an average slope of the five lines, evaluated at (-0.47). By adopting the same procedure and plotting $\log_{10} (\pi_a - 0.73)$ as a function of $\log_{10} (\pi_b)$ for constant values of (π_a) (Fig. 5.5 - 2), the data were best represented by a line of slope (1.08) which is the value for the exponent b_1.

The function B_2 is evaluated by plotting $\log_{10} (\pi_{Nu} - 0.73)$ as a function of $\log_{10} (\pi_a)^{-0.47} + \log (\pi_b)^{1.08}$ (Fig. 5.5 - 3) for the same data used in Figs. 5.5 - 1 and 5.5 - 2 and for further data obtained at a range of tube frequencies from 0 - 2000 rpm and amplitudes from 0 to 1×10^{-2} m (Appendix 4). B_2 is found to be equal to (0.21)
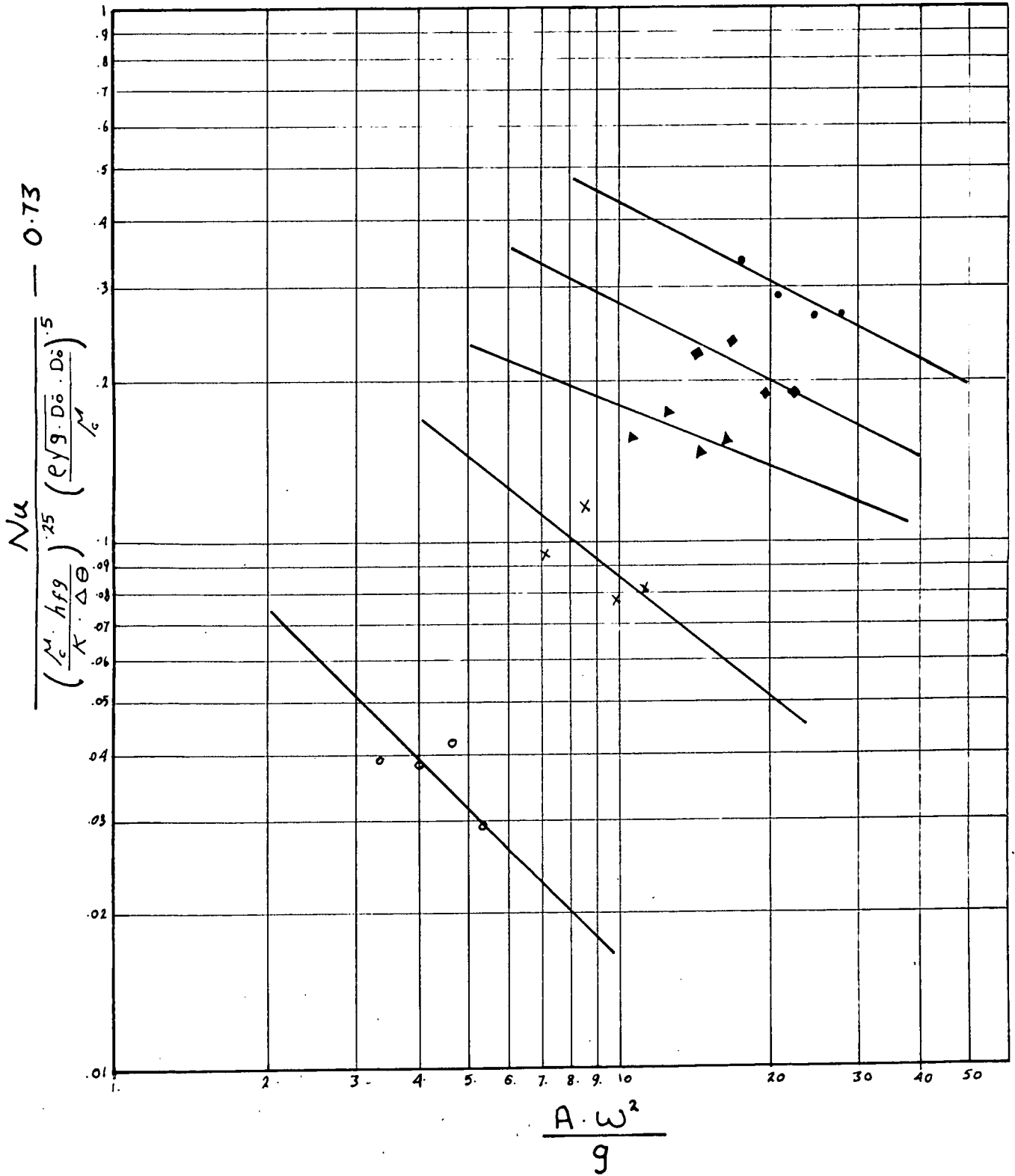
Fig. 5.5-1
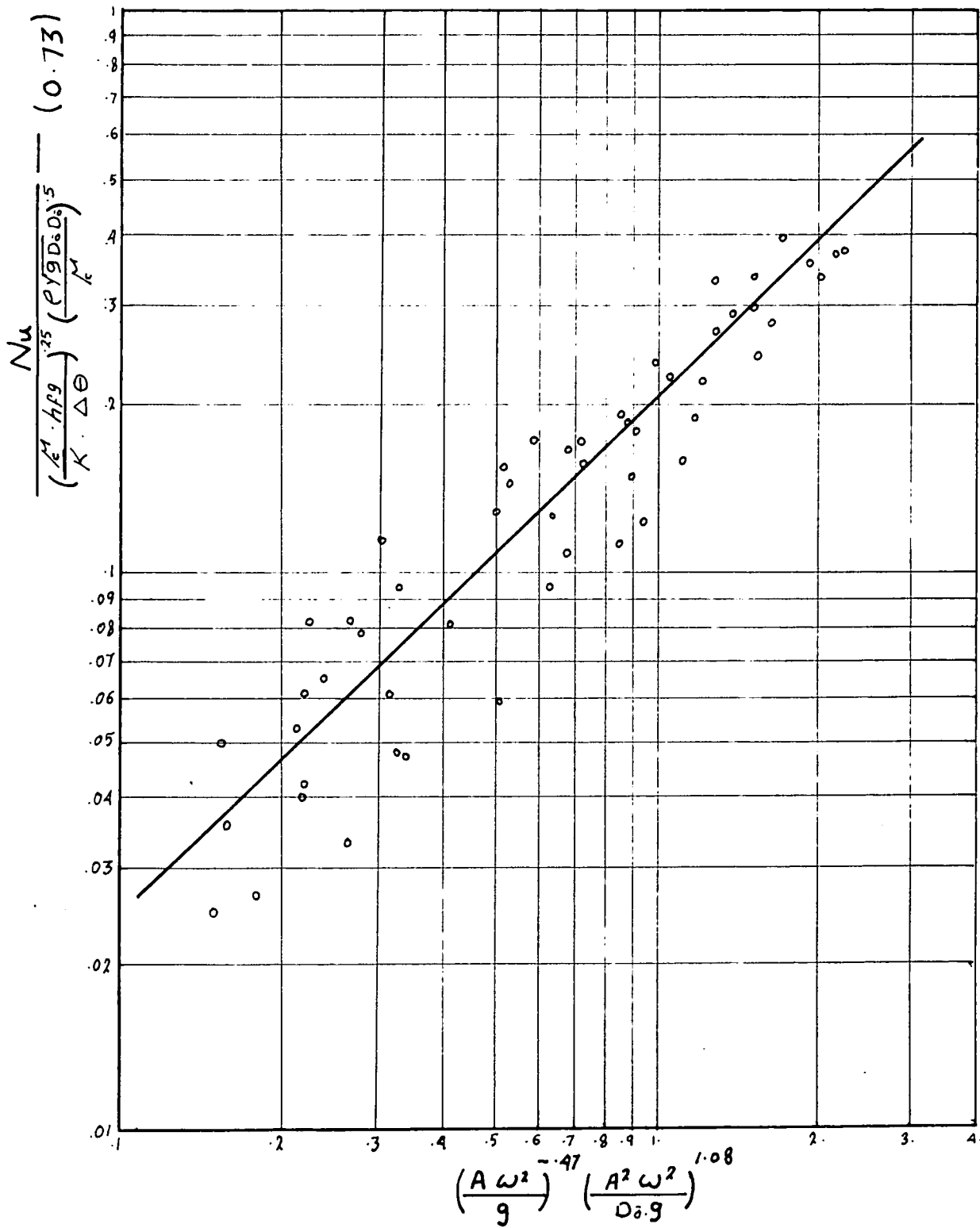
Fig 5.2-3

at the intercept when:

$$\log_{10} \pi_a^{-0.47} + \log_{10} \pi_b^{1.08} = 0 \qquad \text{or}$$

$$(\pi_a)^{-0.47} \times (\pi_b)^{1.08} = 1$$

The experimental data for condensation of steam on vibrating tube can now be represented by the following equation:-

$$\frac{Nu}{\left[\dfrac{\sqrt{\mu} c \cdot \bar{h}_{fg}}{K \cdot \Delta\Theta}\right]^{0.25} \left[\dfrac{\rho \sqrt{g \cdot D\bar{o} \cdot D\bar{o}}}{\sqrt{\mu} c}\right]^{0.5}} = 0.73 + 0.21 \left[\frac{AW^2}{g}\right]^{-0.47} \left[\frac{A^2 W^2}{D_{\bar{o}} g}\right]^{1.08}$$

$$(5.5 - 1)$$

or in alternative form:-

$$\frac{hv}{ho} = 1 + 0.29 \left[\frac{AW^2}{g}\right]^{-0.47} \left[\frac{A^2 W^2}{D_{\bar{o}} g}\right]^{1.08}$$

$$(5.5 - 2)$$

and the Nu_v is determined from equation 5.5 - 1 as:-

$$Nu_v = 0.73 \left[\frac{\sqrt{\mu} c \cdot \bar{h}_{fg}}{K \cdot \Delta\Theta}\right]^{0.25} \left[\frac{\rho \sqrt{g D\bar{o}} \cdot D\bar{o}}{\sqrt{\mu} c}\right]^{0.5} +$$

$$0.21 \left[\frac{\sqrt{\mu} c \cdot \bar{h}_{fg}}{K \cdot \Delta\Theta}\right]^{0.25} \left[\frac{\rho \sqrt{g D\bar{o}} D\bar{o}}{\sqrt{\mu} c}\right]^{0.5} \left[\frac{g}{AW^2}\right]^{0.47} \left[\frac{A^2 W^2}{D_{\bar{o}} g}\right]^{1.08}$$

$$(5.5 - 3)$$

If the exponents a_1 and b_1 are approximated to the values of 0.5 and Unity respectively then equation (5.5 - 3) can be

Fig 5.5-4

The plot shows the dimensionless group
$$\frac{Nu}{\left(\frac{M \cdot h \cdot r g}{K \cdot \Delta \theta}\right)^{.25} \left(\frac{\rho^2 g \cdot D_0^3}{\mu^2}\right)^{.5}}$$
on the vertical axis versus
$$0.2 \left(\frac{A \omega^2}{g}\right)^{-.47} \left(\frac{A^2 \omega^2}{D_0 \cdot g}\right)^{1.08}$$
on the horizontal axis.

-78-
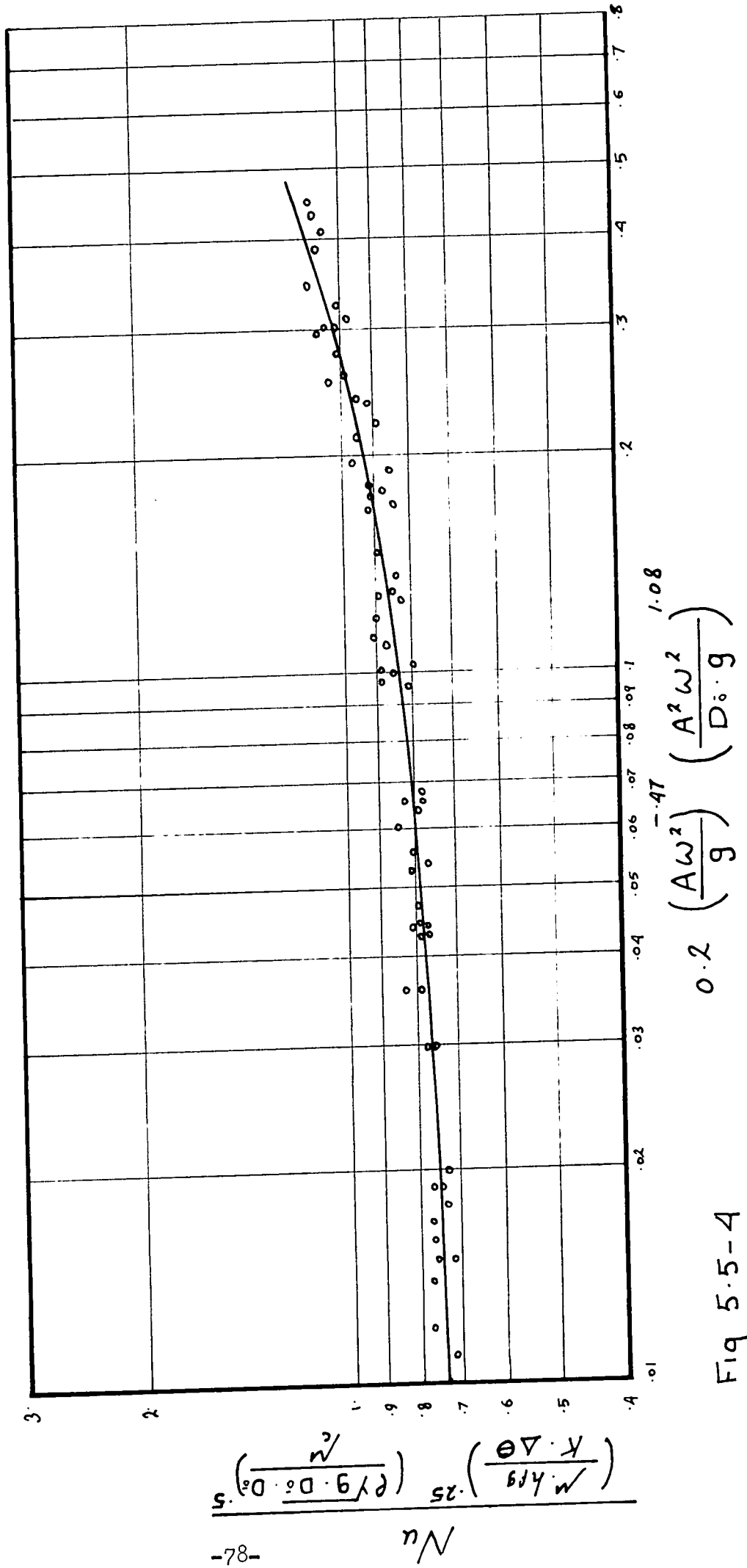
interpreted as:-

$$Nu_v = Nu_o + 0.21 \left[\frac{\mu_c \cdot \bar{h}_{fg}}{K \cdot \Theta}\right]^{0.25} \left[\frac{\rho_c \cdot g \cdot \dot{D}o \, \dot{D}o}{\mu_c}\right]^{0.5} \left[\frac{AW^2}{g}\right]^{0.5} \left[\frac{A}{\dot{D}o}\right]$$

$$(5.5. - 4)$$

The vibrational Reynolds number (Rev) may be formed from this equation giving the relation:-

$$Nu_v = Nu_o + 0.21 \left[\frac{\mu_c \cdot \bar{h}_{fg}}{K \cdot \Theta}\right]^{0.25} \left[Rev\right]^{0.5} \left[\frac{W^2 \cdot \dot{D}o}{g}\right]^{0.25} \left[\frac{A}{\dot{D}o}\right]$$

$$(5.5. - 5)$$

The graphs of Figs. 5.5 - 1, 5.5. - 2, and 5.5. - 3 representing equation (5.5. - 1) reproduce all the data within a deviation of

about $\pm$ 6 per cent. (Fig. 5.5. - 4.) This provides a reasonable

correlation of the experimental results within the employed ranges of

frequencies and amplitudes of vibration.

6. COMPARISON OF THE RESULTS OF CONDENSATION AND COUPLED MECHANICAL OSCILLATION

General

It was reported in section 1.1 - 3, that the available

information on the effect of mechanical vibration on condensation heat

transfer has a very narrow scope and only three different workers have

contributed their knowledge of exploration of this new field.

It would be of interest to compare the available literature by

relating the different results to one parameter and in this way, characteristic

relations between the individual sets of data may be obtained.

Raben et al (14) of the U.S. Department of Interior, were

the first workers who attempted to explore the field of coupled transverse

vibration and condensation on a vertical tube in an effort to promote

dropwise condensation and thereby significantly increase the rates of

heat transfer. Their experimental observations showed no indications

that vibrations of the condenser element could assist in breaking of the

condensate film (see section 6 - 5). Consequently filmwise

condensation was predominant. However increases in heat transfer

coefficient of the order of 58 per cent were obtained. The results

were expressed as a function of frequency and amplitude of vibration

within an accuracy of $\pm$ 5 per cent. Maximum (Rev) employed was

in the order of 200,000.

From his project on condensation of ethanol vapour on a

longitudinally oscillated horizontal tube, Houghey (19) obtained 20

per cent increase in both vapour—side and water-side heat transfer

coefficients at a maximum (Rev) of about 80,000. The increase in heat transfer with vibration was assumed to be a function of (Rev) only, giving an accuracy of correlation of experimental results within $\pm$ 5 per cent of the mean value.

Dent (20) employed transverse mechanical vibration for improving condensation of steam on a horizontal tube. The experiment covered a comparatively small range of vibrational intensities and a maximum (Rev) of 32,000 gave a maximum of 15 per cent increase in the condensation heat transfer coefficient. Gravitational force was the dominating factor in draining the condensate. Analytical correlation of the experimental data was attempted (see section 6.1), but this was found to deviate sharply from the experimental results. The cause is related to poor assumptions made before developing the analysis.

6.1 The Perturbation Parameter

It was pointed out that Dent's (20) experimental results for condensation on a vibrating tube covered a small range of (Rev), thus the contribution of vibration to increasing the heat transfer was relatively small and it was attributed primarily to a better conduction through the condensate film. Correspondingly a perturbation method of analysis was attempted to give an indication of the initial effect of vibration on condensation heat transfer. However this does not describe clearly the actual mechanism involved in the process. The basic approach to the perturbation analysis is stated in section 1.1 - 3. The perturbation parameter (E) introduced in the theory, was based on

similar assumptions stated by Schlichting (40) in his analysis of convection and streaming from horizontal cylinders undergoing a transverse mechanical oscillation.

In order to compare all the available literature concerning the effect of transverse vibration on condensation heat transfer, with relation to the parameter $(ND_o^2/3)$, from perturbation analysis it was necessary to establish a perturbation analysis for condensation on a vertical tube, to account for Raben's results. It was found that the evaluation of the local film thickness under vibrating conditions, is given by a similar expression of the local film thickness for condensation on a horizontal tube, with the exception that the film thickness for the vertical tube case varies with respect to tube length rather than angular position sin $\emptyset$ (as for Nusselt's equation).

The vapour saturation temperature and the outer surface temperature of a condenser must be known if the parameter $ND_o^2/3$ has to be evaluated. Raben did not report any measurements of tube wall temperatures and his calculations for the condensation heat transfer coefficient were based on experimental data for steam and cooling water temperatures, and physical properties as follows:-

The heat flux

$$\dot{Q} = \frac{\sum \Delta T}{1/hc \, \bar{A}o \, + \, Xs/Ks \cdot \bar{A}o \, + \, 1/hw \, Ai}$$

$$(6.2 - 1)$$

where:-

$\triangle T$: Mean overall temperature difference
(steam to inlet water)

A^- : Surface area

ho : Condensate heat transfer coefficient

hw : water side   "   "   "

X_s : Wall thickness

K_s : wall thermal conductivity

i : inside
o : outside
a : average

The water side heat transfer coefficient (hw), was calculated

from empirical formula developed from initial experimental investigation

on the effect of vibration on (hw). The error involved in calculating

(hw) by using this method was reported to be $\overline{+}$ 20%, however it was

necessary to use these values of (hw) for deriving the outer wall

temperature (Θo) as follows:-

$$Q = hw.2.\pi.r_i.L(\Theta_i - Tm)$$

$$(6.2 - 2)$$

L : Tube Length
(Tm : mean cooling water temperature)

and (4.4-3)

and Θo was obtained from equations(4.4 - 2). .Neglecting subcooling,

the temperature drop across the film was found by subtracting Θo

from the saturation temperature. Fig 6.1 - 1 shows all available

data of steam condensation on transversely vibrated tubes, together

with the analytical perturbation results plotted in terms of the ratio

hv/ho as a function of the dimensionless parameter $ND_o^2/3$. All

Computed values (cubic polynomials)
through experimental data

Raben

Auther

Dent

Perturbation
Theory

$$\frac{ND^2}{3} = \frac{4}{3\pi} \left(\frac{A}{D_5}\right) \frac{R_{ev} \cdot l_c}{K} \frac{\mu \cdot hf_4}{\Delta \theta}$$

$\frac{h_v}{h_o}$

Fig 6.1-1

-84-
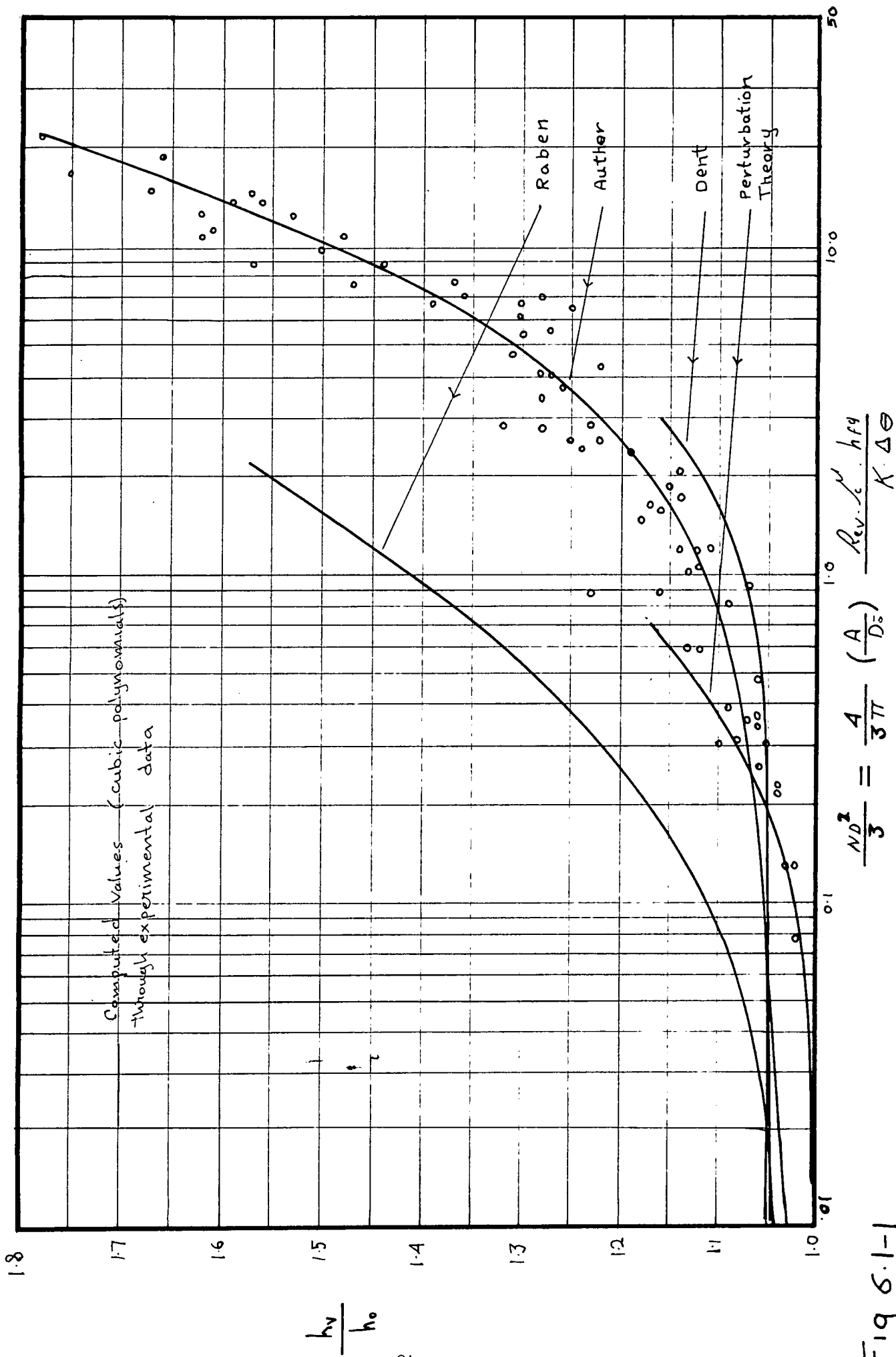
experimental results showed considerable scatter on the graph, and it

was therefore decided to programme each group of results to find mean
α
values from third order polynomial equation of least square fit through
Λ
the experimental points. The curve from the perturbation analysis is

plotted within a comparatively small range of $ND_s^2/3$ since Dent[20] found

that above a value of 0.7, the curve deviates very sharply from the

experimental results. This demonstrates a significant increase in the

rate of heat transfer with vibration. The limitation of this analysis is

governed by the magnitude of the numerical value of the perturbation

parameter (E), which was assumed to be very small. Dent's

experimental results, although very scattered, appear to be in close

agreement with the results given in this report. Raben's experimental

data for condensation on vertical tube seems to demonstrate similar

characteristics of increase in heat transfer with vibration to those for

a horizontal tube.

6.2 The Vibrational Reynolds Number (Rev)

It is very common to display the results of coupled vibration

and heat transfer problems in the form of Nusselt number as a function

of the vibrational Reynold number (Rev). This simple relation can

clearly identify the influence of vibrational intensity on heat transfer.

It was assumed by Houghey (19) that the increase in

condensation heat transfer was solely a function of (Rev) and he

obtained reasonable correlation of his experimental points (see section 6)

considering that the maximum increase in (hv) was about 20 per cent
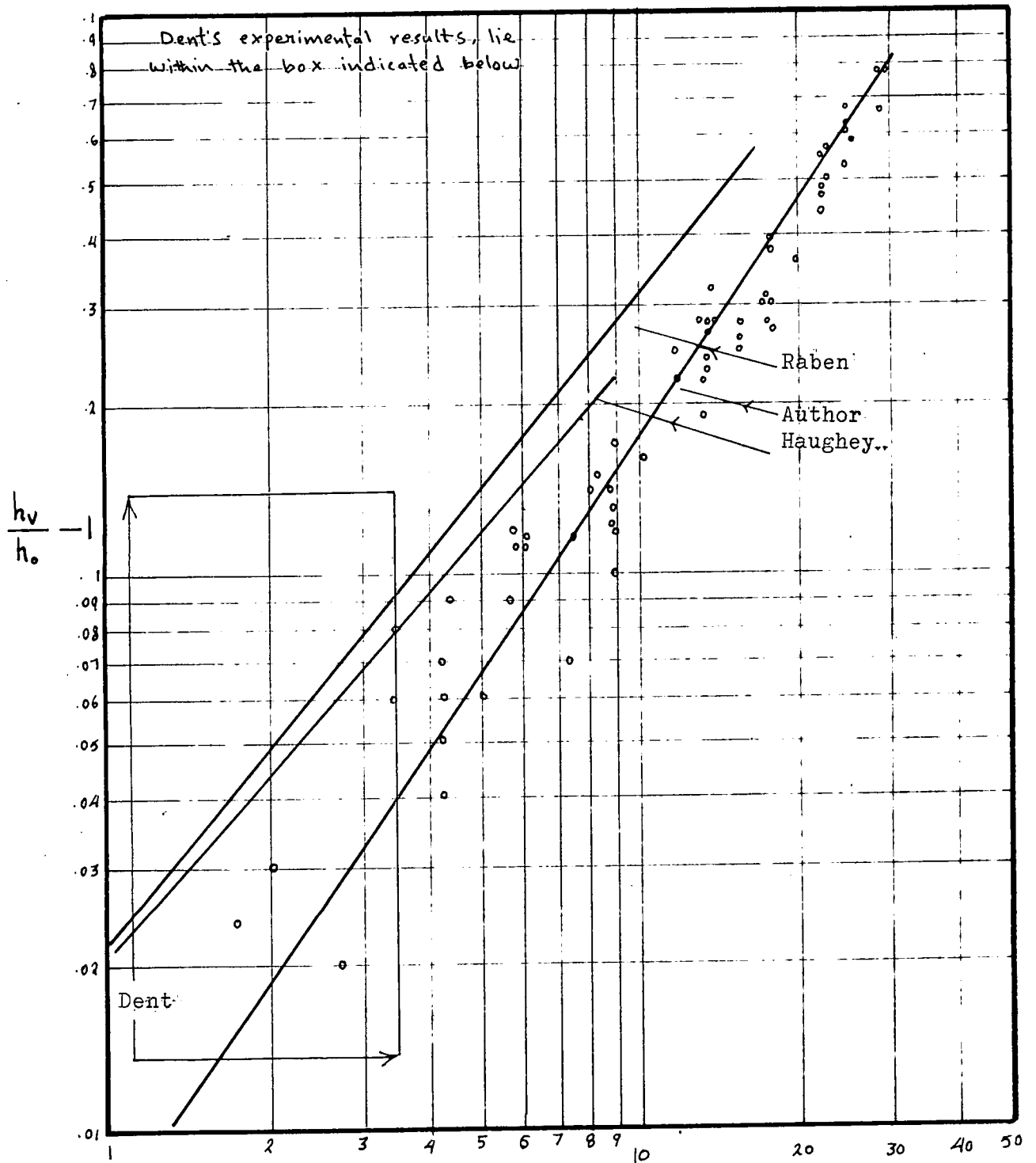
Fig 6.2-1

over (ho). Fig 6.2 - 1 represents a plot of hv/ho as a function of (Rev)

for the results given in this work and those reported by Haughey and

Raben. Dent's results were conducted within a comparatively small

range of (Rev) and also showed a considerable scatter when plotted

on this graph. Fig 6.2 - 1 demonstrates a linear relationship between

hv/ho and (Rev) for longitudinal oscillations. For transverse oscillations,

hv/ho was given approximately as a function of $(Rev)^{1.2}$ for both

horizontal and vertical tubes. The graph also indicates that the

increase in heat transfer coefficient due to transverse oscillations is

more favourable with vertical tubes than with horizontal tubes. This

could well be due to the different nature of drainage of the condensate

film associated with each process (see section 6.4). Haughey's and
Raben's lines in Fig 6.2-1 are within ∓ 8 % of their
experimental data.

6.3 Effect of Cooling Water Temperature on Condensate Nu

The experimental results previously given in this report, were

conducted without control of the inlet water temperature which was

dependent on the temperature of the water stored in the main reservoir.

The inlet temperature varied from 13 to 23 C^o during the entire range

of the experimental results, therefore it is an advantage to find the

effect on condensation Nu of varying the cooling water temperature.

Tests were conducted at a range of inlet water temperatures from 10 to

40 C^o for static conditions and also at a constant tube frequency of

1500 cpm, with a range of amplitudes from 2.2×10^{-3} - 7.5×10^{-3} m

(see appendix 5). These results are shown on Fig 6.3 - 1.

It can be seen that the maximum increases in Nu were obtained

at an inlet temperature of about 32°C and that below this temperature, both the heat flux (Q) and the heat transfer coefficient (h) demonstrated a continuous decrease. Eagle and Ferguson (41) conducted an experimental work to determine the way in which the heat transfer coefficient varies with the physical properties of a fluid. For this investigation an electrically heated 1.9×10^{-2} m diameter tube was used, through which, water was circulated at various constant velocities. Their results showed that an increase in (h) was followed by an increase in the water temperature and also by an increase in the water nominal velocity. The increase in (h) with respect to water temperature was much more rapid at the higher water velocities.

The heat flux is closely dependent on the magnitude of the Reynolds number (Re) of the cooling water and as the cooling water temperature decreases, (Re) decreases very rapidly due to a significant increase in the viscosity. The condensation (Nu) is related to both (Q) and the temperature drop across the film.

The analysis of steam condensation (Nusselt (18)) showed that (h) is less favourable with lower temperatures of condenser surface, since this has the resultant effect of increasing the temperature drop across the film. However, increasing the cooling water temperature towards the boiling point, decreases its viscosity and considerably increases (Re). The value of (Q) will be limited since nucleation will occur on the heating surface, thereby decreasing the surface area through which heat is transferred. It was observed from the experimental tests, that at a mean outlet temperature above 60°C, small vapour bubbles were present in the water outlet line. The bubbles become more

88

pronounced in size and quantity with a further increase in the cooling water temperature and thus the tests were limited to a maximum outlet temperature of about 60°C to avoid the occurrence of a phase change. Raben's experimental results were conducted at a similar value of (Re) to those presented in this report, but at inlet water temperatures ranging from 56 to 80°C and at a saturation temperature of 100 C$^{\circ}$. These results indicated a rapid decrease in ($\dot{Q}$) with an increase in the cooling water temperature, while (h) remained approximately constant over the range of cooling water temperatures employed. This independent relation between (h) and ($\dot{Q}$) was also observed by Birt et al (42) who worked on experimental methods to increase the steam-side heat transfer coefficient. Their results showed for filmwise condensation on a vertical cylinder, that (h) decreased with an increase in ($\dot{Q}$) and they concluded that (h) was largely independent of ($\dot{Q}$) in the range of (h) from Γ 000 to 57, 000 J/m^2.s.$^{\circ}$C. Similar observations were also reported by McAdams (34), Hampson (42) and Nagle (43).

The maximum increase in ($\dot{Q}$) obtained during the experimental tests with vibration, was in the order of 20 per cent over its value with no vibration. Raben's (14) results for vertical tube showed a maximum of 30 per cent increase in ($\dot{Q}$) with vibration. However Dent's (20) results indicated fluctuations in the values of ($\dot{Q}$) in the order of -4.2 to + 8.6 per cent with vibration over the static value.

6.4 Condensate Drainage and Vibration

During experimental tests, the orientation of the condensate

-90-

film was observed under vibrational conditions with the aid of a stroboscope. The nature of the film appeared to be primarily dependent on the vibrational intensity, or (Rev) Fig 6.4 - 1; in the range of (Rev) from 0 to 120,000, drainage of the condensate was strictly from the lower half of the tube. This occurred in the form of drops shearing away from the condensate film and falling downwards under the action of gravity. The draining drops under static tube conditions, appeared to be large in size and the drainage process was comparatively slow.

As the vibrational intensity was increased, the draining drops became more dense (closer to each other) but smaller in size and faster in their downward travel. At higher ranges of vibrational intensity (Rev 120,000 to 180,000), this initially resulted in establishing very thin condensate ridges which appeared to move downward from the top of the tube to its lower half, where they accumulated and drained away rapidly due to the momentum imparted to the condensate by the vibrating tube. The ridges tended to diminish with an increase in the vibrational intensity, but an accumulation of condensate on the top half of the tube became visible in the form of a straight band along the tube. This band varied in width with respect to the tube's cyclic position and appeared to spread during the upper displacement of the tube, and then contract during the lower movement. At vibrational intensities above (Rev) of 180,000, the ridges disappeared, but the condensate accumulating on the top tended to leave the tube during the start of the lower displacement. However it eventually returned under the action of gravity. This stage was predominant at (Rev) up to 220,000. Above this value,

static
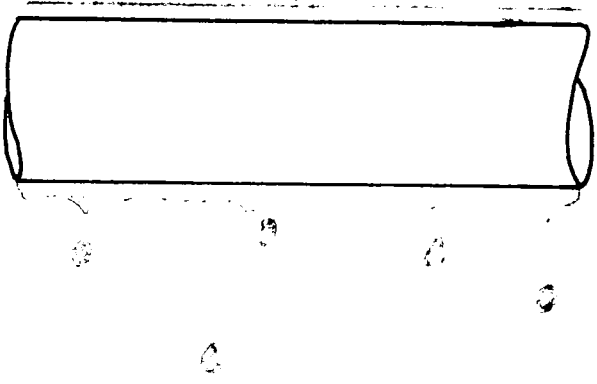
R_{e_v} 120 000

R_{e_v} 180 000

Fig 6.4-1

-92-
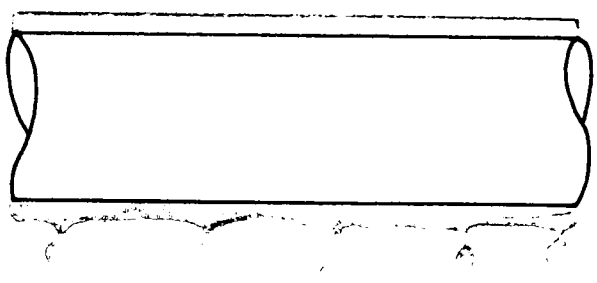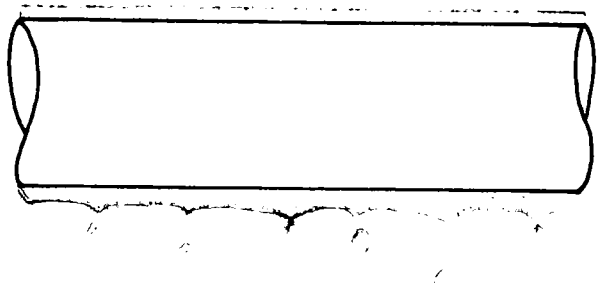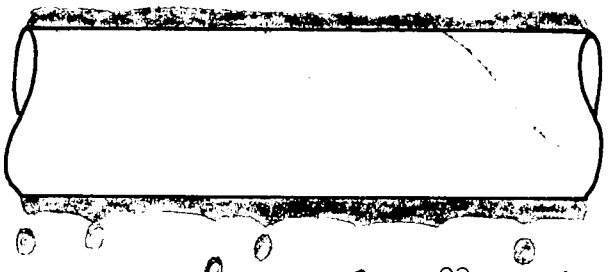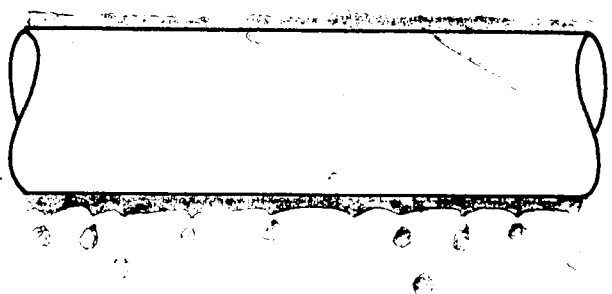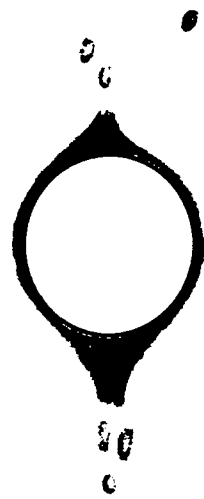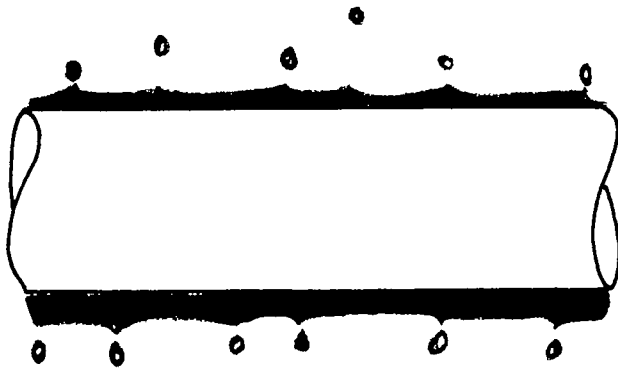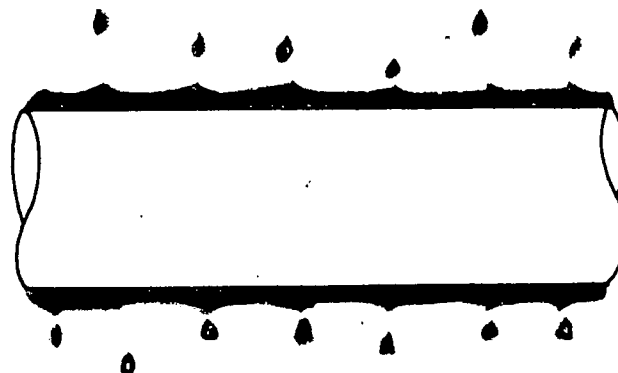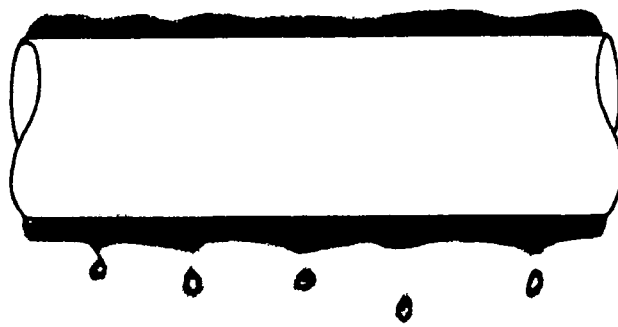
Re_v 220 000

$Re_v > 220\ 000$
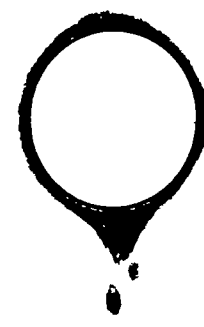
the condensate appeared to have established a highly fluctuating mode of movement and the drainage occurred on both the upper and lower parts of the tube. On the upper part, the condensate drained off during the commencement of the lower displacement, but it spread out on the tube surface during the rest of the cycle.

For condensation on a vertical vibrating tube, Raben reported that the condensate swept back and forth on the tube during each cycle thus forming two stagnant points and very little condensate was thrown free from the tube. Haughey reported formation of standing waves in the condensate film on a longitudinally vibrated horizontal tube. These waves appeared at a critical vibrational intensity (3.2×10^{-2} m/sec) and the wavelength was independent of vibrational intensities. The drainage was observed to take place from the ridges which increased in amplitude with an increase in vibrational intensity.

7. CONCLUSIONS

The purpose of this project was to find the influence of transverse vibration on condensation heat transfer coefficient. The following conclusions can be drawn from the experimental data described in this report:-

1. The average condensation heat transfer coefficient was increased by as much as 78 per cent with oscillations compared to the coefficient without oscillations. This increase was obtained at a maximum vibrational Reynolds number of about 300,000 (or AW = 1.73 m/s) employed during the experimental tests.

2. The improvement in (hv) was generally followed by an increase in frequency and amplitude of vibration.

3. At a vibrational intensity $0 < A.W < 0.46$ m/s, the mechanical vibrations had no appreciable effect on the heat transfer coefficient.

4. The experimental heat transfer coefficients obtained for filmwise condensation on a static tube, agreed with Nusselt's equation (4.2 - 19) to within an error of +8 per cent.

5. An empirical correlation of all experimental data was obtained in the form:-

$$Nuv = 0.73 \left[\frac{\mu_c . \bar{h}_{fg}}{K . \Delta\Theta} \right]^{0.25} \left[\frac{\rho \sqrt{g.D\bar{o}}.D\bar{o}}{\mu_c} \right]^{0.5} + 0.21 \left[\frac{\mu_c . \bar{h}_{fg}}{K . \Delta\Theta} \right]^{0.25}$$

$$\left[\frac{\rho \sqrt{g.D\bar{o}}.D\bar{o}}{\mu_c} \right]^{0.5} \left[\frac{g}{A.W^2} \right]^{0.47} \left[\frac{A^2.W^2}{D\bar{o}.g} \right]^{1.08}$$

This reduces to Nusselt's equation (4.2 - 19) when either A or W tends towards zero.

6.   The visual observation of the condensate film, detected that gravity was the dominant factor in draining the condensate at $0 < \text{Rev} < 120,000$. However, at the higher vibrational intensities ($\text{Rev} > 220,000$), the condensate displayed a cyclic mode of fluctiations and the condensate drainage took place from both the upper and lower parts of the test piece.

7.   The increase in heat transfer coefficient with vibration is assumed to have resulted from a reduced film thickness and agitation of the film.

8.   The experimental data showed a maximum increase of 20 per cent in the heat flux with vibration, over its value at static tube conditions.   The results also indicated that the heat flux was independent of the heat transfer coefficient.

9.   The described method of preparation of the tube surface was found to give a satisfactory film condensation on the stainless steel surface over a prolonged period of the condenser operation.

10.   In comparing the methods of vertical (Raben (19)) and horizontal tube oscillations, the two methods showed a similar characteristic of increase in the heat transfer coefficient with vibration when these results were plotted on a base of the vibrational Reynolds number.

APPENDIX 1

TABLE OF EXPERIMENTAL

RESULTS FOR CORRELATION

WITH NUSSELT'S THEORY

	Units	1	2	3	4	5	6	7
Water flow $\dot{M}$	Kg/hr	1250	1136	1023	909	795	1204	955
Inlet temp T_i	°C	22.1	22.6	23.0	23.4	24.5	26.2	27.0
Outlet temp T_o	°C	37.1	38.4	40.2	42.0	45.0	41.5	44.9
Tube temp $\bar{\theta}_m$	°C	130.2	131.5	133.6	134.4	135.6	131.5	133.7
$T_o - T_i$	°C	15.0	15.8	17.2	18.6	20.5	15.3	17.9
$\dot{Q}_w$	J/s	21770	20841	20430	19631	18923	21389	19848
$\theta_o - \theta_i$	°C	21.9	20.98	20.57	19.77	19.05	21.54	19.99
$\bar{\theta}_o$	°C	141.2	142.0	143.9	144.3	145.1	142.3	143.7
θ_f	°C	150.0	150.4	151.4	151.6	152.0	150.6	151.2
$\theta_{sat} - \theta_{\bar{o}}$	°C	17.6	16.8	14.9	14.5	13.7	16.5	15.1
h_o	$J/m^2.s.°C$	11358	11391	12590	12432	12683	11903	12070
h_{Nu}	$J/m^2.s.°C$	10737	10863	10991	11270	11431	10913	11157
h_o/h_{Nu}	-	1.06	1.05	1.15	1.10	1.11	1.09	1.08
Re_w	-	19000	17300	15750	14080	12300	18600	14800

APPENDIX 2

TABLE OF EXPERIMENTAL RESULTS

FOR DIMENSIONAL ANALYSIS

(Constant $(A \cdot W^2/g)$ Sets)

Test no.	1	2	3	4	5	6	7	8	9
Freq. cpm		1500	1500	1500	1500	1500	1750	1750	1750
Amp $\bar{+}$ A x 10^{-2} m	0	0.22	0.44	0.66	0.89	1.10	0.16	0.33	0.49
T_i °C	13.0	15.8	16.3	16.8	17.2	17.9	14.2	14.3	14.4
T_o °C	30.9	34.3	35.2	35.8	36.8	38.4	32.6	33.1	33.6
$\bar{\theta}_m$ °C	132.7	133.5	134.3	135.1	136.5	137.2	133.0	133.7	134.5
$T_o - T_i$ °C	17.9	18.5	18.9	19.0	19.6	20.5	18.4	18.8	19.2
$\dot{q}_\omega$ J/S	18895	19528	19950	20056	20689	21639	19425	19845	20267
$\theta_o - \theta_i$ °C	19.0	19.7	20.1	20.2	20.8	21.8	19.6	20.0	20.4
θ_o °C	142.2	143.4	144.4	145.2	146.9	148.1	142.8	143.7	144.7
$\theta_{sat} - \theta_{\bar{o}}$ °C	16.6	15.4	14.4	13.6	11.9	10.7	16.0	15.1	14.1
θ_f °C	150.5	151.1	151.6	152.0	152.9	153.5	150.8	151.3	151.8
h J/m².s.°C	10452	11644	12722	13541	15964	18571	11086	12068	13149
hv/hò	-	1.12	1.22	1.3	1.53	1.78	1.06	1.16	1.26
Rev x 10^4	0	5.86	11.73	17.60	23.63	29.25	5.02	10.12	15.13
N Dò²/3	0	0.59	2.53	6.03	12.39	21.30	0.35	1.54	3.68
A²w²/Dòg	0	0.35	1.43	3.24	5.79	8.97	0.25	1.04	2.37
A.w²/g	0	5.41	11.07	16.61	22.26	27.68	5.41	11.07	16.61
Π Nu	0.691	0.755	0.811	0.851	0.970	1.100	0.725	0.778	0.837
Π Nu - 0.73	-	0.025	0.081	0.121	0.240	0.370	-	0.048	0.107
$(\frac{AW^2}{g})^{-0.47}(\frac{A^2W^2}{Dò g})^{1.08}$	0	0.15	0.475	0.950	1.550	2.250	0.100	0.340	0.680

Test no.	10	11	12	13	14	15	16	17	18
Freq. cpm	1750	1750	1750	2000	2000	2000	2000	2000	2000
Amp $\bar{\pm}$ A x 10^{-2} m	0.65	0.81	0.90	0.12	0.25	0.37	0.50	0.62	0.70
T_1 °C	14.7	15.1	15.6	13.5	13.5	13.6	13.8	13.8	14.0
$T_ó$ °C	34.1	35.3	36.1	32.2	32.3	32.7	33.0	33.9	34.3
$\bar{\theta}_m$ °C	135.3	136.2	137.2	132.7	133.3	133.7	134.6	135.4	136.4
$T_o - T_1$ °C	19.4	20.2	20.5	18.3	18.8	19.1	19.2	20.1	20.3
$\dot{Q}$ J/S	20478	21323	21639	19316	19845	20161	20267	21217	21428
$\theta_ó - \theta_1$ °C	20.6	21.5	21.8	19.5	20.0	20.3	20.4	21.4	21.6
$\theta_ó$ °C	145.6	147.6	148.1	142.5	143.3	143.9	144.8	146.1	147.2
$\theta_{sat} - \theta_ó$ °C	13.2	11.8	10.7	16.3	15.5	14.9	14.0	12.7	11.6
θ_f °C	152.3	152.9	153.5	150.7	151.1	151.4	151.8	152.5	153.6
h J/m².s.°C	14246	16594	18299	10881	11757	12425	13293	15341	16962
hv/ho	1.36	1.59	1.75	1.04	1.13	1.19	1.27	1.47	1.62
Rev x 10^4	19.90	20.08	28.10	4.25	8.93	13.18	17.85	22.10	24.90
$ND\bar{o}^2/3$	7.03	13.78	16.63	0.22	1.01	2.31	4.48	7.60	10.6
$A^2.w^2/D\bar{o}.g$	4.25	6.66	8.16	0.19	0.48	1.82	3.31	5.07	6.48
$A.w^2/g$	22.26	27.68	30.85	5.41	11.07	16.61	22.26	27.68	30.85
π Nu	0.889	1.007	1.083	0.716	0.763	0.799	0.842	0.948	1.025
π Nu−0.73	0.159	0.277	0.353	$\pm$	0.033	0.069	0.112	0.218	0.295
$\left(\frac{\Delta W^2}{g}\right)-.47\left(\frac{A^2.W^2}{D\bar{o}.g}\right)^{1.08}$	1.112	1.628	1.930	0.075	0.268	0.510	0.849	1.212	1.510

A P P E N D I X 3

TABLE OF EXPERIMENTAL RESULTS

FOR DIMENSIONAL ANALYSIS

(Constant $(A.W)^2/Do.g$) Sets.)

Test no.	19	20	21	22	23	24	25	26	27
Freq. cpm		2000	2000	2000	2000	2000	2000	1750	1750
Amp ÷ A x 10^{-2} m	0	0.12	0.25	0.37	0.50	0.62	0.70	0.14	0.29
T_i °C	14.0	14.0	14.0	14.0	14.0	14.0	14.6	14.2	14.3
T_o °C	32.6	32.8	33.4	34.2	34.2	34.6	34.8	33.1	33.6
$\bar{\theta}_m$ °C	132.9	133.2	133.6	133.9	134.8	135.7	136.6	133.3	133.6
$T_o - T_i$ °C	18.6	18.8	19.4	20.2	20.2	20.6	20.8	18.9	19.3
$\dot{Q}$ J/S	19633	19845	20478	21323	21323	21745	21956	19950	20373
$\theta_o - \theta_i$ °C	19.77	19.98	20.62	21.88	21.47	21.62	22.11	20.1	20.51
θ_o °C	142.8	143.2	143.9	144.8	145.5	146.5	147.7	143.4	143.9
$\theta_{sat} - \theta_o$ °C	16.6	15.6	149.9	14.0	13.3	12.3	11.1	15.4	14.9
θ_f	150.8	151.0	151.4	151.8	152.2	152.7	153.3	151.1	151.4
h J/m²·s·°C	11268	11681	12620	13986	14722	16234	18164	11896	12556
h_v/h_o		1.04	1.12	1.24	1.31	1.44	1.61.	1.06	1.11
Rev x 10^4	0	4.25	8.93	13.18	17.85	22.1	24.91	4.25	8.93
$ND^2\bar{o}/3$	0	.23	1.05	2.45	4.72	7.85	11.08	0.26	1.20
$A^2w^2/D\bar{o}\,g$	0	.19	.84	1.82	3.31	5.07	6.48	0.19	0.84
$A \cdot w^2/g$	0	5.37	11.18	16.54	22.36	27.72	31.30	4.62	9.9
Π Nu	0.737	0.759	0.812	0.885	0.920	0.996	1.085	0.772	0.808
Π Nu - 0.73	0.007	0.029	0.082	0.155	0.19	0.266	0.355	0.042	0.073
$(\frac{Aw^2}{g})^{-.47} (\frac{A^2 \cdot w^2}{D\bar{o} \cdot g})^{.08}$	0	0.076	0.267	0.512	0.845	0.178	1.49	0.081	0.282

Test no.	28	29	30	31	32	33	34	35	36
Freq. cpm	1750	1750	1750	1750	1500	1500	1500	1500	1500
Amp $\pm$ A x 10^{-2} m	0.48	0.58	0.71	0.80	0.16	0.34	0.50	0.67	0.83
T_i °C	14.4	14.7	14.9	15.	15.6	16.1	16.5	17.0	17.6
T_o °C	34.4	35.0	15.6	16.3	34.4	35.6	36.3	37.4	38.2
θ_m °C	134.0	134.6	135.4	136.2	133.21	134.2	135.0	135.4	135.8
$T_o - T_i$ °C	20.0	20.3	20.7	21.3	18.8	19.5	19.8	20.4	20.7
$\dot{Q}$ J/S	21111	21428	21850	22484	19845	20584	20906	21534	21850
$\theta_o - \theta_i$ °C	21.26	21.58	22.0	22.64	19.98	20.73	21.04	21.68	22.0
θ_o °C	144.8	145.4	146.4	147.5	143.4	144.6	145.5	142.6	146.8
$\theta_{sat} - \theta_o$ °C	14.0	13.4	12.4	11.3	15.4	14.2	13.3	12.6	12.0
θ_f °C	151.8	152.1	152.6	153.2	151.1	151.7	152.2	152.5	152.8
h J/m²·s·°C	13847	14684	16181	18271	11833	13312	14430	15694	16720
hv/ho —	1.23	1.30	1.44	1.62	1.05	1.18	1.28	1.39	1.48
Rev x 10^4	13.13	17.9	22.1	24.91	4.25	8.93	13.13	17.85	22.1
$ND^2\bar{o}/3$	2.83	5.42	8.93	12.45	.31	1.49	3.47	6.71	10.68
$A^2 \cdot w^2/D\bar{o} \cdot g$	1.82	3.31	5.07	6.48	0.19	0.84	1.82	3.31	5.07
$A \cdot w^2/g$	14.57	19.62	24.3	30.26	4.0	8.49	12.49	16.81	20.82
π Nu	0.876	0.919	0.994	1.097	0.768	0.846	0.903	0.968	1.019
π Nu - 0.73	0.146	0.189	0.264	0.366	0.038	0.116	0.173	0.238	0.289
$(\frac{AW^2}{g})^{-.47}(\frac{A^2 \cdot w^2}{D\bar{o} \cdot g})^{1.08}$	0.542	0.907	1.287	2.17	0.087	0.303	0.583	0.969	1.386

APPENDIX 4

TABLE OF EXPERIMENTAL RESULTS

AT VARIOUS FREQUENCIES AND

AMPLITUDES OF VIBRATION.

Test no.	37	38	39	40	41	42
Freq. cpm	1500	1250	1250	1250	1250	1250
Amp $\pm$ A x 10^{-2} m	0.94	0.19	0.40	0.59	0.80	1.00
T_i °C	18.0	19.5	19.8	20.0	20.4	20.7
T_o °C	39.5	37.8	38.8	40.0	40.2	41.6
$\bar{\theta}_m$ °C	136.3	133.4	134.0	134.6	135.4	136.2
$T_o - T_i$ °C	21.5	18.9	19.3	20.0	20.2	20.9
Q J/S	22695	19950	20371	21111	21321	22061
$\theta_{\bar{o}} - \theta_i$ °C	22.85	20.09	20.51	21.26	21.47	22.21
$\theta_{\bar{o}} -$ °C	147.7	143.5	144.3	145.2	146.1	147.3
$\theta_{sat} - \theta_{\bar{o}}$ °C	11.1	15.3	14.5	13.6	12.7	11.5
θ_f °C	153.4	151.2	151.6	152.0	152.5	153.1
h J/m²·s·°C	18775	11974	12901	14254	15416	17615
hv/ho	1.67	1.06	1.14	1.27	1.37	1.56
Rev x 10^4	24.91	4.25	8.93	13.18	17.85	22.01
$N\,D\bar{o}^2/3$	29.65	0.37	1.73	4.02	7.90	13.51
$A^2 w^2/D\bar{o}\cdot g$	6.48	0.19	0.84	1.82	3.31	5.07
AW^2/g	23.54	3.33	7.07	10.41	14.01	17.35
$\pi\,Nu$	1.122	0.769	0.824	0.896	0.953	1.062
$\pi\,Nu - 0.73$	0.392	0.039	0.094	0.166	0.223	0.332
$\left(\frac{AW^2}{g}\right)^{-.47}\left(\frac{A^2 w^2}{D\bar{o}\cdot g}\right)^{1.08}$	1.708	0.970	0.331	0.636	1.053	1.513

Test no.	43	44	45	46	47	48	49	50	51
Freq. cpm	0	800	1300	1680	800	1100	1300	1650	0
Amp ± A x 10^{-2} m	0	0.43	0.58	0.76	0.57	0.67	0.77	0.98	0
T_i °C	13.9	17.9	16.2	16.0	18.8	18.8	19.0	18.9	16.3
$T_{\bar{o}}$ °C	31.9	36.8	35.4	36.4	37.5	37.9	38.4	39.6	34.2
$\bar{\Theta}_m$ °C	132.6	133.1	134.9	135.5	133.8	134.3	134.7	136.3	133.2
$T_{\bar{o}} - T_i$ °C	18.0	18.9	19.2	20.4	18.7	19.1	19.4	10.8	18.3
$\dot{Q}$ J/S	19000	19950	20267	21534	19739	20161	20479	21955	19317
$\Theta_{\bar{o}} - \Theta_i$ °C	19.3	20.1	20.4	21.7	19.9	20.3	20.6	22.1	19.4
$\Theta_{\bar{o}}$ °C	142.4	143.7	145.1	146.4	143.8	144.5	145.0	147.4	142.4
$\Theta_{sat} - \Theta_{\bar{o}}$ °C	16.4	15.1	13.7	12.4	15.0	14.3	13.8	11.4	15.9
Θ_f °C	150.6	151.3	152.0	152.6	151.3	151.6	151.9	153.1	150.9
h J/m².s.°C	10638	12132	13584	15946	12084	12946	13627	17684	11156
h_v/h_o	-	1.14	1.28	1.50	1.14	1.22	1.28	1.66	-
Rev x 10^4	0	6.05	13.45	22.58	8.05	13.12	17.80	28.79	0
N D$\bar{o}^2$/3	0	1.20	4.01	9.70	2.09	4.33	7.01	18.55	0
A^2w^2/Dog	0	0.39	1.87	5.30	0.66	1.78	1.39	8.56	0
Aw^2/g	0	3.04	-10.96	32.82	4.05	9.06	9.45	29.93	0
π Nu	0	0.783	0.855	0.918	0.778	0.824	0.854	1.063	0.73
π Nu - 0.73	0	0.053	0.125	0.188	0.048	0.094	0.129	0.333	0
$(\frac{Aw^2}{g})^{-.47}(\frac{A^2w^2}{D\bar{o}\cdot g})^{1.08}$	0	0.213	0.639	1.175	0.331	0.625	0.495	2.053	0

Test no.	52	53	54	55	56	57	58	59	60
Freq. cpm	600	1000	2000	1500	1000	2000	0	1000	1320
Amp ± A x 10^{-2} m	-0.17	0.20	0.39	0.28	0.20	0.39	0	0.37	0.39
T_i °C	16.3	16.4	20.4	22.0	22.4	22.8	12.3	14.6	14.8
T_o °C	34.8	35.7	40.8	40.8	41.0	42.8	30.8	34.2	34.8
θ_m °C	133.2	133.7	134.6	135.5	133.9	134.8	133.0	133.4	134.0
$T_{\bar{o}} - T_i$ °C	18.5	19.3	20.4	18.8	18.6	20.0	18.5	19.2	20.0
$\dot{Q}$ J/S	19529	20372	21533	19844	19633	21111	19528	20266	21111
$\theta_{\bar{o}} - \theta_i$ °C	19.66	20.51	21.68	19.48	19.77	21.26	19.66	20.41	21.26
$\theta_{\bar{o}}$ °C	143.1	143.5	145.4	143.5	143.8	145.4	142.8	143.6	144.0
$\theta_{sat} - \theta_{\bar{o}}$	15.7	15.3	13.4	15.3	15.0	13.6	16.0	15.2	14.8
θ_f °C	151.0	151.2	152.1	151.2	151.3	152.1	150.8	151.2	151.4
$\bar{h}$ J/m².s.°C	11422	1227	14756	11910	12019	14254	11208	12243	13098
h_v/h_o	1.024	1.100	1.320	1.070	1.080	1.280	-	1.09	1.17
Rev x 10^4	1.76	3.46	13.89	7.35	3.46	13.86	-	5.61	9.05
$ND_{\bar{o}}^2/3$	0.13	0.31	2.85	0.93	0.32	2.81	-	0.82	1.64
$A^2w^2/D_{\bar{o}}.g$	0.03	0.50	2.02	0.55	0.12	2.02	-	0.45	0.87
Aw^2/g	0.66	4.36	17.44	6.92	2.18	9.81	-	4.14	28.6
Π Nu	0.744	0.791	0.924	0.772	0.774	0.896	0.733	0.791	0.841
Π Nu - 0.73	0.014	0.061	0.194	0.042	0.044	0.166	0.003	0.061	0.111
$(\frac{Aw^2}{g})^{-.47}(\frac{A^2w^2}{D_{\bar{o}}.g})^{1.08}$	0.035	0.176	0.558	0.218	0.070	0.731	-	0.220	0.178

Test no.	61	62	63	64	65	66	67	68	69
Freq. cpm	1500	1700	2000	0	1000	1250	1500	1700	0
Amp ± A x 10^{-2} m	0.44	0.51	0.64	0	0.16	0.19	0.22	0.25	0
T_1 °C	15.0	15.6	16.2	19.2	19.9	19.8	19.8	19.4	13.9
$T_{\bar{o}}$ °C	35.4	36.1	36.6	37.2	38.1	38.5	38.8	39.2	31.9
$\bar{\Theta}_m$ °C	134.5	134.8	136.0	132.9	132.9	133.1	133.4	133.7	132.8
$T_{\bar{o}} - T_i$ °C	20.4	20.5	21.0	18.0	18.2	18.6	19.0	19.3	18.0
$\dot{Q}$ J/s	21534	21639	22167	19000	19211	19634	20055	20373	19000
$\Theta_{\bar{o}} - \Theta_1$ °C	21.68	21.79	22.32	19.13	19.34	19.77	20.19	20.51	19.13
$\Theta_{\bar{o}}$ °C	144.7	145.7	147.2	142.5	142.6	143.0	143.5	144.0	142.4
$\Theta_{sat} - \Theta_{\bar{o}}$ °C	14.1	13.7	11.6	16.3	16.2	15.8	15.3	14.8	16.4
Θ_f °C	151.8	152.3	153.0	150.7	150.7	150.9	151.2	151.4	150.6
h J/m².s.°C	14024	14295	17547	10703	10884	11411	12036	12641	10638
hv/ho	1.25	1.28	1.57	-	1.02	1.07	1.13	1.18	-
Rev x 10^4	11.75	15.50	22.79	-	2.76	4.23	5.87	1.73	-
N $D_{\bar{o}}^2/3$	2.59	4.08	8.88	-	0.08	0.36	0.60	0.87	-
$A^2 w^2 / D_{\bar{o}} \cdot g$	1.43	2.48	5.38	-	0.09	0.19	0.37	0.61	0
$A w^2 / g$	10.73	16.51	28.61	-	1.79	3.34	5.61	8.17	0
π Nu	0.889	0.901	1.06	0.701	0.716	0.745	0.78	0.812	0.701
π Nu - 0.73	0.159	0.171	0.33	-	-	0.015	0.05	0.082	-
$\left(\frac{A w^2}{g}\right)^{-.47} \left(\frac{A^2 w^2}{D_{\bar{o}} \cdot g}\right)^{1.08}$	0.483	0.720	-	0.056	0.094	0.152	0.152	0.221	0

Test no.	70	71	72	73	74	75	76	77	78
Freq. cpm	800	1300	1680	500	800	1000	0	1000	1310
Amp ± A x 10^{-2} m	0.14	0.20	0.25	0.39	0.43	0.47	0	0.85	0.75
T_i °C	14.2	14.6	14.8	17.4	16.9	16.7	15.3	16.7	18.4
T_o °C	32.4	33.2	33.8	35.6	35.6	35.8	33.6	37.0	39.0
θ_m °C	133.0	133.4	133.8	133.4	133.6	133.5	132.6	133.9	134.7
$T_o - T_i$ °C	18.2	18.6	19.0	18.2	18.7	19.1	18.5	20.3	20.6
$\dot{Q}$ J/S	19211	19634	20056	19211	19734	20161	19527	21428	21745
$\theta_{\bar{o}} - \theta_i$ °C	19.3	19.8	20.2	19.3	19.4	20.3	19.7	21.6	21.9
$\theta_{\bar{o}}$ °C	042.7	143.3	143.9	143.1	143.6	143.7	142.7	144.7	145.0
$\theta_{sat} - \theta_{\bar{o}}$ °C	16.1	15.5	14.9	15.7	15.2	15.1	16.1	14.1	13.8
θ_f °C	150.8	151.1	151.4	151.0	151.2	151.3	150.8	151.8	151.9
h J/m^2·s·°C	10956	11632	12360	11236	11921	12260	11137	13955	14470
hv/ho	1.03	1.09	1.16	1.06	1.12	1.15	–	1.25	1.30
Rev x 10^4	2.05	4.45	7.52	3.45	6.05	8.39	–	15.23	17.49
$ND_{\bar{o}}^2/3$	0.13	0.39	0.89	0.59	1.19	1.84	–	6.43	6.70
$A^2w^2/D_{\bar{o}}\cdot g$	0.04	0.20	0.66	0.11	0.39	0.72	0	2.38	2.82
Aw^2/g	1.01	3.59	8.36	1.05	3.04	5.27	0	9.5	14.39
Π Nu	0.719	0.576	0.795	0.732	0.770	0.791	0.731	0.877	0.914
Π Nu - 0.73	–	0.026	0.065	0.002	0.040	0.061	0.001	0.147	0.186
$(\frac{Aw^2}{g})^{-.47}(\frac{A^2w^2}{D_{\bar{o}}\cdot g})^{1.08}$	0.031	0.096	0.236	0.090	0.215	0.321	0	0.885	0.876

APPENDIX 5

TABLE OF EXPERIMENTAL RESULTS

FOR NUSSELTS NUMBER X COOLING

WATER TEMPERATURE.

Freq. cpm	0	0	0	0	0	0	0
Inlet Ti °C	19.2	31.3	39.4	20	14.4	28.4	33.4
Outlet To °C	37.2	50.1	57.6	38.7	44.	47.8	52.4
Tube θm °C	132.9	135.5	135.9	133.3	134.1	134.6	135.1
To - Ti °C	18	18.8	18.2	18.7	19.6	19.4	19
Q J/s	19000	19845	19211	19739	20689	20478	20056
θō - θi °C	19.13	19.98	19.34	19.88	20.83	20.62	20.19
θō °C	142.5	145.5	145.6	143.2	144.5	144.9	145.2
θf °C	150.7	152.2	152.2	151	151.7	151.9	152
θ sat - θō °C	16.3	13.3	13.2	15.6	14.3	13.9	13.6
h J/m².s.°C	10703	13701	13364	11619	13285	13528	13542
Nu	535	685	668	581	664	676	677

Freq. cpm	0	0	0	0	0	0	0
Inlet Ti °C	10.8	18.1	19.6	23.6	27.6	35	38.2
Outlet To °C	28.7	36.3	38.6	42.7	46.7	54.3	56.6
Tube θm °C	132.8	133.0	133.5	133.9	134.4	134.9	135.7
To - Ti °C	18.0	18.2	19.0	19.1	19.1	18.6	18.4
Q J/s	19000	19211	20056	20161	20161	19634	19423
θō - θi °C	19.1	19.3	20.2	20.3	20.3	19.77	19.56
θō °C	142.4	142.7	143.6	144.1	144.6	144.8	145.5
θf °C	150.6	150.8	151.2	151.5	151.7	151.8	152.2
θsat - θō °C	16.4	16.1	15.2	14.7	14.2	14.0	13.3
h J/m².s.°C	10639	10957	12116	12594	13038	12878	13410
Nu	532	548	607	630	652	644	671

Freq. cpm	1500	1500	1500	1500	1500	1500
Inlet Ti °C	19.8	24.0	28.8	35.0	37.0	30.6
Outlet To °C	39.0	44.4	48.9	54.9	56.8	40.2
Tube Θ_m °C	133.9	134.5	135.2	135.8	136.0	135.4
Amp $\mp$ A $\times 10^{-2}$ m	0.22	0.22	0.22	0.22	0.22	0.22
To - Ti °C	18.8	19.3	19.7	19.1	18.7	19.2
$\dot{Q}$ J/S	19844	20373	20795	20161	19739	20267
$\Theta_{\bar{o}} - \Theta_i$ °C	19.83	20.51	20.94	20.30	19.88	20.41
$\Theta_{\bar{o}}$ °C	143.9	144.8	145.6	146.0	145.9	145.6
Θ_f °C	151.4	151.8	152.2	152.4	152.4	152.2
$\Theta_{sat} - \Theta_{\bar{o}}$ °C	14.9	14.0	13.2	12.8	12.9	13.2
h $J/m^2.s.°C$	12230	13363	14466	14465	14051	14098
Nu	612	668	723	723	703	705

Freq. cpm	1500	1500	1500	1500	1500	1500
Inlet Ti °C	15.6	20.4	26.3	31.2	36.2	42.0
Outlet To °C	35.3	40.5	47.5	52.1	56.8	61.0
Tube Θ_m °C	136.1	136.5	137.0	137.5	137.9	138.4
Amp $\mp$ A $\times 10^{-2}$ m	0.75	0.75	0.75	0.75	0.75	0.75
To - Ti °C	19.7	20.1	21.2	20.9	20.6	19.9
$\dot{Q}$ J/S	20794	21216	22378	22061	21745	21005
$\Theta_{\bar{o}} - \Theta_i$ °C	20.94	21.36	22.53	22.21	21.90	21.15
$\Theta_{\bar{o}}$ °C	146.6	147.2	148.3	148.6	148.9	149.0
Θ_f °C	152.7	153.0	153.6	153.7	153.9	153.9
$\Theta_{sat} - \Theta_{\bar{o}}$ °C	12.2	11.6	10.5	10.2	9.90	9.8
h $J/m^2.s.°C$	15651	16795	19571	19861	20170	19682
Nu	783	840	979	993	109	984

Freq. cpm	1500	1500	1500	1500	1500	1500
Inlet Ti °C	13.6	18.5	22.3	28.5	31.4	37.6
Outlet To °C	40.0	37.5	41.8	48.3	51.0	56.5
Tube $\bar{\theta}_m$ °C	135.1	135.5	136.0	136.6	137.0	137.5
Amp $\pm$ A x 10^{-2} m	0.49	0.49	0.49	0.49	0.49	0.49
$\bar{T}_o - T_i$ °C	18.4	19.0	19.5	19.8	19.6	18.9
$\dot{Q}$ J/s	19423	20055	20583	20900	20689	19950
$\bar{\theta}_o - \theta_i$ °C	19.56	20.19	20.7	21.04	20.83	20.09
$\bar{\theta}_o$ °C	144.9	145.6	146.4	147.1	147.4	147.5
θ_f °C	151.9	152.2	152.6	153.0	153.2	153.5
$\theta_{sat} - \bar{\theta}_o$ °C	13.9	13.2	12.4	11.7	11.4	11.3
h J/m².s.°C	12831	13952	15242	16403	16665	16212
Nu	642	697	762	820	833	810

REFERENCES

1. J.A. Scanlan.

    Effect of surface vibration on laminar forced
    convection heat transfer.
    Ind. Enging. Chemistry.
    V. 50, No. 10, Oct. 1958.

2. R.C. Marinelli and
    L.M.K. Boelter.

    The effect of vibration on heat transfer by
    free convection from a horizontal cylinder.
    Proc. of fifth Int. Prog. for Applied
    Mechanics, 1930.

3. W.R. Penney and
    J.B. Jefferson.

    Heat transfer from oscillating horizontal wire
    to water and ethylene Glycol.
    Trans. ASME Series (C)
    V. 88, 359, 1961.

4. F.K. Deaver,
    W.R. Penney and
    T.B. Jefferson.

    Heat transfer from an oscillating horizontal
    wire to water.
    Trans. ASME   Journal of heat transfer.
    V. 84, 251, 1962.

5. R. Lemlich and
    M. Anandha.

    The effect of transverse vibration on free
    convection from a horizontal cylinder.
    Int. Jour. Heat Mass Transfer,
    V. 8, 27, 1963.

6. R. Lemlich.

    Effect of vibration on natural convection heat
    transfer.
    Ind. Eng. Chemistry
    V. 47, 1175, June 1955.

7. R.M. Fand and
    J. Kay.

    The influence of vertical vibration on heat
    transfer by free convection from a horizontal
    cylinder.
    Trans. ASME, Jour. of Heat Transfer.
    V. 83, 133, 1961.

8. R.M. Fand and
    E.M. Peebles.

    A comparison of the influence of Mechanical
    and Acoustical vibration on free convection
    from a horizontal cylinder.
    Trans. ASME   Jour. of Heat Transfer.
    V. 84, 268, 1962.

9. G. Morrell.

    An empirical method for calculating heat
    transfer rates in resonating gaseous pipe.
    Jet Propulsion, Dec. 1958.

10. T.W. Jackson,
    W.B. Morrison and
    W.C. Boteler.

    Free convection, forced convection and acoustic
    vibrations in a constant temperature vertical
    tube.
    Trans ASME Jour. Heat Transfer, Feb. 1959.

11. R. Lemlich.

    Vibration and pulsation boast heat transfer.
    Chemical Engineering,
    May 15th, 1961.

12. C.E. Feiler and
    E.B. Yeages.

    Effect of large amplitude oscillations on heat
    transfer.
    NASA Report No. TR R - 142, 1962.

13. R.M. Fand and
    J. Kaye.

    Acoustic Streaming near a heated cylinder.
    Jour. Acoustic Soc. of America.
    V. 32, 1960.

14. I.A. Raben
    G. Commerford and
    R. Dietert.

    An investigation of the use of acoustic vibration
    to improve heat transfer rates and reduce scaling
    in distillation units used for saline water.
    U.S. Dept. of Interior, Office of Saline
    Water Research and Development.
    Report No. 49, (1961)

15. J.C. Dent.

    The calculation of heat transfer coefficient for
    condensation of steam on a vibrating vertical
    tube.
    Int. Jour. of Heat and Mass Transfer.
    V. 12, No. 9, 1969.

16. P.V. Danckwerts.

    The sigjificance of liquid-film coefficients in
    gas absorption.
    Ind. Eng. Chemistry,
    43, 1960, 1951.

17. H.S. Mickley and
    D.F. Fairbanks.

    Mechanism of Heat Transfer to Fluidized Beds.
    A.I. Ch. E. Jour.
    NO. 1, 334, 1955.

18. W. Nusselt.

    Zeitchr. d. ver. dentsch. Ing.
    V. 60, 514, 1916.

19. D.P. Haughey.

    Heat transfer during condensation on vibrating
    tube.
    Tran. Inst. Chem. Engrs.
    V. 43, No. 2, 1965.

20. J.C. Dent.

    Effect of vibration on condensation heat
    transfer to a horizontal tube.
    Proc. Inst. Mech. Engrs.
    V. 184, No. 5, 1969.

21. O. Reynolds   An experimental investigation of the circumstances which determine whether the motion of water shall be direct or sinuous. Phil. Trans. Roy. Soc., London. V. 174, 1883.

22. W.H. McAdams   Heat Transmission. McGraw - Hill, New York, 1942.

23. L.A. Bromley, R.S. Bradkey and N. Fishman.   Heat transfer in condensation. Ind. and Enging. Chem. V. 44, 2962, 1962.

24. G.G. Watson and R.D. Clark.   Determination of tube wall temperature in a heat exchanger from the tube resistance. NEL Report, No. 272, 1961.

25. G.W. Kaye and T.H. Laby.   Table of physical and chemical constants. Longmans Green and Co. Ltd.

26. J.D. Link   The ABC of thermocouples. Foulsham - Sams W. Foulsham and Co. Ltd., 1968.

27. T.B. Drew, W.M Nagle and W.Q. Smith.   The condition of dropwise condensation of steam. Trans. A.I.Ch.E. V. 31, 1935.

28. M.S. Plesset.   The Dynamics of Cavitation bubbles. Trans. ASME Journal of Applied Mechanics. V. 16, 1949.

29. G.W. Sutton.   A photoelastic study of strain waves caused by cavitation. Journal of Applied Mechanics. V. 24, Part 3, 1937.

30. F.L. Shea and N.W. Krase.   Trans. A.I.Ch. E. V. 36, 436, 1940.

31. M. Jackob.   Heat Transfer. John Wiley and Sons, New York. V.1, 1949.

32. L.A. Bromley.   The effect of heat capacity of condensate. Ind. and Enging. Chemistry. V. 44, 2966, 1952.

33. B.O. Pierce.   A short table of integrals.
                          Green and Co.
                          Boston, Mass. 1929.

34. W.H. McAdams and   Ind. and Enging. Chemistry.
    T.H. Frost   V. 14, 13, 1922.

35. J.L. Wallace and   Ind. and Enging. Chemistry,
    A.W. Davison.   V. 30, 948, 1938.

36. D.F. Othmer.   Ind. and Enging. Chemistry,
                          V. 21, 576, 1929.

37. W.R. Rohsenow.   Heat transfer and temperature distribution
                          in laminar film condensation.
                          Trans. ASME.
                          V. 78, 1645, 1956.

38. E.M. Sparrow and   A Boundary-Layer treatment of laminar
    J.L. Gregg.   film condensation.
                          Trans. ASME Series (C).
                          Journal of Heat Transfer.
                          V. 81, 13, 1959.

39. E.M. Sparrow and   Laminar condensation heat transfer on a
    J.L. Gregg.   horizontal cylinder.
                          Trans. ASME Series (C).
                          Journal of Heat Transfer.
                          V. 81, 4, 1959.

40. H. Schlichting.   Boundary-Layer theory.
                          Pergamon Press, 1935.

41. A. Eagle and   The coefficient of heat transfer from tube to
    R.M. Ferguson.   water.
                          Proc. Inst. Mech. Engrs.
                          No. 4, 1930.

42. D.C.P. Birt et al.   Methods of improving heat transfer from
                          condensing steam and their application to
                          condensers and evaporators.
                          Trans. Inst. Chem. Engrs.
                          V. 37, 1959.

43. H. Hampson.   Engineering. London.
                          1955, 179, 464.

44. W.M. Nagle,
    G.S. Blendenman and
    T.B. Drew.

Trans. Am. Inst. Chem. Engrs.
1935, 31, 593.

45. L. Prandtl.

Fluid Dynamics.
Blackie and Son Ltd., 1957.

46. A.J. Ede.

An Introduction to Heat Transfer.
Pergamon Press, 1967.

47. J.R. Welty,
    C.E. Wicks and
    R.E. Wilson.

Fundamentals of Momentum Heat and Mass
Transfer.
John Wiley and Sons.   1969.